**[P13.01]**

# Carbon based electrochemical sensors with nafion coating for selective detection of drug molecules

E. Mynttinen*[1], N. Wester[1], J. Etula[1], E. Kauppinen[1], E. Kalso[2,3], T. Lilius[2], J. Koskinen[1], T. Laurila[1]

*[1]Aalto University, Finland, [2]University of Helsinki, Finland, [3]Helsinki University Hospital, Finland*

Novel carbon materials, such as tetrahedral amorphous carbon (ta-C) and various carbon nanostructures, have shown great promise in sensitive and selective electrochemical detection of biological molecules [1,2]. The selectivity of such sensors can be further improved with cation exchange polymers, such as Nafion, exhibiting permselective properties [3]. In hospital environments, accurate determination of drug molecule concentrations is essential in pain management for efficient and safe dosing. However, the current analysis methods are both time consuming and laborious, and are thus not sufficient for adaptive pain treatment. For this purpose, carbon based electrochemical sensors coated with permselective Nafion films can enable fast and effortless detection without compromising sensitivity and selectivity.

The permselective properties of Nafion appear to be affected by differences in the surface roughness of the electrode, and thus the selectivity of the sensor could be tailored by modifying its topography. We have generated two types of carbon based thin film electrodes coated with Nafion for the detection of biological molecules: a smooth ta-C surface and a carbon nanotube (CNT) thin film with larger surface roughness.

In this work, we will evaluate the effect of surface roughness of the underlying carbon material on the permselective properties with cyclic voltammetry (CV) and differential pulse voltammetry (DPV). The physical, chemical and electrochemical properties of ta-C electrodes have been characterized in detail in previous work [1,4,5]. The electrochemical properties of the prepared Nafion coated sensors will be assessed with several outer and inner sphere probes. In addition, the materials will be characterized by SEM, AFM and Raman spectroscopy. The sensor performance will be evaluated with various biological molecules (Fig.1). It is anticipated that with these novel electrode materials, fast, sensitive and selective detection of various drug molecules with clinical relevance can be achieved.

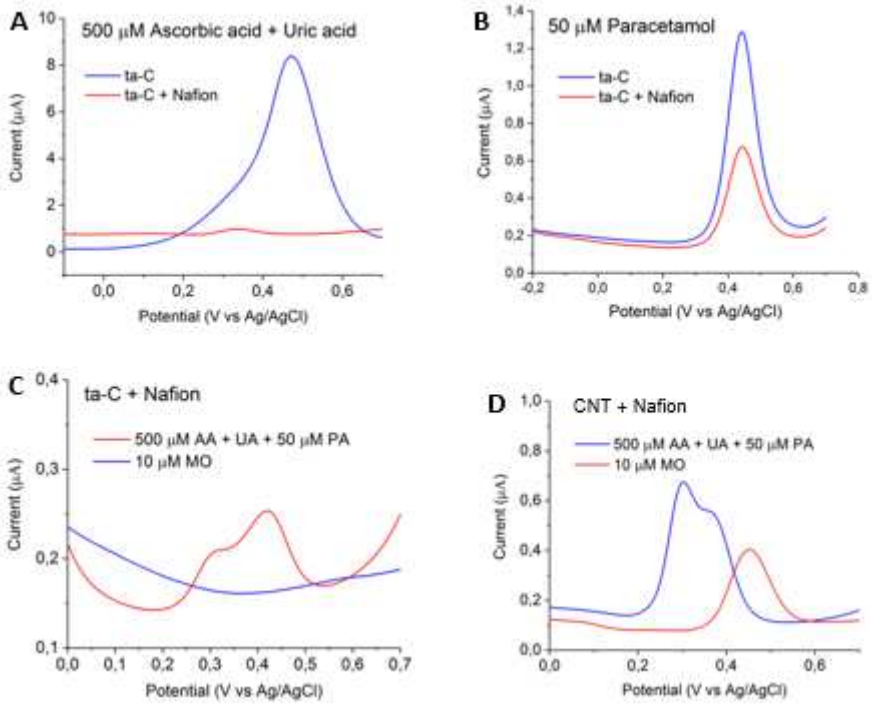


Figure 1. Differential pulse voltammograms for ta-C and ta-C coated with Nafion in 500 µM of AA and UA (A) and 50 µM PA (B). ta-C coated with Nafion (C) and CNT coated with Nafion (D) in 500 µM of AA and UA and 10 µM MO. On ta-C, the polymer film greatly reduces the signals of AA and UA (A) while still preserving its ability to detect PA (B). However, this sensor completely fails to detect MO (C), in contrast to the nanostructured surface (D). On the other hand, the CNT sensor seems to have an unfavorable response for UA and PA in respect to each other, compared to that of ta-C.

1. Laurila, T., et al. "New electrochemically improved tetrahedral amorphous carbon films for biological applications". Diamond and Related Materials 49 (2014): 62-71.

2. Sainio, S., et al. “Integrated Carbon Nanostructures for Detection of Neurotransmitters”. Molecular Neurobiology 52 (2015): 859-866.

3. Ribeiro, J. A., “Electrochemical sensors and biosensors for determination of catecholamine neurotransmitters: A review”. Talanta 160 (2016): 653-679.

4. Protopopova, V. S., et al. "Ultrathin undoped tetrahedral amorphous carbon films: thickness dependence of the electronic structure and implications for their electrochemical behaviour". Physical Chemistry Chemical Physics 17.14 (2015): 9020-9031.

5. Palomäki, T., et al. "Electron transport determines the electrochemical properties of tetrahedral amorphous carbon (ta-C) thin films". Electrochimica Acta 225 (2017): 1-10.

Keywords: Carbon nanotube, Tetrahedral amorphous carbon, Electrochemical sensor, Nafion

**[P13.02]**

# Carbon coated GaN sensors

I.B. Usman*, N.J. Coville, B.W. Mwakikunga, D.M. Wamwangi
*University of the Witwatersrand, South Africa*

Gallium nitride (GaN) is a wide-band gap (3.39 eV) semiconductor with excellent thermal stability for applications in optoelectronic devices [1 - 3]. As sensors GaN does not operate at room temperature. In this study carbon coated GaN nanostructures are investigated for the role of carbon defects in room temperature sensor applications. The optical and electronic properties of defects in GaN is of great importance for evaluating the degree to which they affect the devices' performance. The carbon coated GaN (C-GaN) was synthesised using a horizontal chemical vapour deposition (CVD) setup at 600 °C. The physico-chemical properties of the C-GaN have been carried using XRD, TEM, SEM, TGA, Raman, PL and XPS procedures to establish the disorder of the carbon on the surface of GaN. TGA showed that more carbon is coated on the surface of GaN when argon was used as a carrier gas compared to nitrogen. The PL spectrum of C-GaN showed that the intensity of the YL peaks for all the samples containing carbon is suppressed compared to pure GaN. This is attributed to anti site ($C_N$) defects. As a proof of concept C-GaN were tested for gas sensing applications through measurements of the change in electrical resistance of the C-GaN as a function of analyte composition (0-100 ppm) at varying temperatures (300K-500K). The results will be described.

## REFERENCES

1. X.M. Cai, et al., Thin Solid Films, 2006. 515

2. F. Choa et al., Appl. Phys. Lett., 1996. 69(24); S. Nakamura et al., Jpn. J. Appl. Phys., 1997. 36

3. R. Armitage et al., Appl. Phys. Lett. 92 (2002) 2575

Keywords: Carbon coated GaN, TGA, PL

**[P13.03]**

# Development of the direct methanol fuel cell electrocatalyst using marimo nano carbon as a novel electrode material

K. Saito*[1], K. Nakagawa[1,2], T. Ando[3]

*[1]Kansai University, Japan, [2]HRC, Japan, [3]NIMS, Japan*

Direct methanol fuel cell (DMFC) uses a carbon supported Pt catalyst for electrode. Carbon black is generally used the catalyst support material. However, a lot of Pt particle was loaded in the inner micro pore of carbon black. Because methanol cannot get into the micro pore, the activity of Pt loading carbon black catalyst is not high. Therefore, we demonstrated marimo nano carbon (MNC) for a novel catalyst support material. MNC is spherical carbon nanofilaments (CNFs). CNFs were synthesized radially from oxidized diamond (O-dia) supported catalysts for the core. MNC has meso size interfiber voids. We expected Pt particle supported inside of MNC was effective, evaluated the catalyst activity and power generation performance.

MNCs were synthesized by CCVD method. Ni/O-dia and Co/O-dia were used as catalysts. Pt supported on MNCs was prepared by the modified nanocolloidal method. Pt supported on Vulcan XC72 (carbon black: CABOT) was also prepared for comparison. Pt loading level was 5 wt%. The catalyst activity was measured by cyclic voltammetly measurements (CV). The I-V performances were measured by unit cell for DMFC. The Pt metal state was analysed using X-ray photoelectron spectroscopy (XPS).

Figure 1 shows cyclic voltammograms of Pt loading catalysts. Methanol oxidation reaction peaks were observed in the region of 0.6 V. The peak current density of Pt/MNC(Ni) was the highest. Figure 2 shows the results of I-V measurement. The max power density of unit cell using Pt/MNC(Ni) in both electrode was the highest. Figure 3 shows the XPS spectra of Pt4f in the Pt loading catalysts. Pt peak intensity was the highest when using MNC(Ni) for catalyst support. Because electrochemically active Pt was supported on the surface of CNFs.

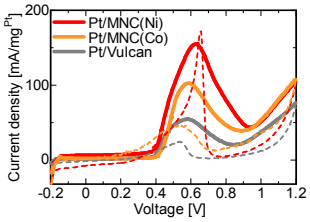


Fig.1 Cyclic voltammograms of Pt loading catalysts.

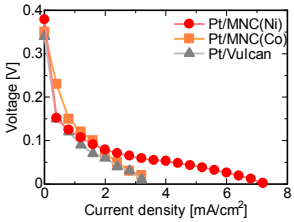


Fig.2 I-V characteristic of DMFC.

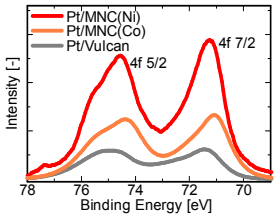


Fig.3 XPS spectra of Pt4f on Pt loading catalysts.

Using MNC(Ni) as catalyst support, the Pt catalyst activity and the power generation performance of DMFC was increased.

Keywords: Marimo nano carbon, Direct methanol fuel cell, Oxidized diamond, Carbon nanofilament

**[P13.04]**

# Oxygen Reduction Reaction on N-doped activated carbons obtained from chitin and chitosan

A. Ilnicka*[1], J.P. Lukaszewicz[1], K. Shimanoe[2], M. Yuasa[3]

*[1]Nicolaus Copernicus University, Poland, [2]Kyushu University, Japan, [3]Kindai University, Japan*

Recently, porous carbon materials doped with heteroatoms, such as oxygen and nitrogen have attracted considerable attention to some electrochemical energy devices (supercapacitors, fuel cells, metal-air batteries) due to several unique properties of heteroatom incorporating surface active sites. In this research we used chitin and chitosan as the carbon source to synthesize the N-doping catalysts.

Chitin and chitosan were subjected to an different activation procedures. In order to improve the electrocatalytic activity, the prepared catalyst is further subjected to the urea impregnation. Then, the nitrogen sorption isotherm, scanning electron microscopy, elemental analysis, and X-ray photoelectron spectroscopy were used to study the microstructure and composition. The catalytic voltammetry and rotating-ring-disk electrode methods were used to investigate the electrochemical behaviour for the oxygen reduction reaction (ORR). The research presents how urea-treatment influenced several textural, chemical and electrocatalytic properties of N-doped activated carbons obtained from renewal resources like chitosan and chitin. The urea-treatment resulted in a spectacular increase in nitrogen content by weight (up to 68%) and the improvement of the surface area (up to 42%) along with total/micro-/mezo- pore volume (up to 49%).

In summary, we have, for the first time, prepared N-doping carbon materials with or without urea from chitin and chitosan. The results revealed that both the pyrolysis temperature and the optionally treatment of urea yielded significant effect on the specific surface area, nitrogen doping and, thus, the electrocatalytic activity, as well. Additionally, it was found that the treatment in urea could further improved the electrocatalytic activity and selectivity to the ORR. All the N-doped carbon materials exhibit higher catalytic performance compared to a commercial Pt/C electrode. This fact indicating on avenues for the development of novel, efficient, metal-free ORR catalysts.

Acknowledgments

This work was created as a result of the research project No. 2014/15/N/ST8/03399 funded by the National Science Centre.

Keywords: nitrogen-doped carbon, oxygen reduction reaction, chitin, metal-free electocatalysts

**[P13.05]**

**Low resistivity of heavily nitrogen doped carbon**

D.A. Zherebtsov*[1], K.R. Smolyakova[1], R.F. Yantsen[1], E.V. Bartashevich[1], D.E. Zhivulin[2], V.E. Zhivulin[2], R.S. Morozov[1], D.A. Vinnik[1], V.V. Avdin[1]

*[1]South Ural State University, Russia, [2]South Ural State Humanitarian Pedagogical University, Russia*

Carbon nitride and nitrogen doped carbon outstanding electrical, photocatalytic, sensing properties makes it a valuable material for producing of semiconducting, photovoltaic, electrochemical devices, liquid and gas sensors. Four series of carbon – nitrogen samples were synthesized at 500 °C from mixtures of 0, 10, 20, ... 90, 100 % of melamine and four kind of pitch: medium temperature coal pitch, high temperature coal pitch, petroleum pitch, shale pitch.

The X-ray powder diffraction, IR spectra, SEM, EDX, mass change, nitrogen adsorption, electric resistivity and magnetic susceptibility measurements were used to analyze structure, composition and properties of the samples.

It is found that in all four series in a range 0-50 mass % pitch the samples consist of two phases: pure $C_3N_4$ and saturated $C_3N_4$ solid solution in graphitic coke. In a range of 50-100 mass % pitch all samples are single phase $C_3N_4$ solid solutions in graphitic coke. Maximal concentration of nitrogen correspond to formula $C_5N_2$ or $C_{0.71}N_{0.29}$ or to 32 mass % N. The electric resistivity of pressed powdered samples of this composition is 1-100 Ohm*m, that is 100-1000 times lower than resistivity of pure coke samples. Resistivity of g-$C_3N_4$ powder estimated to be $10^{10}$ Ohm*m.

PXRD pattern of saturated $C_3N_4$ solid solution in graphitic coke is very similar to that of pure coke, supposing that N atoms are randomly distributed in graphene-like sheets. IR spectra of solid solutions confirm no long range ordering of N atoms in g-$C_3N_4$ motif (no $C_3N_4$ islands). Pure coke is highly paramagnetic ($\chi$=5.0*10$^{-6}$ cm$^3$/g), but N doping decrease magnetic susceptibility fast so that $C_{0.71}N_{0.29}$ is diamagnetic ($\chi$=-1.1*10$^{-6}$ cm$^3$/g).

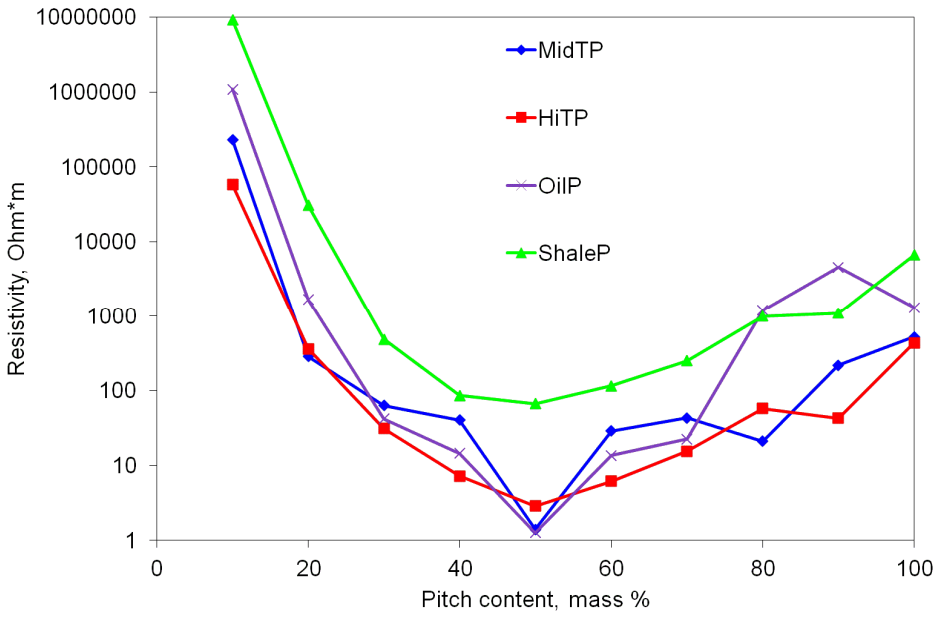


Keywords: nitrogen doped carbon, resistivity, pitch, melamine

**[P13.06]**

**Carbon for energy storage**

P. Jagdale*[1], J. Nair[1], G. Rius[2], F. Bella[1], G. Meligrana[1], A. Tagliferro[1], C. Gerbaldi[1]

*[1]Politecnico di Torino, Italy, [2]Institute of Microelectronics of Barcelona, Spain*

Lithium (Li) metal anodes with an organic electrolyte result in non-uniform passive film formation on the anode surface. This effect causes dendrite growth of Li metal, which detrimentally affects cell performance and safety upon long-term charge/discharge cycling. Advantageously, electrochemical intercalation of Lithium ion ($Li^+$) into carbonaceous materials can solve these issues. Precursor and preparation method are controlling the structure and orientation of mesostructured carbon, which is one of the major factors governing the intercalation of $Li^+$. Recently, the scientific community reconsidered disordered carbon materials. They may store $Li^+$ differently from e.g. graphite, which provides evident advantages in some specific applications.

For this study, carbon from methane, biochar (dried tea leaf powder) as well as waste cellulose fibres precursors were selected. Microwave plasma enhanced chemical vapour deposition (MPE-CVD) technique was used to grow carbon nano walls (CNWs) from methane. Instead, pyrolysis technique was adopted for carbonisation of biochar and cellulose waste. Constant current charge/discharge cycles and Li intercalation on different structural orientation in carbon are thoroughly investigated and here reported. The carbon from biochar showed the capacity of 63.31 mAh g−1. The superior cycling behaviour (>1000 cycles) was demonstrated by CNWs, which also showed stable and prolonged reversible cycling, excellent durability, good specific capacity, and capacity retention when subjected to ultrafast current regimes. Carbon from waste cellulose fibre is currently under study, and preliminary results are promising. Noteworthy, the battery components used can be almost completely recovered after operation. Such an approach opens up a new way of thinking for advanced sustainable batteries.

References:

- Asian Journal of Experimental Science, 22, 2, 2008, 89-93.
- Electrochimica Acta, 182, 2015, 500–506.
- Carbon, 107, 2016, 811-822.

Keywords: Carbon nano walls, tea leaves biochar, Carbon fibres, Lithium

**[P13.07]**

## Green production of carbon nanomaterials in molten salts and their applications

A.R. Kamali*
*Northeastern University, China*

Large scale production of low cost and high quality carbon nanomaterials such as graphene and nanodiamonds from abundant raw materials using eco-friendly methods is a critical step towards the widespread and sustainable use of these so-called “wonder materials”. This paper discusses the progress made on molten salt electrochemical preparation of graphene nanosheets and nanodiamonds having all the characteristics mentioned above. These methods use readily available commercial graphite electrodes as the carbon source which is both abundant and cheap. Apart from graphite, the other consumables are H2, water and electricity. These methods are not only eco-friendly but also very efficient. It offers a production rate of 450 g graphene per litre of molten salt per day. A molten LiCl volume of 10 L should be able to produce 4.5 kg graphene in a day. In molten NaCl graphene can be produced by a rate of about 2.0 kg graphene in a day. The graphene product showed a high conductivity which can be as high as 5.8 × 105 S m−1. The bench-scale production of high quality graphene, on a scale of tens of grams, was achieved using a novel two working electrode electrolysis cell, operating at a current density of about 1 A cm−2 which is at least an order of magnitude higher than any other electrochemical exfoliation method which has been used so far for the preparation of graphene. The mechanism involved in the process is discussed. The graphene nanosheets showed a high oxidation temperature of 663 °C when heated in air at 40 °C min−1. The application of graphene nanosheets in Li-ion batteries, supercapacitors and ceramic-based composites is also discussed.

Keywords: Molten salts exfoliation, Graphene, Energy, Composites

**[P13.08]**

**Plasma functionalization of a 3D interconnected carbon structure - Aerographite**

J. Marx*[1], T. Schepers[1], K. Kröning[1], S. Garlof[1], D. Smazna[2], R. Adelung[2], K. Schulte[1], B. Fiedler[1]

*[1]Hamburg University of Technology, Germany, [2]University of Kiel, Germany*

The manufacturing of the 3D interconnected carbon structures, called Aerographite, is based on a two-step process. First, the template of zinc oxide (ZnO) is prepared in a flame transport synthesis (FTS) [1]. The conversion to a graphitic structure is carried out in the chemical vapour deposition (CVD) process [2]. These structures have a super hydrophobic character, which makes it difficult to use them for applications based on contact with water, e.g. supercapacitors. The application area can be extended by a functionalization treatment of Aerographite, in which the hydrophilic character can be reduced and at the same time the interfacial bonding to resin systems for polymer composites can be improved. The functionalization of carbon structures can be carried out either by the chemical or plasma functionalization. The plasma functionalization is a cost-effective and rapid treatment process, when compared to the chemical functionalization. The morphological characterisation of the samples was carried out by scanning electron microscopy with energy-dispersive X-ray microanalysis (SEM/EDX) and transmission electron microscopy (TEM). Further, the influence of the plasma treatment time on both, the electrical conductivity was investigated by custom designed 4-point measurement system and the hydrophobic character via the measurement of the contact angle. In addition the formation of defects was analysed via Raman spectroscopy and thermal gravity analysis (TGA). The electrical conductivity of these structures increase with increasing number of functional groups and at the same time the contact angle decreases. A change in the Raman spectra as well as in the temperature stability can be observed. Furthermore, the plasma treatment has an influence on the atomic structure of the carbon tetrahedrons.

References

[1] Y. K. Mishra, et al., Part. Part. Syst. Charact. 30, 775 (2013).

[2] Mecklenburg M., et al., Advanced Materials 24, 3486 (2012).

Keywords: CVD process, TEM, electrical conductivity, contact angle

**[P13.09]**

**Deposition of atomically dispersed noble metals on carbon materials**

U. Petek*[1,2], F. Ruiz Zepeda[1], P. Jovanovic[1], M. Bele[1], M. Gaberscek[1,2]

*[1]National Institute of Chemistry, Slovenia, [2]Faculty of Chemistry and Chemical Technology, Slovenia*

Carbon materials are a common support for metallic catalysts. Generally, the metal is dispersed on the carbon as nanoparticles. However, the metal can also be atomically dispersed and anchored on the carbon surface via ligands, functional groups or defects. In recent years, there has been increased interest in atomically dispersed noble metals as an alternative to nanoparticle-based noble catalysts. Despite the increased attention, our understanding of the structure, activity and stability of such supported single atoms is still poor.

In this contribution, wet chemical deposition of atomically dispersed noble metal on carbon supports will be described. The materials were characterized with aberration-corrected scanning transmission electron microscopy to confirm atomic dispersion of metal. Electrochemical properties of the materials were tested by the thin-film rotating disk electrode method and compared to nanoparticle-containing carbon materials. Thermal and electrochemical stability of the single atoms were also investigated.

Atomic distribution of metals on carbon support was obtained by adjusting the metal loading and conditions of the deposition. With increased loading metallic nanoparticles were formed in addition to the single atoms. Figure 1 shows an example of atomically dispersed Pt on porous N-doped carbon support. Comparison of the material before and after mild electrochemical treatment (100 potential cycles, from 0.05 to 1.0 V vs. RHE in 0.1 M $HClO_4$) suggests that single atoms do not aggregate or significantly dissolve under electrochemical conditions. Even after heating the material to 800 °C Pt remained atomically dispersed.

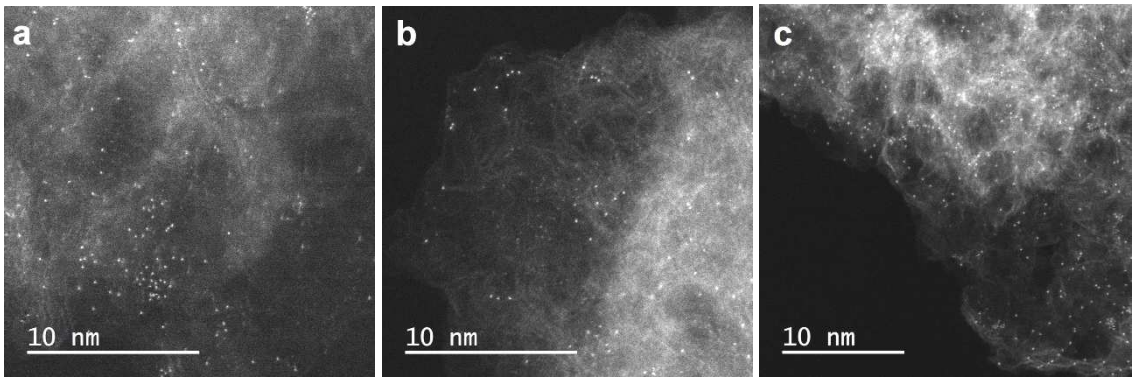


Figure 1. Atomically dispersed Pt on porous N-doped carbon heated to 400 °C for 1 h, shown before (a) and after (b) electrochemical cycling, and the same material heated to 800 °C for 1 h (c).

Our findings suggest that atomic distribution of noble metals can be readily obtained on various carbon supports. Single atoms were stable against aggregation under thermal treatment and electrochemical tests. In contrast to some recent reports and speculations, they displayed no electrochemical activity typical for metallic nanoparticles.

Keywords: single atom catalysis, carbon suport, electrocatalysis

**[P13.10]**

**Carbon nanostructers grafted biopolymers for medical applications**

P. Zakova*, N. Slepickova Kasalkova, P. Slepicka, V. Svorcik

*University of Chemistry and Technology, Czech Republic*

Enhancing biopolymers with carbon nanostructures leads to creation of attractive materials suitable for diverse medical application i.e. tissue engineering. We study surface properties and cytocompatibility of amine functionalized carbon nanoparticles (CNPs) grafted on biopolymer film. Poly-*L*-lactic acid and poly-3-hydroxybutyrate, in form of polymer films, were treated in an inert argon plasma discharge and, subsequently, grafted with three types of amine-functionalized carbon nanoparticles. The surface properties were studied using multiple methods (goniometry, X-ray photoelectron spectroscopy, atomic force microscopy). Cytocompatibility was studied *in vitro* by studying adhesion, proliferation and viability of vascular smooth muscle cells (VSMCs) from the aorta of a rat. Cell-substrate interactions on pristine and modified substrates were compared to standard tissue culture polystyrene (TCPS). Our results show that CNPs affect surface wettability, surface chemistry and morphology, and therefore adhesion, proliferation and viability of cultured cells.

Keywords: carbon nanoparticle, biopolymer, surface properties, cytocompatibility

**[P13.12]**

**Experimental manifestation of electrodynamical forbiddance of a strong quadrupole light - molecule interaction in methane and fullerene**

V.P. Chelibanov[1], A.M. Polubotko*[2]

*[1]State University of Information Technologies, Mechanics and Optics, Russia, [2]A.F. Ioffe Physico-Technical Institute, Russia*

As it is well known, the main feature of SERS, SEHRS and SEIRA, is appearance of strong forbidden lines in the spectra of molecules with sufficiently high symmetry. They are caused by so-called strong quadrupole light - molecule interaction, arising in surface fields strongly varying in space near rough metal surfaces. It is associated with the terms of light-molecule interaction Hamiltonian with so-called main quadrupole moments. However in molecules with cubic and icosahedral symmetry groups there is a factor $div\mathbf{E} = 0$ before the term of the light-molecule interaction Hamiltonian with the main quadrupole moment and the quadrupole interaction is forbidden. The forbidden lines must be absent and the enhancement of the spectra is caused only by the enhancement of the electric field. This weak enhancement of the SERS spectrum was observed in methane. The absence of forbidden lines associated with the vibrations with the irreducible representation $T_{1u}$ of the icosahedral symmetry group, which describes transformational properties of the dipole moments was observed in the SERS spectra of fullerene $C_{60}$. The enhancement factor of the spectrum was $\sim 10^4$ instead of the value $\sim 10^6$, characteristic for SERS. In addition one did not observe the forbidden lines caused by vibrations with the unit irreducible representation in the SEIRA spectrum of $C_{60}$. Of a special interest is observation of the SERS spectra of $C_{60}$ in the single molecule regime. Since the huge enhancement in this case is caused exclusively by the strong quadrupole light-molecule interaction, one must observe a significantly weaker enhancement because of the forbiddance of this interaction. The observed enhancement for $C_{60}$ was $\sim 10^8$ that is significantly lower than $\sim 10^{14} - 10^{15}$ characteristic for the usual one in single molecule SERS. Thus the above experimental results strongly support the SERS and SEIRA theories, based on the concept of the strong dipole and quadrupole light-molecule interaction.

Keywords: strong quadrupole light-molecule interaction, electrodynamical forbiddance, fullerene C60, SERS, SEIRA

**[P13.13]**

**Laser beam excitation to study transitions in fullerene molecule**

T.K. Subramaniam, P. Rajaraman, R Premanand*

*Sri Sairam Engineering College, India*

Infrared laser beam can be a good choice for studying the absorption and emission characteristics of Buckminsterfullerene molecule due to its strong absorption around 700-800nm region. Many scientists have already studied both photo physical and photochemical properties by ordinary methods of radiation. Even optical properties of Buckminster fullerene are well known. Buckminsterfullerene has much weaker inter-molecular forces than diamond, it has a much lower melting/boiling point and therefore less energy is required to break the forces of attraction. Since it is known to accept electrons, laser interactions with carbon atoms, can break the carbon bonds, creating more free electrons through excitation, resulting in transitions that can provide information on fluorescence properties or on formation of new compounds.

Keywords: Infrared laser;, inter-molecular, Photo physical, fluorescence;

**[P13.14]**

# An AFM, TEM, XRD and luminescence study of carbon nanomaterials obtained from cork industry wastewater

J.V. Prata*[1,2], O.C. Monteiro[3], A.J. Silvestre[1,3], A.S. Viana[3], A.I. Costa[1,2]
[1]*Instituto Politécnico de Lisboa, Portugal,* [2]*Universidade de Trás-os-Montes e Alto Douro, Portugal,* [3]*Universidade de Lisboa, Portugal*

*Quercus suber L. (cork oak)* contributes significantly to the economies of several European Union countries. The industrial processing of cork planks involves a cooking operation in which the textural and plastic properties of cork are improved. The resulting wastewater (ca. 400 L/ton of processed cork) is rich in water-soluble extractives, namely phenol- and polyphenol-based compounds and pectins. While the presence of these and other compounds usually defy several spent water treatment processes owing to their inherent poor biodegradability, they represent otherwise a huge opportunity to produce high-valued carbon-based materials.

Some of us have recently shown that luminescent carbon nanomaterials can be directly produced from cork industry wastewater [1], which displayed remarkable sensitivity/selectivity as protein biosensors [2].

Preliminary TEM analysis of the as-synthesized materials reveal that they mainly consist of spherical shaped particles, some of them fitting into the carbon-dot accepted sizes (< 10 nm) while others show much larger dimensions (up to 50 nm), probably as a result of aggregation. On the other hand, AFM results point to nanostructured carbon materials (C-dots) with typical heights below 3 nm. Moreover, aqueous solutions of these nanoparticles display an unusual and interesting behavior as they tend to self-assemble, being the phenomenon apparently modulated by temperature. The rationale behind the aforementioned features is nonetheless complicated by the presence of inorganic salts in the medium. Results from the studies conducted to tentatively ascertain the precise morphology of the C-dots mostly freed from inorganics, as well as the impact such changes induce on the self-assembling properties and luminescence of nanoparticles, will be further disclosed and discussed in this contribution.

Acknowledgments

We thank FCT/MCTES for financial support (UID/QUI/00616/2013, UID/MULTI/00612/2013 and UID/CTM/04540/2013).

References

[1] Provisional Portuguese Patent Application, nº109379, May 10th 2016.

[2] Provisional Portuguese Patent Application, nº109725, November 7th 2016.

Keywords: Carbon-dots, TEM, AFM, Luminescence

**[P13.15]**

# Highly sensitive and selective NO gas sensors using defect-induced single-walled carbon nanotubes with simultaneous polyethylenimine functionalization

J-Y. Jeon, T-J Ha, S.H. Kim, Y.T. Byun*
*Korea Institute of Science and Technology, Republic of Korea*

This work describes the development of a nanotechnology solution for the non-invasive detection and monitoring of diseases, such as asthma and chronic obstructive pulmonary disease (COPD), by identifying and measuring the concentration of nitric oxide (NO) in exhaled breath. NO is a known breath biomarker, correlating the amounts of NO in breath with various airway diseases [1]. However, NO-targeting diagnostic breath analysis based on NO detection and monitoring remains a challenge, primarily due to the lack of affordable NO sensors of high sensitivity and selectivity.

One-dimensional semiconductor nanostructures have attracted increasing attention due to their fundamental scientific interest and potential applications in a variety of functional devices. In particular, the large surface-to-volume ratio makes them highly sensitive in gas sensors. Among them, single-walled carbon nanotubes (SWCNTs) have a great potential as an ultimate candidate for highly sensitive gas sensors.

In order to enhance the selectivity and sensitivity of NO sensors, a SWCNT thin film with random networks was first formed on a thermally grown $SiO_2$ layer on top of a Si substrate using an air spray gun equipped with a 0.18 mm nozzle. Subsequently, we performed post annealing process to obtain defect-induced SWCNTs for improved sensitivity of NO sensors [2]. Finally, defect-induced SWCNTs were surface-treated by Polyethylenimine (PEI) to improve the selectivity of NO sensors. The sensing performances of both PEI- and defect-functionalized SWCNTs have been investigated. As a result, bi-functionalized SWCNTs exhibit high selectivity towards NO gas, compared to carbon monoxide, ammonia, benzene, and toluene. In addition, they show high sensitivity to 10 ppb of NO at room temperature.

Acknowledgment

This work was supported by the Industrial Strategic Technology Development Program (10047909) and the KIST Institution Research Program (2E27260).

References

[1] S.A. Kharitonov et al., American Journal of Respiratory and Critical Care Medicine, 163, 1693 (2001).

[2] Jaeseong Kim et al., Sensors and Actuators B, 228, 688(2016).

Keywords: single-walled carbon nanotube(SWCNT), defective SWCNT, SWCNT functionalized with PEI, nitric oxide sensor

**[P13.16]**

**Preparation of highly packed SWNT film using chitosan nanofiber for improved electrical and mechanical property**

C.K. Lee*, S.B. Lee, H.J. Kim, E.A. Shin

*Korea Institute of Industrial Technology, Republic of Korea*

Highly packed single-walled nanotubes (SWNT) film were prepared by solvent casting using chitosan nanofiber which was dispersed in water. The chitosan nanofiber offered an individually separated SWNTs without any surfactant that can form high concentrated SWNT solution and packed morphology of SWNTs mat. As the concentration of SWNT increases, highly packed SWNTs were like aligned SWNT mats. The further packed of SWNT produced a substantial improvement in the electrical conductivity (under 30 ohm/sq) and the specific capacitance of the resulting chitosan nanofiber/SWNT non-woven mats. Moreover, chitosan nanofiber/SWNT non-woven mats showed higher and flexible mechanical properties. It is concluded that the sensory non-woven mats are demonstrated to have excellent tailor-ability, electrochemical stability, and damage reliability. In this study, the morphology of the chitosan nanofiber-SWNT non-woven mat was characterized by scanning electron microscopy (SEM), transmission electron microscopy (TEM), atomic-force microscopy (AFM) and 3D laser scanning confocal microscopy.

Keywords: single-walled nanotubes, Chitosan, Nanofiber, composite film

**[P13.17]**

# Sorting of arc-discharge single-walled carbon nanotubes by selective dispersion with polymers

L. Scharfenberg*[1], M. Mertig[1,2]

*[1]Technische Universität Dresden, Germany, [2]Kurt-Schwabe-Institut für Mess- und Sensortechnik e.V. Meinsberg, Germany*

A single-walled carbon nanotube (SWCNT) is a cylindrical nanostructure consisting of a hexagonal lattice of $sp^2$-hybridized carbon atoms. The intrinsic electronic properties of SWCNTs enable a broad spectrum of applications, e.g. the use of SWCNTs as source-drain channels in field-effect transistors (FETs). For the assembly of FETs, however, the SWCNTs need to be semiconducting (sc). Consequently, the as-produced tubes have to be sorted according to their electronic properties prior to their application.

A fast method of sorting is the selective dispersion of SWCNTs with aromatic polymers, which structure is similar to the carbon lattice of the SWCNTs. The ordered alignment of the polymer on the SWCNT is defined by the tube diameter whereby only definite chiralities are effectively dispersed, leading to the desired sorting effect. To this aim, the polymer PFO-BPy was used to sort large-diameter SWCNTs with high efficiency [1, 2]. Here we have used the same polymer for the dispersion of arc-discharge CNTs (diameter: 0.9 nm - 1.6 nm) in organic solvent by tip sonication. The samples were characterized with UV/VIS spectroscopy (Figure 1) and the content of sc tubes was calculated from the amplitudes of the first derivative of the absorbance [3], which effectively allows to neglect the background of the absorption spectrum in the analysis.

We achieved an enrichment of sc-SWCNTs up to 99 %. A comparable treatment of the raw material with the anionic surfactant sodium cholate (SC) led only to an unsorted SWCNT dispersion. For the latter, a subsequent sorting step by density gradient ultracentrifugation was necessary to achieve an enrichment of sc-SWCNT of up to 98 %. Thus, the wrapping of SWCNTs with aromatic polymers is less technically complex, large scalable, and nevertheless, more efficient as other sorting methods. Additionally, photoluminescence measurements support our results and provide information about contained chiralities.

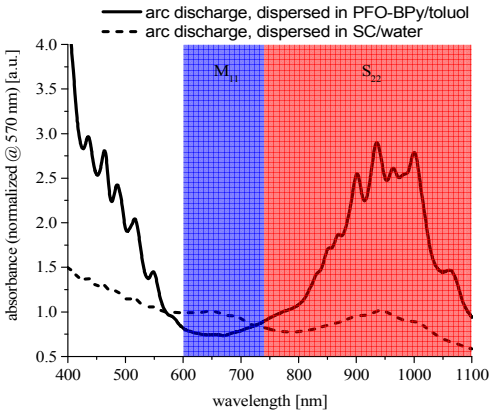


Figure 1: UV/VIS spectra of arc discharge CNTs dispersed in PFO-BPy/toluol (solid line) and in SC/water (dashed line) at similar sonication conditions. For a better comparison, the curves were normalized at 570 nm. The blue background area indicates the first metallic transition and the red background area indicates the second semiconducting transition.

[1] K. S. Mistry, B. A. Larsen, and J. L. Blackburn, ACS Nano **7**, 2231-2239 (2013).

[2] G. J. Brady, A. J. Way, N. S. Safron, H. T. Evensen, P. Gopalan, and M. S. Arnold, Sci. Adv. **2**, e1601240 (2016).

[3] L. Scharfenberg, and M. Mertig, Phys. Status Solidi A **212**, 1395-1398 (2015)

Keywords: sorting, single-walled carbon nanotubes, selective dispersion

**[P13.18]**

# Nanocalipers as novel molecular scaffolds for carbon nanotubes

N. Komatsu*, G. Liu, Y. Miyake
*Kyoto University, Japan*

We have been developing host–guest chemistry for separation of carbon nanotubes (CNTs) according to diameter, metallicity, and even handedness.

The host molecules named “nanotweezers” consisting of a rigid core and two receptors were designed and applied to CNT separation. To apply this methodology for separation of a wider range of CNTs with better selectivity, “nanocalipers” have been designed, which include a core, two corners, and two receptors. In this paper, we focus on “nanocalipers”, new host molecules next to the nanotweezers, from their molecular design and synthesis to CNT separation.

References

1. G. Liu, Y. Miyake, N. Komatsu* "Nanocalipers as novel molecular scaffolds for carbon nanotubes" Org. Chem. Front. (Review Article), in press (DOI:10.1039/C7QO00158D).

2. G. Liu, Y. Saito, D. Nishio-Hamane, A. K Bauri, E. Flahaut, T. Kimura and N. Komatsu* "Structural Discrimination of Double-Walled Carbon Nanotubes by Chiral Diporphyrin Nanocalipers", J. Mater. Chem. A, 2 (44), 19067-19074 (2014).

3. G. Liu, A. F. M. M. Rahman, S. Chaunchaiyakul, T. Kimura, Y. Kuwahara, and N. Komatsu,* "Bis(tert-butylpyrene) Nanotweezers and Nanocalipers: Enhanced Extraction and Recognition Abilities for Single-Walled Carbon Nanotubes", Chem. Eur. J., 19 (48), 16221-16230 (2013) [highlighted at the front cover].

4. G. Liu, F. Wang, S. Chunchaiyakul, Y. Saito, A. K. Bauri, T. Kimura, Y. Kuwahara, and N. Komatsu,* "Simultaneous Discrimination of Diameter, Handedness, and Metallicity of Single-Walled Carbon Nanotubes with Chiral Diporphyrin Nanocalipers", J. Am. Chem. Soc., 135 (12), 4805-4814 (2013) [highlighted in Chemical & Engineering News, 91 (12), p. 34, March 25, 2013].

Keywords: separation, molecular recognition, host-guest chemistry, handedness

**[P13.19]**

# Oxygen-functionalised carbon nanotubes for supercapacitors

E.T. Mombeshora*[1], P.G. Ndungu[2], A.L.L. Jarvis[1], V.O. Nyamori[1]
[1]*University of KwaZulu-Natal, South Africa,* [2]*University of Johannesburg, South Africa*

Several shaped carbon nanomaterials (SCNMs) are suitable materials for applications in energy conversion systems.[1] In particular, multiwalled carbon nanotubes (MWCNTs), have found applications in several energy devices such as dye sensitized solar cells,[2] bulk heterojunction organic solar cells[3] and supercapacitors.[4] Modification of physicochemical characteristics of MWCNTs by either composite synthesis or attachment of appropriate moieties are common strategies used to enhance their functionality in typical energy devices. The current work focused on modifying MWCNT walls with oxygen moieties by use of five different reagents and investigating the associated physicochemical properties. Oxygen-containing groups were introduced onto MWCNTs using an ultrasound water-bath treatment with $HNO_3$, HCl, $H_2O_2$ or HCl/$HNO_3$ solution. Physicochemical properties were thoroughly investigated by means of various techniques such as Fourier transform infra-red, Raman and electrochemical impedance spectroscopies; scanning and transmission electron microscopies; thermal gravimetric analysis; textural characteristics and cyclic voltammetry. The current study linked numerous physicochemical properties of oxygen-modified MWCNTs with their suitability as supercapacitor electrodes using group one sulfates. $HNO_3$ treatment introduced the highest oxygen-containing moieties and achieved highest specific capacitance in $Li_2SO_4$ and $Na_2SO_4$ electrolytes of 36.200 F $g^{-1}$ (77 times better than pristine) and 45.100 F $g^{-1}$ (2.5 times enhancement), respectively. For $K_2SO_4$ it was 33.600 F $g^{-1}$ (4.9 times better) with $HNO_3$/HCl treated samples. The dominating charge storage mechanism was pseudo and $Na_2SO_4$ was the best electrolyte amongst the three group one sulfates investigated.

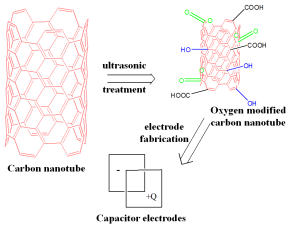


Fig. 1 The graphical abstract

---

1. W. Gu and G. Yushin, Wires energy environ, 2013, 3, 423-473.

2. E. T. Mombeshora, R. Simoyi, V. O. Nyamori and P. G. Ndungu, S. Afr. j. chem, 2015, 68, 153-164.

3. G. Keru, P. G. Ndungu, V. O. Nyamori and G. T. Mola, J Mater Sci: Mater Electron, 2015, 26, 9891- 897.

4. S. Hussain, R. Amade, E. Jover, E. Bertran, J Mater Sci, 2013, 48,, 7620-7628.

Keywords: electrochemical properties, multiwalled carbon nanotubes, group one sulfate electrolytes, oxygen-containing

**[P13.20]**

**Electrical performance of lightweight CNT-Cu composite wires and the impact of surface and internal Cu spatial distribution**

R. Sundaram*, T. Yamada, K. Hata, A. Sekiguchi

*National Institute of Advanced Industrial Science and Technology, Japan*

We report the fabrication of ultralong conducting lightweight multiwall carbon nanotube (MWCNT)-Cu composite wires by two-step Cu electrodeposition into industrial MWCNT wires. Further, we present the effect of Cu spatial distribution at composite wire surface and bulk on the overall electrical performance, including resistivity (ρ), temperature dependence of resistance, and stability to current measured as current carrying capacity (CCC). Our study shows that a continuous Cu matrix with homogeneous MWCNT distribution, i.e., maximum internal Cu filling *within* MWCNT wires, is critical to achieving high overall electrical performances. Composite wires with maximum internal Cu filling exhibit (i) low room temperature ρ, 1/100th that of the starting MWCNT wires, (ii) suppressed resistance-rise with temperature-increase and temperature coefficient of resistance (TCR) ½ that of Cu, and (iii) CCC 28% higher than Cu. In addition, due to the uniform distribution of MWCNTs with high volume fraction (~45 vol%) in a continuous Cu matrix throughout, the composite wire density is only 2/3$^{rd}$ that of Cu. Our MWCNT-Cu wires demonstrate real-world applicability with ease of soldering and integration into practical circuits with Cu wires. We believe that these lightweight MWCNT-Cu wires with optimal internal Cu filling and promising electrical performance are attractive as conductors for weight-reducing applications to supplement or replace Cu wiring. Additionally, the low TCR is specifically advantageous for stable and efficient high-temperature operation, e.g., in motor windings.

Keywords: CNT-Cu wires, Electrical resisitvity, Temperature coefficient of resisitance, current carrying capacity

**[P13.21]**

**Synthesis of highly-crystalline single-walled carbon nanotubes dispersed ink for construction of a planar field electron emitter**

S. Kumon*[1,2], N. Shimoi[1]

*[1]Tohoku University, Japan, [2]DOWA Holdings CO. Ltd., Japan*

Highly-crystalline single-walled carbon nanotubes (HC-SWCNTs) are known to exhibit excellent field emission electron source based on their high aspect structures with nano-ordered diameter [1]. However, the wet dispersion process resulted in a deterioration of the HC-SWCNT crystallinity; it is difficult to disperse isolated HC-SWCNTs in solution without including crystal defects due to the strong cohesion force of about 100 MPa that exists between individual SWCNTs [2]. Therefore, it is important to confirm the extent of SWCNT crystallinity deterioration during wet dispersion processes. In this work, we aim to clarify the relationship between the crystallinity and dispersibility of HC-SWCNTs to synthesize a homogeneous SWCNTs dispersion ink for a planar field emitter.

As a result of dispersion process using wet-jet milling, the SWCNTs result to dispersoid of 50 nm mode diameters with practical aggregation stability. We notice that thermogravimetric curve of the dispersed SWCNTs is very similar with its curve of the raw SWNCTs. It is suggested that the crystallinity of HC-SWCNTs did not deteriorate in the dispersion process. The observed relationship between crystallinity and concentration of HC-SWCNT dispersions prepared using a wet-jet milling process suggested that the degree of crystallinity could be controlled. We achieved a HC-SWCNT dispersion concentration whilst maintaining an extraordinarily high degree of crystallinity, which dispersion energy was higher than the cohesive energy depending on the high-order structure of the HC-SWCNTs. We have succeeded in obtaining SWCNTs ink for construction of a planar field electron emitter. Detailed relationships between the crystallinity, dispersibility and emission properties of the SWCNT emitter will be discussed at the symposium.

[1] Y. Saito, S. Uemura, “Field emission from carbon nanotubes and its application to electron sources”, Carbon, 38 (2) (2000), 169-182.

[2] Y.Y. Huang and E.M. Terentjev, “Dispersion of Carbon Nanotubes: Mixing, Sonication, Stabilization, and Composite Properties”, Polymers, 4 (1) (2012), 275-295.

Keywords: SWCNTs, electron source

**[P13.22]**

**A high-performance field emission x-ray tube with carbon nanotube emitters**

S. Park*[1], J.W. Kim[1], J.T. Kang[1], J.W. Lee[1,2], E. Go[1,2], H. Jeon[1,2], J.W. Jeong[1], Y.H. Song[1,2]
*[1]ETRI, Republic of Korea, [2]UST, Republic of Korea*

Field emission x-ray tubes with carbon nanotube (CNT) emitters have some advantages such as the ability to operate in fast digital operation, ease of size reduction and high-voltage insulation, and relatively compact system as compared to x-ray tube with thermionic emitters owing to the removal of heating elements. For achieving the commercial-level field emission x-ray tube, we need to obtain the highly stable and reliable emission characteristic of CNT field emitters avoiding degradation of the emitters. In this point of view, we have intensively investigated fully vacuum-sealed x-ray tubes with CNT emitters for several years [1-2] and successfully manufactured them. In the present study, we report the great improvement in vacuum sealed CNT field emission x-ray tubes enough to commercialize them to medical imaging application especially dental imaging. With the consideration of the required tube spec, we used a triode configuration with focus-functional gate [2] for independent control of the electron emission and acceleration in parallel with for obtaining small focal spot size. The manufactured CNT field emission x-ray tube had a length of 6 cm and an outer diameter of 1.5 cm, which is much smaller than the conventional thermionic x-ray tubes. We have obtained a quite good x-ray image of a human tooth by operating the CNT x-ray tube in an anode voltage of 65 kV, an emission current of 3 mA, and a pulse duration of 0.5 s, which is comparable to that of the conventional commercial thermionic x-ray tube. Furthermore, we performed lifetime test of the developed CNT x-ray tube which showed an excellent stability and reliability with x-ray shots more than 250,000 times, satisfying the commercial-level performances. We could confirm the superior properties of CNT field emission vacuum devices through the first demonstration of commercial level CNT x-ray tubes.

References

[1] J.-W. Jeong, J.-W. Kim, J.-T. Kang, S. Choi, S. Ahn, and Y.-H. Song, *Nanotechnology* **24**, 085201 (2013).

[2] J.-W. Jeong, J.-T. Kang, S. Choi, J.-W. Kim, S. Ahn, and Y.-H. Song, *Appl. Phys. Lett.* **102**, 023504 (2013).

Keywords: CNT, Field emission, X-ray tube

**[P13.23]**

# The planar field emission of SWCNTS bundle in atmosphere

C. Lin, J. Zhang*
*Peking University, China*

## Introduction

CNT is a formidable candidate of nano-electronic devices, sensors and interconnect wires [1]. As for striding into practicality, thorough characterizing the failure of CNTs is crucial [2]. Most of CNT-based devices work in atmosphere and FE must arise after CNTs breakdown. Almost all knowledge on field emission (FE) phenomenon is under the vacuum condition [3]. This paper reports the characterization of planar FE of SWCNTs in air.

## Method

Our samples are Au-SWCNTs bundle-Au structure on $SiO_2$/Si substrate (Fig.1a). The SWCNTs bundle was self-assembled by DEP (Fig.1b). Then, scanning voltage was applied to achieve SWCNTs breakdown (Fig.2). Thirdly, the samples with breaking point at the contact of SWCNT and Au were picked out by SEM as experimental samples. Finally, 0-100V scanning and current monitoring were carried out by HP4156B.

## Results

The typical I-V curve was shown in Fig.3. At low voltage, there is a 10-11A current rising linearly with voltage, being the leakage current between the SWCNTs bundle and substrate. Then, current rise with voltage non-linearly at the range of 10-9A to 10-7A, indicating the domination of FE current, but distinctly different from exponential curve predicted by F-N theory. The statistic result of the FE threshold voltage is shown as Fig.4. Samples with higher threshold voltage tend to have lower FE current.

## Discussion

Firstly, different from most CNT FE experiments, our samples have planar structure instead of vertical structure, which leads to larger leakage current before threshold voltage. Secondly, field emission in air is, without doubt, affected by multiple factors which make it deviate the FN theory. Thirdly, the Joule heating effect will result in the failure of the FE tips, in consequence, the FE current in air is much lower than that in vacuum. The successively failure and switch of the FE tips also bring about the multi-interval phenomena.

## References

[1] Xining Zang, Qin Zhou, et al, *Microelectronic Engineering,* vol. 132, pp. 192-206, 2015.

[2] Anshul A. Vyas, et al., *Interconnect Technology Conference,* pp. 203-205, 2016.

[3] Erich J. Radauscher, et al, *IEEE Transactions on Electron Devices*, vol. 63, pp. 3753-3760, 2016.

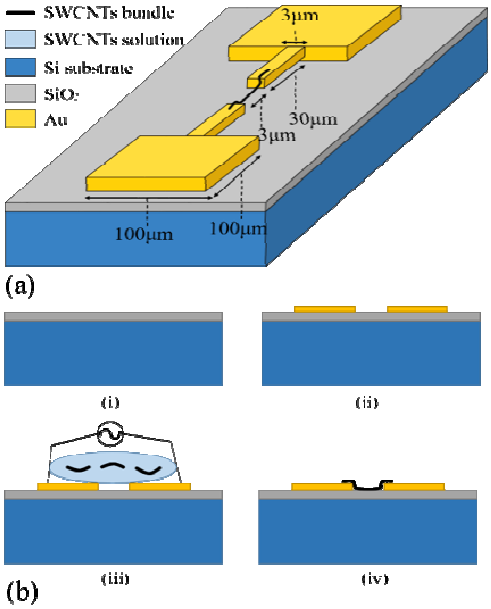


*Figure 1(a): A schematic diagram of the device; (b): The fabrication process flow of our device.*

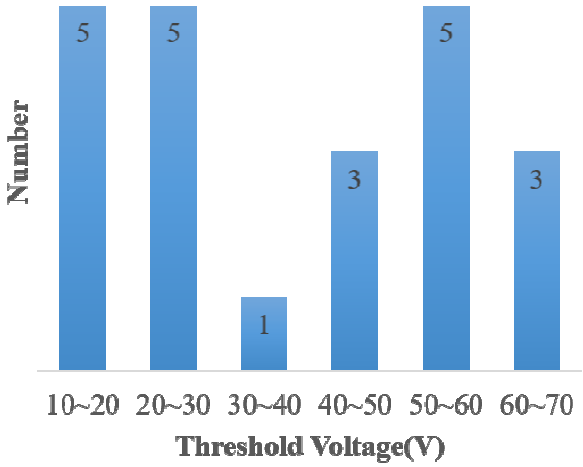


*Figure 4: A statistic result of the threshold voltage of the field emission domination.*

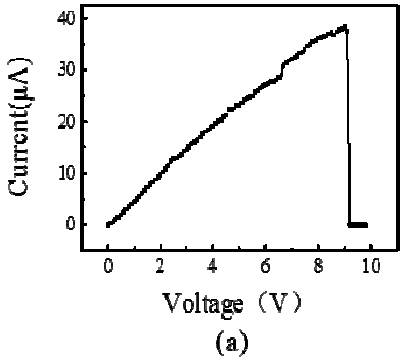


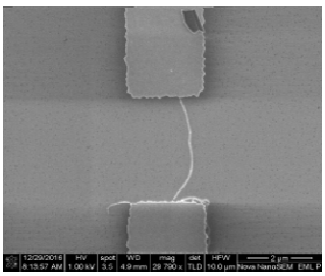


*Figure 2(a): I-V curve of the breajdown of the SWCNTs bundle; (b): The SEM picture of a sample broken at the contact with electrode.*

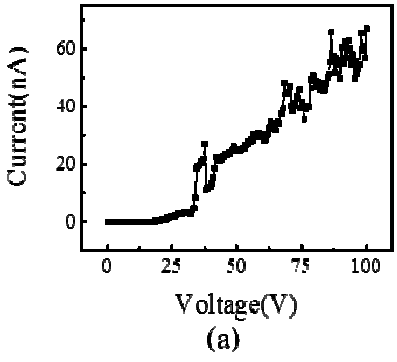


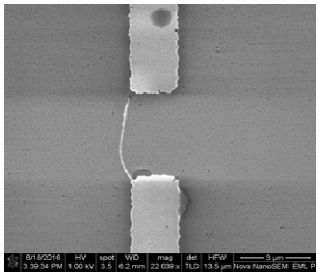


*Figure 3(a): I-V curve of the field emission experiment of a sample; (b): The SEM picture of a sample after field emission process.*

Keywords: SWCNTs, field emission, planar structure, atmosphere

**[P13.24]**

**n-Type CNTs/polymer hybrid for organic thermoelectrics**

Y. Shiraishi*, K. Oshima, Y. Yanagawa, Y. Du, N. Toshima

*Tokyo University of Science Yamaguchi, Japan*

The utilization of unused heat energy like natural heat and waste heat below 150°C has received much attention recently. In fact, two thirds of chemical energy from the fossil fuels has been discharged as heat energy without use. Thermoelectric technology is used to convert heat energy to electric energy and vice versa, which is an exciting technology to recover electric energy from the waste heat. In order to fabricate effective Π-form thermoelectric devices both positive-type (p-type) and negative-type (n-type) semiconductors are expected to be used for the fabrication. There are a few reports on n-type organic thermoelectric materials and they are usually unstable in air. Here, we report the considerable stabilization of n-type carbon nanotubes/hydrazine hybrid films by mixing a common polymer, poly(vinyl chloride) (PVC) and poly(vinylidene difluoride) (PVDF). The n-type carbon nanotubes were synthesized by dispersion of super growth carbon nanotubes (SG-CNTs) into hydrazine hydrate in NMP (*N*-methyl-2-pyrrolidone). The SG-CNT/Hydrazine/PVC hybrid films were fabricated by a simple method to drop-cast the mixtures on a glass substrate. To evaluate the air durability of SG-CNT/Hydrazine/PVC hybrid film, the samples were kept in air and the temporal change of the thermoelectric properties in air was measured. After 150 min Seebeck coefficients of n-type SG-CNT without polymer changed from -5.0 μV $K^{-1}$ to 7.0 μV $K^{-1}$. On the other hand, the SG-CNT/Hydrazine/PVC hybrid films were rather stable in air and kept negative Seebeck coefficient even after 28 days. The developed CNT/Hydrazine/Polymer hybrid films are expected to be novel hybrid organic materials for future thermoelectric devices, which could have advantages in terms of flexibility and long lifetime. We envisage that such materials could be applied for recovering electric energy from waste heat as well as providing electric resources for environmental sensors.

Keywords: Carbon nanotubes, Thermoelectric, Organic thermoelectrics, Negative-type semiconductors

**[P13.25]**

**Heat characteristics of carbon fiber heating elements coated by polyimide**

E.W. Son[1,2], D.U. Kim[1], J.W. Lim[2], K.S. Kim*[1] et al

*[1]Korea Institute of Industrial Technology, Republic of Korea, [2]Chonbuk National University, Republic of Korea*

Carbon fibers (CFs) are considered as materials of energy-saving heating elements because the CFs have several advantages such as short response time, space heating and electromagnetic shielding. However, due to the serious drawback of being easily oxidized in high temperature environments, actual applications have been limited to usage at low temperatures and vacuum environment. Conventional approaches to improve oxidation resistance are epoxy composite manufacturing and metal plating. These significantly reduce both heating temperature and far-infrared emissivity of CF heating elements due to their low electrical conductivity and poor far-infrared absorption, respectively. In this study, polyimide (PI) was coated to improve oxidation resistance and far-infrared emissivity. The thickness and surface roughness of PI coated on CFs were observed by field emission scanning electron microscopes and three-dimensional surface profiler, respectively. The heating temperature and far-infrared properties of the CF heating elements coated by PI were evaluated using thermocouple and Fourier transform infrared spectroscopy. The experimental results show that far-infrared emissivity decreases when surface roughness and thickness of PI coated on CF increase. Also, the CF heating elements coated by PI cause the changes in their heat flow and thermal conversion efficiency due to surface roughness and thickness of PI. Therefore, the CF heating elements coated by PI are expected to replace the conventional heating elements based on metal coils for high-temperature heaters.

Keywords: Carbon fiber, Polyimide, heating elements, Heat characteristics

**[P13.26]**

**Plasma treatment of graphene coated cotton cellulose for enhanced electro-conductive properties**

K. VinishaRani, B. Sarma*, A. Sarma
*VIT University, India*

Graphene oxide (GO) is synthesised using modified Hummer's method. The prepared GO are characterised using X-ray diffraction (XRD). Scanning electron microscopy (SEM) imaging of the synthesised GO reveals that it has sheet-like morphology. Initially, cotton fabrics are treated with dc glow discharge plasma to enhance the surface roughness property. Cotton fabrics are then functionalised by GO using a dip dry method. Finally, this coating is chemically converted by vapor reduction using hydrazine hydrate to reduced graphene oxide (rGO) for restoration of a high electrical conductivity at the fabric surface. The phase and functional group of the coated and uncoated fabrics are analysed by XRD and Fourier transform infrared spectroscopy. The surface morphology of the coated fabrics is analysed using SEM. Elemental analysis has been carried out using energy-dispersive spectroscopy. It confirms the presence of carbon along with cellulose on the surface of the fabric. The electrical conductivity of the fabricated cotton fibre is also investigated which depicts enhanced electrical behaviour. Our results provide a way to develop reduced graphene oxide (rGO) based devices for the biomedical applications for improving health care; smart textiles with the integration of sensors or various electronic items which may be employed for defence purpose too.

Keywords: rGO, Electrical conductivity, SEM, FTIR

**[P13.27]**

# Fast synthesis of 3D multilayer graphene nanoflakes by mesoplasma chemical vapour deposition

S. Wu*[1], Z. Lu[1], X. Chen[2], D. Wang[1], J. Sheng[1], J. Ye[1]
*[1]Chinese Academy of Sciences, China, [2]Tsinghua University, China*

Three-dimensional Multilayer Graphene nanoflakes (3D-MGNFs), also called vertically oriented graphene (VG), carbon nanowalls (CNW), are a special type of nanostructure that are oriented vertically on a substrate. These carbon nanostructures have received a great attention for the application of energy storage (e.g. super capacitor and Li ion batteries), filed emitters, gas- and bio- sensors, due to their unique features such as large surface-to-volume ratio, sharp edges, and vertical morphology. They are also attractive as they can be fabricated without the use of catalysts, although the growth mechanism is still not well understood.

Many techniques have been employed to synthesize MGNFs, such as microwave plasma chemical vapor deposition (CVD), direct current glow discharge plasma CVD, inductively coupled plasma CVD with a planar-coiled antenna. However, the growth rate is on the order of 10 μm/h and a rapid growth process for such films is expected for their mass applications.

In this work, we report a new plasma based technology for the rapid and controllable growth of MGNFs by means of mesoplasma CVD. Due to its high atomic H density and high carbon atom flux, a 12-μm-thick branched film has been synthesized in 2 minutes from Ar-$H_2$-$CH_4$ mixture, corresponding to a growth rate of 360 μm/h, which is about one order faster than that of the conventional technologies. These branched films have been confirmed to be the 3D-MGNFs by SEM, Raman, and TEM analysis. Each of these nanoflakes is consisted of 5-25 graphene layers. By increasing the dilution ratio of $H_2$/$CH_4$, these branched nanostructures can be controlled to be vertically oriented as the second nucleation on the growth site can be suppressed. This fast and controllable growth process for the 3D-MGNFs is suggested to be effective for their mass application.

Keywords: multilayer graphene nanoflakes, mesoplasma chemical vapor deposition, fast rate synthesis, controllable structure

**[P13.28]**

# Investigation of carbon nanoparticles processing by sublimation

A.A. Kovalchuk*[1,2], A.V. Prikhodko[1], N.N. Rozhkova[2], O.I. Konkov[1,3]

*[1]Peter the Great St. Petersburg Polytechnic University, Russia, [2]Institute of Geology Karelian Research Centre Russian Academy of Sciences, Russia, [3]Russian Academy of Sciences, Russia*

Carbon nanoparticles have unique properties. At present, there are many ways of the nanoparticles production.

The main goal of this project was to apply of the sublimation method to natural carbon and to study its structural features.

The subject of the study was a thin powder of shungite type I from Shun'ga deposit (Russia). The particle size of the powder was 0.01 - 1 μm.

On completion of the sublimation process a carbon film was formed on the substrate.

The evaluation of structural features was carried out by Raman spectroscopy (RS). The study of the morphology of the film was conducted by scanning electron microscopy (SEM).

It was found that the main peaks of the RS of the film coincided with the RS spectra of shungite carbon nanoprticles in the stable aqueous dispersion, but the G-band of the RS of the film was biased towards lower frequencies, that was characteristic of the starting shungite powder.

When the RS of the film was compared with the RS of the starting powder, it could be pointed out that there was strong broadening of the D- and G-bands, while the ratio of maxima of the intensities decreased considerably.

It could be inferred that the structures of carbon in the film and in the dispersion did not differ.

The SEM study showed the presence of carbon nanoparticles forming a deformed net. An average particle size ranged from 50 to 100 nm, which was consistent with the results of dynamic light scattering for the aqueous dispersions of carbon nanoparticles.

The film could be regarded as a new nanocarbon object. The main difference of carbon in the film from nanoparticles of aqueous dispersion was the absence of the hydration component. It was for the first time when the basic elements of shungite carbon could be picked out without water.

Keywords: carbon, film, Raman scattering, scanning microscopy

**[P13.29]**

**The influence of processing conditions on the structure and properties of 3D graphene**

C. Banciu*, A. Bara, M. Lungulescu, V. Marinescu, A. Teisanu, D. Patroi

*National Institute for Research and Development in Electrical Engineering ICPE-CA, Romania*

Graphene is a distinctive two-dimensional carbon material, which was recognized for its special physical, chemical, optical and electrical properties. Graphene has high mobility and optical transparency, in addition to flexibility, robustness and environmental stability. Thus, graphene has true potential in photonics and optoelectronics.

The use of graphene involves some experimental constrains related to their planar structure, which could be overcome by using their 3D counterpart. Such 3D graphene structures have a large specific surface area, which in combination with the unique properties of graphene have the potential to be useful in the field of optoelectronics.

3D graphene foam was prepared by using nickel foam as the template in a CVD process at ambient pressure and 1000°C with methane as carbon source at different deposition times. The obtained 3D graphene was investigated by scanning electron microscopy, which brought out a continuous structure and by Raman spectroscopy in order to evaluate the influence of deposition time on the thickness of the graphene layer. The 3D graphene obtained by CVD are single-layer and multi-layer-graphene that are free of defects.

In order to obtain the freestanding 3D graphene, we proceeded to nickel foam etching in hydrochloric acid. After nickel removing, the 3D graphene was characterized by scanning electron microscopy and energy dispersive X-ray analysis, in order to evaluate the rate of nickel removal. In addition, we used Raman spectroscopy in order to evaluate the influence of etching process to the freestanding 3D graphene structure. 3D graphene structures were also characterized in terms of specific surface area, thermal and electrical conductivity.

In conclusion, 3D graphene foam was obtained by CVD on nickel foam substrate at different deposition times. After nickel foam removal, freestanding 3D graphene was characterized by different techniques. Such materials could be further used in optoelectronic applications.

Keywords: 3D graphene, CVD, optoelectronics

**[P13.30]**

**Macroporous hybrids of ZnO and 3D graphene: a new material for electrode technologies**

L.M. Veca*[1], F. Nastase[1], C. Banciu[2], C. Pachiu[1], R. Popa[1], T. Sandu[1], C. Romanitan[1], A. Dinescu[1]

*[1]National Institute for Research and Development in Microtechnologies - IMT Bucharest, Romania, [2]National Institute for Research and Development in Electrical Engineering ICPE-CA, Romania*

For efficient energy storage and conversion, electrode materials represent a prevalent bottleneck that attracts extended design and synthesis research.

The favorable optoelectronic, photocatalytic and fluorescent properties of zinc oxide, combined with the large specific surface area of graphene when remodeled as a defect-free 3D network, suggest a promising pathway towards the development of hybrid structures with improved electrical and photocatalytical properties.

The main technological challenge for the realization of these hybrids is the bottom-up growth of the active metal oxide materials directly on the graphene surface. In this context, we have used nickel foam as both catalyst and scaffold for the 3D graphene growth to obtain uniform and high-quality coverage. Subsequently, the resulted structure was covered with a thin film of ZnO in an atomic layer deposition (ALD) process.

Robust and highly porous 3D-graphene networks were grown on nickel foam by thermal CVD, using methane and hydrogen, at 1000°C and atmospheric pressure. The SEM analysis confirmed the formation of a continuous graphene network which replicates the structure of the nickel foam and structural characterizations revealed the presence of both single and multi-layer graphene with insignificant defect formation. Notably, the 3D graphene shell preserved the network structure even after the complete chemical etching of the nickel scaffold. Subsequently, after a thorough hydrophobicity adjustment of graphene surface, a thin zinc oxide film was deposited by ALD. Surface morphology, as well as crystallinity of the ZnO films deposited on the surface of the 3D graphene network have been investigated by SEM and X-ray diffraction, respectively. The importance of the surface chemistry for a successful coverage with continuous and robust thin ZnO films will be underlined.

In conclusion, combining 3D growth of CVD graphene with conformal ALD-deposited ZnO films we prepared self-supported, mesoporous ZnO-3D graphene hybrids that show good promise for various electrode applications.

Keywords: 3D graphene, ALD ZnO deposition, hybrid

**[P13.31]**

**Preparation of graphene flake thin film by kinetic spraying of graphite powder**

D.M. Chun*[1], M.N.E.A.A. Nasim[2], M.M.M. Mohammed[1], W.S. Chu[3], S.H. Ahn[3], C.S. Lee[1]

*[1]University of Ulsan, Republic of Korea, [2]RMIT University, Australia, [3]Seoul National University, Republic of Korea, [4]Hanyang University, Republic of Korea*

Carbon-based materials such as graphite, graphene, carbon nanotubes, and carbon fibers play an important role in today's technology. Recently, the graphene flake structure has attracted great interest to researchers in a variety of applications. Some methods such as chemical vapor deposition have been reported in the preparation of graphene flake thin films, but have limitations such as the use of high temperature, toxic chemicals and small deposition areas. This work demonstrates the formation of graphene flake thin films directly from graphite particles using kinetic spraying at room temperature. A nano-particle deposition system, which is a one of kinetic spray method commonly used for the deposition of metals and ceramics, has been introduced to deposit graphite particles. Graphite powder was deposited on a copper substrate without using a binder and the deposited thin film was characterized. The deposited thin film was evaluated using scanning electron microscope, X-ray diffraction and Raman spectroscopy, and showed a small, few-layer graphene flake structure. We also propose a mechanism in which a small number of graphene flake structures are formed during thin film preparation. The proposed mechanism was interlayer separation of micron sized graphite particles and cracking of particles into small pieces during deposition due to the high impact velocity of the graphite particles.

Keywords: Graphene flake thin film, Kinetic spraying, Nano-particle deposition system, Graphite powder

**[P13.32]**

**Possible nature of SERS on graphene**

V.P. Chelibanov[1], S.A. Ktitorov[2], A.M. Polubotko*[2], Y.A. Firsov[2]

*[1]State University of Information Technologies, Russia, [2]A.F. Ioffe Physico-Technical Institute, Russia*

At present it is well known that there is SERS on graphene, which is named as GERS. The GERS enhancement coefficient is $\sim 10^2$. The most accepted opinion is that GERS is determined by the "chemical" enhancement mechanism. In addition researchers note the existence of the first layer effect, which one associates with this mechanism or with the direct interaction of the molecules with the substrate. However we demonstrated in our previous works that the "chemical" mechanism in SERS has a pure electrodynamical nature and is associated with very large difference in the strength of the electromagnetic field in the first and the second layers of adsorbed molecules. As it is well known graphene is a very conductive material and is not an ideal plane. There are so-called ripples, which are a roughness as a matter of fact. Therefore there is a full analogy in the reasons of classical SERS and GERS. As it is well known strong SERS arises on silver rough surfaces, which have a very high conductivity. Therefore from our opinion GERS arises due to enhancement of the electromagnetic field on the tops of these ripples, and due to a very high conductivity and mobility of electrons in graphene. Those fact that graphene is not a bulk material but only a single atomic layer results in a weak enhancement, compared with usual SERS. As it is demonstrated from experiments on GERS, usual Raman scattering and infrared absorption on pthalocianine molecules ($H_2Ph$) the quadrupole interaction in GERS is very low and does not manifest practically.

Keywords: SERS, graphene, ripples

**[P13.33]**

# Nanocrystalline graphene: theoretical and practical investigations of its potential for plasmonic applications

T. Sandu*, A. Avram, C. Pachiu, M. Veca, R. Popa

*National Institute for Research and Development in Microtechnology - IMT-Bucharest, Romania*

Nanocrystalline graphene (NCG) films are increasingly investigated for their promise to replace transferred graphene in electronic and MEMS/NEMS applications[1-5]. Films of controllable thickness and viable mechanical[2,4,8,9], as well as optical/electronic properties[1,2,5-7,9] are successfully deposited on various substrates, enabling unlimited freedom for micro/nano-patterning.

As NCG films grown directly on dielectric present superior processability when compared to graphene, they have the potential to become a more practical plasmonic material, provided that they are able to offer also graphene's low-losses advantage, according to the high carrier mobility. In fact, carrier mobilities of NCG films attained [$cm^2V^{-1}s^{-1}$] values of: 2.49 [3], 10 [10], 40 [11] or 90 [6], but are reaching as high as 720$cm^2V^{-1}s^{-1}$ [12], close to those of graphene nanodots and nanoribbons (≈/≥1000$cm^2V^{-1}s^{-1}$).

We have grown NCG films on insulating substrates showing tunable morphologies, spectroscopical and electrical properties and we will present theoretical and practical investigations on their usage as viable plasmonic materials.

Experimentally, NCG films of various $I_D/I_G$ ratios have been grown on insulating substrates (Figs.1,2) at low-temperature (600°C) in a capacitively coupled, dual-frequency plasma CVD, using Ar-rich/$CH_4/H_2$ mixture. Estimated grain sizes varied between ~7-17nm and proved controllable by gas pressure, substrate temperature, HF/LF power proportion, and Ar concentration.

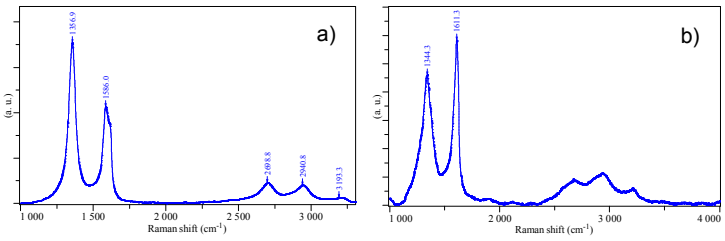


Fig.1 - HR Raman spectra (488nm/1mW excitation) of nanographene samples: a) $P_{RF}$ 300W, 10sccm $CH_4$/190sccm/Ar, 300mTorr, 600°C, $I_D/I_G$=1.7; b) $P_{RF}$ 300W, $P_{LF}$ 20W, 10sccm $CH_4$/20sccm $H_2$/360sccm/Ar, 4500mTorr, 600°C, $I_D/I_G$=0.8.

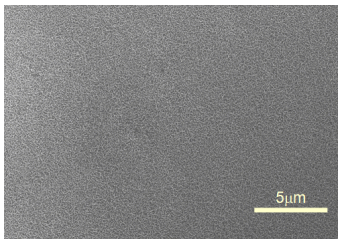


Fig.2 - Typical SEM micrograph of synthesized NCG films.

On the theoretical side, we use a figure-of-merit that characterizes the *localized plasmon resonances* (LPR) on nanoparticles, represented by the ratio between plasmon resonance

frequency and the damping constant ($\gamma$). This FOM takes the form $\omega_p \sqrt{1/2 - \chi_j} \big/ \gamma$ for Drude-like metals, where $\omega_p$ is the bulk plasma frequency and $\chi_j$ is an eigenvalue of the electrostatic operator defined on the boundary of the nanoparticle[13]. Damping constants as high as ~100fs were measured in case of LPRs in graphene dots, at a mobility of 780cm$^2$V$^{-1}$s$^{-1}$[14]. Based on the findings in [12] and [14] we assume that, at optical frequencies, graphene nanodots and NCG nanoparticles might behave similarly.

Numerically, we considered a 4.5nm diameter graphene disk and an NCG nanoparticle as a cylinder of the same diameter. Based on our method[13], we simulated the corresponding LPRs (Fig.3), where we observe that, unlike the graphene nanodots, the NCG nanoparticles exhibit LPRs for both polarizations of the electric field, thus providing richer plasmonic features and greater flexibility in the design of plasmonic devices. Investigative ellipsometry and angle-dependent light reflection measurements on NCG films will be presented.

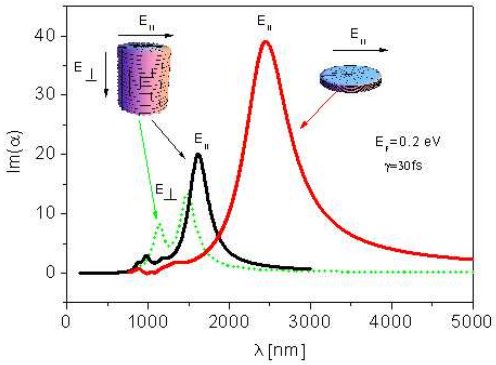


Fig.3 - Volume normalized polarizability of a graphene dot and of a NCG nanoparticle. The arrows indicate the field polarizability.

[1] L.Zhang, Nano Res. 4(3):315, 2011.

[2] W.Yang, et al., Small 8:1429, 2012.

[3] M.E.Schmidt, et al., Mater. Res. Express 1, 2:25031, 2014.

[4] J.Sun, et al., Nanoscale 8(12):6659, 2016.

[5] Q.Zhang, et al., Carbon 111:1, 2017.

[6] N.Kurra, et al., Nanotechnology 23:425301, 2012.

[7] G.Kalita, et al., RSC Adv.2:3225, 2012.

[8] S.J.Fishlock, et al., Microelectronic Engineering 159:184, 2016.

[9] A.Riaz, et al, Nanotechnology 26:325202, 2015.

[10] N. Lindvall, et al., Micro & Nano Lett., 7, 8:749, 2012.

[11] J.Sun, et al., J.Appl.Phys 111:044103, 2012.

[12] N.-E.Weber, et al, Carbon 112:201, 2017.

[13] R. C. Voicu, T. Sandu, Proc. R. Soc. A 473: 20160796, 2017.

[14] Z. Fang et al., ACS Nano, 7: 2388, 2013.

Keywords: Nanocrystalline graphene, Plasmonics

**[P13.34]**

**Flexible conducting films based on multiple layer graphene (ultrathin graphite) nanobelts**

S.A. Moshkalev*[1], A.R. Vaz[1], M.A. Canesqui[1], A. Alaferdov[1], G.M. Trindade[2], U. Lima[2], A.S. Souza[2]

*[1]UNICAMP, Brazil, [2]Nacional de Grafite Ltda, Brazil*

In this study we prepared and characterized a series of thin flexible free standing conducting films (also known as buckypapers) with thickness ranging from 15 up to 100 microns. Buckypapers were prepared using a vacuum filtering process from a liquid solutions of thin graphite (graphene) nanobelts in isopropanol. Nanobelts were supplied by Nacional de Grafite Ltda and have thickness ranging from 10 to 50 nm and high aspect ratios (length/width ~10, length/tickness ~1000). Systematic study of buckypapers (BPs), as well as fabrication of BP based devices, requires development of reliable technologies for successive preparation, manipulation, contacting and measurements of electrical and thermal properties. Here the buckypapers were characterized as deposited and after pressing (~1000 kgf/cm$^2$). The best results were obtained for medium thickness of BP (~60 microns), with the values for electrical and thermal conductivities of 200 microOhms-cm and 1400 W/m.K, respectively, comparable with best results reported in the literature.

Keywords: multilayer graphene, graphite nanobelts, electrical and thermal characterization, buckypaper

**[P13.35]**

# Facile synthesis of graphitic carbon-coated nanopowders for EMI shielding and thermal diffusion

D.H. Ko, H.B. Na*
*Myongji University, Republic of Korea*

## 1. Introduction

The market of personal electronic devices has been growing with the advent on virtual reality and augmented reality which facilitates the development of wearable devices. Electronic devices, in particular, miniaturized or wearable devices need efficient electromagnetic interference (EMI) shielding, and thus metals such as copper and nickel and magnetic materials have been used as EMI shielding enclosures or films. The development of high performance and miniaturized devices has brought another important issue, the heat diffusion, because the concentrated heat damages customers as well as devices. Graphite film is popularly used as a heat emitter for electronic devices due to their quick thermal diffusion because of high anisotropic conductivity along length and width (X-Y-direction). Here, we report the synthesis of metal-carbon composites consisted of metal nanoparticles with EMI shielding and carbon matrix with high heat diffusion.

## 2. Method and Results

Ni nanopowders were mixed with sucrose aqueous solution. After evaporation of water at 100 □, resulting paste was heated to 160 □ for caramelization. The as-synthesized material was carbonized under $N_2$ atmosphere at 900 □. The nanopowders were characterized by XRD, TEM and Raman spectroscopy. Characterization results confirmed that prepared nanopowders have composite structures of metal Ni and graphitic carbon.

## 3. Discussion

Graphitic carbon-coated nanopowders were synthesized by a simple carbonization of sucrose. Graphitic carbon was prepared at low temperature by catalytic effect of metal nanoparticles. This facile synthesis can offer scalable process to prepare multi-functional materials of EMI shielding and thermal diffusion for various personal electronic devices.

Keywords: Metal nanopowders, Graphitic carbon

**[P13.36]**

## High temperatures processing of thin graphite nanobelts

S.A. Moshkalev*[1], A. Alaferdov[1], R. Savu[1], M.A. Canesqui[1], N. Rozhkova[2], Y. Kopelevich[1], R.R. Silva[1], G.M. Trindade[3], U.B. Lima[3], A.S. Souza[3]

*[1]UNICAMP, Brazil, [2]KRC RAS, Russia, [3]Nacional de Grafite Ltda, Brazil*

Ultrathin graphite nanobelts (obtained from Nacional de Grafite Ltda, Brazil) were thermally processed in a neutral atmosphere. Samples were treated at medium temperatures (1500C) for 10 minutes and at high temperatures (up to 2950C) for 5 seconds. The nanobelts were obtained by liquid phase chemically assisted exfoliation and have following dimensions: thickness 10-50 nm, width 2-5 microns, length 10-50 microns. Analysis of XRD-spectra showed that original samples consist predominantly (up to ~ 70 %) of the turbostratic graphite (t-graphite). After thermal processing at 1500C strong restructuring of graphite to higher crystalline quality Bernal (H-graphite) stacking and rhombohedral (Rh-graphite) structures was observed. Further increase of the temperature of thermal treatment (up to 2950C), even for shorter times, leads to increasing part of H-graphite up to ~ 80 % (part of Rh-graphite decreases down to ~ 20 %). Analysis of Raman spectra of the thermally treated sample showed also improving crystalline structures as evidenced by changes of FWHM of G-band from 30 $cm^{-1}$ to ~ 20 $cm^{-1}$ and decreasing ID/IG ratios from 0.39 to 0.15. Further, by employing the vacuum filtration of graphite nanobelts (GNBs) suspensions, free standing thin films of nanobelts (buckypapers) were prepared from original and thermally treated samples. Electrical measurements were performed to reveal that sample resistivities decrease strongly with thermal processing, down to ~100 microOhms-cm, also confirming the improvement of samples crystallinity.

Keywords: multilayer graphene, graphite nanobelts, electrical and structural characterization, buckypaper

**[P13.37]**

**Gas jet deposition of diamond structures by thermal activation inside of cylinder**

A.K. Rebrov*, M.N. Andreev, T.T. Bieiadovskii, A.A. Emelyanov, K.V. Kubrak

*Kutateladze Institute of Thermophysics, Russia*

A new method of diamond structures deposition by activation of carbonaceous gas mixtures on extended surfaces has already been described in sufficient details [1, 2]. Recently, the authors had being conducted systematic experimental studies to synthesize crystals and films from a mixture of hydrogen and methane, depending on temperature of activating surfaces, substrate temperature, mass flow of hydrogen, percentage of methane and the pressure in the vacuum chamber. During the film deposition on the molybdenum surface, a strong dependence of the film morphology on the temperature of the tungsten surface was observed in the range of 2040 - 2140□C, which is explained by changing of atomic hydrogen concentration. The optimal substrate temperature was defined. The value of the pressure in the reaction zone of the vacuum chamber corresponding to maximum deposition rate was determined. First time for this method experiments on the diamond deposition were conducted on the seed crystals grown by the HPHT method. The most difficult task was to find optimal structure of the interlayer between diamond and steel substrate for its friction properties to improve. As a result of the experiments, ways of minimizing the carbidization of the activation surfaces were found. The general conclusion is that for all indicators, except scaling, the method is surpasses the widely used HWCVD technology.

This work was supported by the Russian Science Foundation (grant № 15-19-00061).

[1]. A. K. Rebrov, M. N. Andreev, T. T. B'yadovskiy, K. V. Kubrak, and I. B. Yudin. The reactor–activator for gas-jet deposition of diamond structures // Rev. Sci. Instrum. – 2016. Vol. 87 – P. 103902:1-8. DOI: 10.1063/1.4964704.

[2] A. K. Rebrov. Gas jet deposition of diamond structures by thermal activation on an extended surface // Diamond & Related Materials 72 (2017) 20–25.

Keywords: gas jet deposition, diamond structure, thermal activation

**[P13.38]**

**Stress and defects distribution around crystal junction in diamond mosaics: Mapping with confocal Raman spectroscopy**

G. Shu*[1], B. Dai[1], V. Ralchenko[1,2], A. Khomich[2,3], E. Ashkinazi[2], A. Bolshakov[1,2], K. Liu[1], J. Zhao[1], J. Han[1], J. Zhu[1] et al

[1]*Harbin Institute of Technology, China,* [2]*General Physics Institute RAS, Russia,* [3]*Institute of Radio Engineering and Electronics RAS, Russia*

Preparation of diamond mosaics, CVD diamond films homoepitaxially grown on seed single-crystalline (SC) diamond substrates oriented and arranged in close proximity, is one of the ways to produce large-area SC diamond plates [1]. Although the quality of the main part of such mosaics could be high, the structure of the material grown in the junction area between the crystals typically is defected, and reveals a significant stress [1,2]. Therefore, the study of defects and stress distribution within the crystal junctions is important to obtain reliable growth of large-area mosaics. In the present work we used a high resolution Raman mapping of stress and defect abundance both in cross-section and on growth surface of (100) oriented mosaic crystals, in order to monitor how the junction region evolves with the growth process.

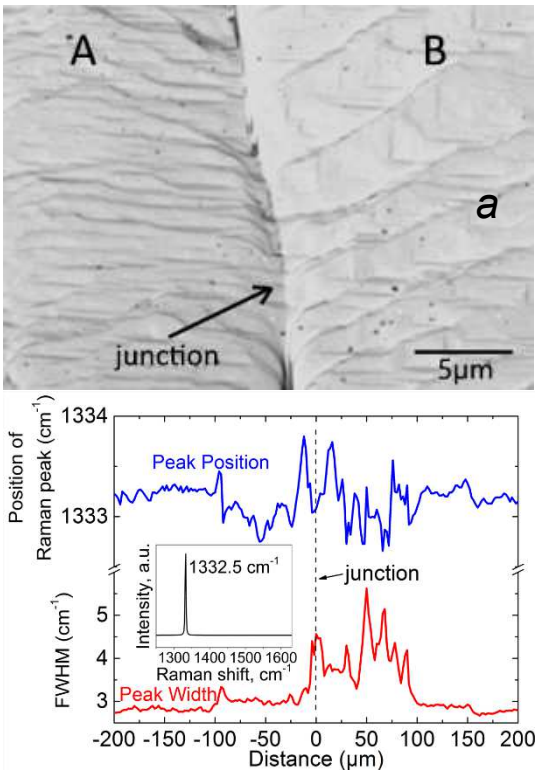


We found the existence of a zone with enhanced stress and defects around the junction between crystals A and B (Fig. 1*a*) as evidenced from Raman peak shift and broadening (Fig. 1*b*). A monotonic increase of the width of defected and strained zone, extending up to several hundred microns, with the film thickness was observed. The stress distribution forms a complex pattern, often asymmetric, the stress building up to 0.7 GPa within this zone. In some samples, however, the stress zone as narrow as ~ 30μm was observed. The results are further complemented with SEM and XRD characterization of the CVD diamond mosaics.

[1] H. Yamada, et al. Diam. Relat. Mater. 57 (2015) 17

[2] G. Shu et al. J. Cryst. Growth 463 (2017) 19

Keywords: stress and defects, mosaic diamond, microwave plasma CVD, Raman spectroscopy

**[P13.39]**

**Alteration of diamond crystals types depending on the metal-solvent composition and growth temperature at HPHT crystallization**

V. Lysakovskyi*, T. Kovalenko, S. Ivakhnenko et al
*Institute for Superhard Materials NAS of Ukraine, Ukraine*

Transitions metals, such as Fe, Co, Ni, were reported as solvents for diamond crystallization. But search for new solvents remains an important topic to modify properties of grown diamonds.

Diamond growth experiments were performed in a high-pressure apparatus of the "toroid" type at 5.5-6.0 GPa and 1380-1420 °C in a Fe-Co-Ti(Zr)-C system and at 7.5-7.7 GPa and 1700-1900 ° C in Fe-Al-Mg-C system.

It is known that diamond crystals grown in the Fe-C system are type Ib with nitrogen content up to 600 ppm. Doping Fe-C system with cobalt in an amount of 45 at. % does not change the crystal type but the nitrogen content in crystals decreases to 30-35 ppm. Adding to Fe55-Co45 alloy Ti(Zr) an amount up to 2.7 (1.25) at. % leads to reduce the concentration of nitrogen up to 18-23 ppm. Increase the Ti(Zr) content up to 3.6 (2.25) at. % allows to changing crystal type Ib→IIa.

Doping Fe–C system with Al and Mg up to ~ 6 at. % and 9.2 at. %, respectively, does not change the type of crystals, they contain nitrogen in an amount of ≥28 ppm, but when these concentrations increase to 8 at. % Al and 10 at. % Mg the crystals type modify to type IIa. Doping this system with ≥30 at.% Mg leads to growing semiconducting type IIb crystals without the addition of boron or boron-containing compounds.

Doping of the Fe-C growth system with Mg, Ti, Zr allows a significant change in the defect-impurity content and the type of diamond crystals. All these features can be explained by the change in the thermodynamic activity of the main impurities in the diamond crystal lattice (nitrogen and boron) on crystallization front depending on the composition of the growth system and the growing temperature.

Keywords: Diamond, crystal, alloy-solvent, thermodynamic activity

**[P13.40]**

**Development conditions for cube and octahedron faces of diamond single crystals**

V. Lysakovskyi*, O. Hutsu, S. Ivakhnenko et al
*Institute for Superhard Materials NAS of Ukraine, Ukraine*

The development diamond single crystals of the cube and octahedron faces depends on the solvent composition and the growth temperature.

The present investigation was carried out for diamond single crystals which were grown with solvents Fe – Ni, Fe – Ni – Sn (6 – 16 at.%) and Fe – Ni – Pb (1,5 – 11,5 at.%) by the temperature gradient method. Pressure and temperature for research were 5.8 – 6 GPA and 1385 – 1425 oC, respectively; growth time was from 50 to 80 hours. The structurally perfect crystals of Ib type had mass 0.2 – 0.3 ct and size 3 – 3.5 mm.

Using Fe – Ni as a solvent, the ratio between cube and octahedron face was 65 : 35 (%), increasing temperature from 1385 °C to 1460 °C, this ratio was changed to 73 : 27 (%).

Solvent Fe – Ni – Pb (11 at.%) provided the relation of cube faces development about 79 and 86 % at temperature 1385 – 1420 oC, respectively.

For Fe – Ni – Sn alloys (12 at.%), the ratio between the development degrees of cube and octahedron faces was 85 % at temperature 1385 °C; temperature increase to 1425 °C led to the cube faces development up to 96%. A further temperature increase to 1470 °C led to a decrease in the degree of the cube face development to 72%.

Thus, diamond single crystals growth using solvents in the Fe – Ni → Fe – Ni – Pb → Fe – Ni – Sn sequence, led to an increase in the degree of development of the cube faces. Research showed that alloy doping Fe – Ni with tin and lead makes it possible to grow diamond crystals at a temperatures 1420 – 1425 °C, which cube faces is developed 86 – 96 %.

Keywords: Diamond, octahedron faces, cube faces, alloys

**[P13.41]**

# Double - layer model for T - gradient method of diamond growth

A. Burchenia, V. Lysakovskyi*, S. Ivakhnenko et al
*Institute for Superhard Materials NAS of Ukraine, Ukraine*

Structurally perfect single diamonds crystals are grown by Strong-Wentorf temperature gradient method in one growing layer with application of high pressure devices. The development of high pressure equipment led to the creation of high-pressure machines with volume of working space ~ 500 cm3 and there was a possibility of increasing growing layers for this kind of machines. In order to use multi-layer model one needs to precise control of temperatures and temperature gradients. Therefore, the implementation of multi-layer models is challenging.

Our investigations with usage of high pressure device type “toroid” conducted by us earlier, show that the main conditions for growing single diamond crystal in double – layer system is that the temperatures and temperature gradients in the region of seed crystals must be 1400 ºC ± 30 ºC, 4 – 6 0C/mm respectively.

To conduct the present study was used 6 – anvil high pressure device model CS VII with volume of working space about 180 cm3. In the process of designing the growth cells was used the finite element method. This method allowed to optimize the growth cell dimensions parts and choose the necessary configuration of resistive heating system. Calculations of the temperature distribution were performed for each of the growth layer and for entire workspace. Results of the calculations showed that temperature gradients in the growth layers would be 5 – 7 ºC/mm , the temperature in a region of seed crystals would be 1390 – 1410 ºC.

As a result of the experiments were received single type IIa diamond crystals where the average weight for each layer was about 14 ct, the average weight of a single crystal was about 0.7 ct. Study by the method of IR-spectroscopy showed that the nitrogen content in crystals is less than 5 ppm.

Keywords: Diamond, high pressure equipment, growth layer, alloys

**[P13.42]**

**High-speed deposition of uniform diamond coatings on wc-co milling cutters in ac glow discharge plasma**

S.A. Linnik*, A.V. Gaydaychuk, V.V. Okhotnikov

*Tomsk Polytechnic University, Russia*

We report about the development of new PACVD reactor for high-speed uniform diamond deposition on 3D cutting tools (milling cutters, drills). In this reactor, plasma lines are used for gas activation like the hot filaments in HFCVD reactors. Our construction allowed minimizing the plasma edge effect which usually resulted non-uniform heating of cutters in all other plasma CVD systems. The growth rate of polycrystalline diamond film in such reactor reached 10 μm/h. The opportunity of construction the film with multilayer structure is also shown. The uniformity of deposition was tested for milling cutters with a diameter 6-16 mm and cobalt content 6-10 %. We also studied the impact of argon addition, deposition pressure, methane content and volt-ampere characteristics. This system is characterized by high stability and growth rate of diamond films, simplicity of scaling potential. In the long term, this system can become a serious competitor of HFCVD systems for cutting tools deposition.

Keywords: Glow discharge plasma, High-speed deposition, WC-Co cutting tools, uniform coating

**[P13.43]**

**Complementary analysis of macro- and micro-stress in (111)-oriented heteroepitaxial diamond by X-ray diffraction and µ-Raman spectroscopy**

B-C. Gallheber*, M. Fischer, M. Mayr, J. Straub, M. Schreck
*University of Augsburg, Germany*

For homoepitaxial as well as for heteroepitaxial growth, the (001) surface represents the preferred crystallographic orientation for the synthesis of high quality single crystal diamond. Despite its several drawbacks like significantly lower growth rates and increased structural instability towards defect formation, growth of (111)-oriented diamond has attracted great interest, especially in the context of doping. High level p-type boron doping, n-type doping by phosphorous and the formation of epitaxial heterojunctions between diamond and wurtzite type compound semiconductors are current fields of research. Additionally, its potential for the construction of neutron monochromators is under investigation.

In the present work, heteroepitaxial growth of diamond on Ir(111) surfaces by microwave plasma chemical vapor deposition (MWPCVD) has been studied. Ir/YSZ/Si(111) substrates with different off-axis angles & directions have been used and gas composition as well as substrate temperature have been varied. The resulting macro- and micro-stresses have been analyzed and compared using X-ray diffraction (XRD) and µ-Raman spectroscopy, respectively.

Highly anisotropic stress states showing a pronounced variation with off-axis parameters and process conditions have first been measured by XRD. Well-defined orientations of the principal axes of the stress tensors have been found. The strain tensors derived from XRD were used to calculate the shift in phonon frequencies even for complex stress states. These predictions were then compared with measurements of the diamond Raman line position in order to investigate the potential of Raman spectroscopy for the analysis of tri-axial stress states.

Maps of width and absolute position of the diamond Raman line show clear correlations with surface topographic structures. They provide deeper insight into the mechanisms that control defect incorporation and interaction between the surface and threading dislocations during growth on (111) surfaces.

Keywords: heteroepitaxy, (111) orientation, iridium, stress

**[P13.44]**

**Impact of the methane hydrogen ratio onto deposition temperature, growth rate and residual stress in an atmospheric laser-based plasma CVD process**

M. Prieske*[1], S. Müller[2]

*[1]BIAS - Bremer Institut für angewandte Strahltechnik GmbH, Germany, [2]Carl von Ossietzky Universität Oldenburg, Germany*

Polycrystalline diamond coatings are highly promising for various applications in the industrial sector due to its outstanding properties. They are for example deployed for heat sinks in electrical circuits because of the high thermal conductivity or as coating on tools due to high hardness. In this study the process window for diamond deposition of a laser-based plasma chemical vapour deposition (LaPlas CVD) process without a chamber at atmospheric pressure was characterized. Polycrystalline CVD-diamond coatings were deposited onto tungsten carbide. The methane hydrogen ratio was varied from 0.2 % to 5.0 % and the temperature range experimentally investigated in which the diamond coating is growing. The diamond coatings were examined by Raman spectroscopy, laser scanning microscopy and scanning electron microscopy (SEM). The results showed, that the deposition temperature can be lowered significantly by lowering the methane hydrogen ratio. This leads to a decrease of residual compressive stress which is detected by the shift of the diamond peak in the Raman spectra. The advantage of the high methane hydrogen ratio is the high growth rate of the diamond coating of higher than 30 µm/h. This study shows in detail the influence of the methane hydrogen ratio to the deposition temperature, the growth rate and the regarding residual compressive stress in an atmospheric LaPlas CVD process.

Keywords: polycrystalline diamond, residual stress, growth rate, atmospheric

**[P13.45]**

**Evaluation of PAni deposition time on the PAni/diamond/CF ternary composite performance**

L.M. Silva, D.A.L. Almeida, S.S. Oishi, A.B. Couto, N.G. Ferreira*

*National Institute for Space Research - INPE, Brazil*

The energy demand has increased dramatically over the last few decades due to the intensive urbanization that has taken place. Electrochemical energy storage devices have been emerging as potential substitutes for the fossil fuel energy, since they are rechargeable and environmentally friendly. Among them, supercapacitors play an important role in the technological evolution since they have high power density, which makes them preferred over batteries in a wide range of applications. In addition to carbon based electrode materials widely used in supercapacitors, intrinsically conducting polymers, such as polyaniline (PAni), are emerging as electrode materials for this purpose. Therefore, this work presents the production and characterization of the PAni/B-doped diamond/carbon fiber (CF) ternary composite, aiming its application as electrode for supercapacitor device. Diamond films were grown on CF in two different morphologies, boron doped nano and microcrystalline diamond (BDND/BDD) films. PAni deposition times were varied for 30 and 60 min in order to improve the composite responses for both films morphologies. For PAni synthesis, BDD/CF and BDND/CF samples were immersed in NaCl/HCl solution with distilled aniline. An aqueous solution of $(NH_4)_2S_2O_8$ in NaCl/HCl was used as oxidant. FEG-SEM images showed the differences on the amount of PAni deposited for each condition. Raman and FTIR analyses confirmed the PAni deposition in its conductive form, for all electrodes. TGA analyses exhibited the samples thermal behavior, highlighting the diamond film influence on the ternary composite. Electrochemical characterizations allowed studying the PAni deposition time as well as the diamond morphology influences. Diamond grain size influence was better observed on samples prepared for 30 min. However, electrodes prepared for 60 min presented higher current density and capacitance response associated to greater charge storage capacity and lower charge transfer resistance.

Keywords: Composite, Diamond, Polyaniline, Carbon Fiber

**[P13.46]**

# Lattice sites and annealing of radiation damage in Fe implanted natural and CVD diamond

K. Bharuth-Ram*, D. Naidoo, H.P. Gunnlaugsson, R. Mantovan, G. Weyer
[1]*Durban University of Technology, South Africa,* [2]*University of the Witwatersrand, South Africa,*
[3]*Ubiversity of Iceland, Iceland,* [4]*5Laboratorio MDM, IMM-CNR, Italy*

Conventional doping of single crystalline diamond, during growth or by diffusion, is hampered by its metastability as well as the low mobility of potential dopants in the lattice. Ion implantation, therefore, has been investigated as an alternative means to incorporate dopant atoms into the diamond lattice. However, lattice damage which is invariably produced and the resulting compensating defects and lattice strain in the neighbourhood of the dopants must be annealed out before diamond based semiconductors can be realised.

In this contribution we report on use of $^{57}$Fe Mössbauer spectroscopy, following the implantation of radioactive parent $^{57}Mn^{+}$ ions, to investigate the lattice sites of the implanted probe ions and the annealing of implantation induced lattice damage in a natural and a CVD diamond.

Radioactive $^{57}$Mn+ ions ($T_{1/2}$= 85.4 s) were produced at the ISOLDE facility at CERN by 1.4 GeV proton-induced fission in a heated $UC_2$ target and element selective multi-photon laser ionization. The Mn ions were implanted with 60 keV energy into a natural type IIa diamond and a CVD diamond, held at 300–1100 K. The Mn parent isotopes are found to be implanted into defect sites of non-cubic symmetry, which anneal partially with increasing temperature during the $^{57}$Mn lifetime. The annealing of implantation damage and the lattice sites of the probe ions have been tracked with emission Mössbauer spectroscopy measurements on the 14.4 keV □-rays emitted by the $^{57}$Fe daughter nuclei populated in the $^{57}$Mn □-decay.

The lattice damage is found to anneal more rapidly in the CVD diamond than in the natural diamond, with approx. 30% of the Fe ions located at defect-free substitutional sites and approx. 5 % on interstitial sites after annealing at temperatures above 900 K.

Keywords: Diamond, Fe ion implantation, lattice sites, Emission Mossbauer Spectrosocpy

**[P13.47]**

**Conformal nano-crytalline diamond growth at low temperature using micro-wave antennas at low pressure by chemical vapour deposition**

O. Antonin*[1,2], M. Gabureac[1], L. Petho[3], R. Schoeppner[3], D. Rats[4], J. Michler[3], P. Raynaud[5], T. Nelis[1]

*[1]Berne University of Applied Science, Switzerland, [2]Toulouse University, France, [3]EMPA, Switzerland, [4]NEOCOAT, Switzerland, [5]University of Toulouse, France*

Nano crystalline diamond deposition [1] at low substrate temperature (< 350 °C) has several potential industrial applications [2]. However, one crucial issue is the possibility of deposition NCD films on substrate with a complex shape with high the highest possible 3D conformity. The work presented here concentrates on this important aspect.

We present results on the NCD growth on 3D features (trenches with different aspect ratio) obtained by standard photolithography and dry etching (Bosch process) on a Si wafer. Prior to deposition, the substrate was seeded with 5 nm diamond crystals. NCD was deposited using 4-7 Hi-Wave coaxial elementary sources each connected to a 200 W micro-wave power generator (both Sairem, France) [3], using a gas mixture (50 Pa) of $H_2$, $CH_4$ and $CO_2$. Discharge conditions as gas concentration, plasma power densities and substrate temperature directly influence the NCD growth and morphology. The NCD character of the films was confirmed using Raman spectroscopy (Fig. 1), XRD and TEM.

Trenches as deep as 100 µm and with aspect ratio as low as 1:10 (Fig. 2), as well as the sidewalls (including scallops) were fully covered by NCD, with thickness variations scaling with the solid angle opening. This proves that, while the seeding process cover the entire surface, the CVD growth was mass transport limited. The 3-D conformity obtained using the array of micro-wave sources is compared to results obtained by hot filament CVD deposition.

The results demonstrate for the first time the NCD deposition at low temperature on 3D structured substrate. The aspect ratios are compatible with requirements of the MEMS, watch and med-tech industry. Work on the adhesion of NCD films deposited on stainless steel is on-going in our laboratories.

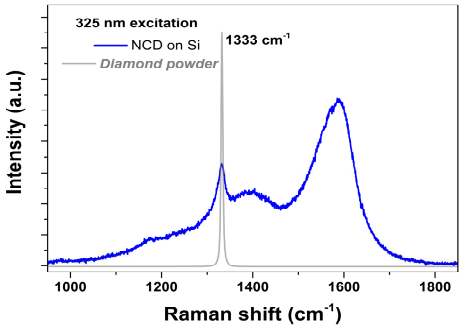


Figure 1. NCD on Si and reference.

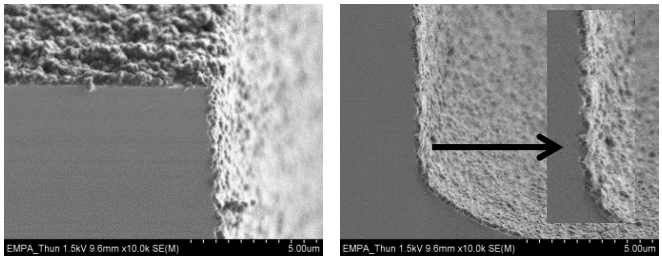


Figure 2. NCD on 3D trenches,

a) top, b) bottom and zoom in insert.

1. Mehedi, H.A., et al., Low temperature and large area deposition of nanocrystalline diamond films with distributed antenna array microwave-plasma reactor. Diamond and Related Materials, 2014. **47**: p. 58-65.

2. Baudrillart, B., et al., Nanocrystalline diamond films grown at very low substrate temperature using a distributed antenna array microwave process: Towards polymeric substrate coating. Diamond and Related Materials, 2017. **75**: p. 44-51.

3. SAIREM, SAIREM - US-2014-0197761-A1. 2014.

Keywords: Nano-Crystalline Diamond, Low Pressure, Low Temperature, 3D Conformal

**[P13.48]**

**Surface pre-treatments of diamond HPHT (100) substrates for P- epitaxial layer growth**

C. Barbay, J-C. Arnault* et al
*CEA Saclay, France*

Diamond is a promising candidate for high power-electronic applications. However, electronic properties of diamond films are directly impacted by the HPHT substrate quality. Indeed, they contain structural defects like dislocations which could propagate into the diamond epilayer. Additionally, substrate polishing step induce defects over a depth of several microns and leave polishing lines at the surface which strongly influence the diamond layer crystalline quality (1). Surface pre-treatment is needed to remove dislocations in the defective subsurface to better control the early stages of growth of diamond epilayers.

We investigate the etching of diamond substrates via a mixture of Ar/O2 performed in a RF-sputtering PVD system. The pre-treatment efficiency in terms of etching rate and surface smoothing was studied versus the Ar/O2 ratio, the gas pressure, the applied power. The Ar/O2 plasma provides a high-speed etching rate (9 um/h) and decreases RMS roughness according to AFM measurements.

The efficiency of this pre-treatment to improve the crystalline quality of a Sumitomo Ib (100) substrate was confirmed by High Resolution XRD and X-ray reflectometry. The HRXRD pattern showed a significant reduction of the diffuse scattering due to initial subsurface damages. A comparative study was led using optimized conditions of etching on two half-etched substrates from different producers (Sumitomo Ib and New Diamond Technology IIa). Both substrates were characterized by Raman Spectroscopy and Cathodoluminescence to confirm the enhancement of the surface crystalline quality. Then, a plasma H2/O2 was applied to reveal the emerging dislocations at the surface through the formation of etch pits in order to estimate the dislocation densities by image analysis.

Finally, the crystalline quality of low boron doped thin layers grown on etched substrates was studied and compared with as-received substrates. Crystallinity improvement should increase transport properties of such p- layers involved in the architecture of a diamond MOSFET for power electronics applications.

(1) A. Tallaire et al. Identification of Dislocations in Synthetic Chemically Vapor Deposited Diamond Single Crystals. Crystal Growth and Design, American Chemical Society, 2016, 16 (5), pp.2741-2746.

**This project has received funding from the European Union's Horizon 2020 Programme under Grant Agreement no. 640947 (Greendiamond).**

Keywords: etching, dislocations, single-cristal, growth

**[P13.49]**

**Observation of cross sections of bulk single-crystal diamond with millimetre thickness**

H. Yamada*, Y. Asahara, S. Ohmagari, A. Chayahara, Y. Mokuno

*AIST, Japan*

For industrial use of single-crystal diamond, especially in the field of the electronic devices, inch-sized wafers with sufficient quality are indispensable. While wafer process has been developed to some extent, such as the lift-off process [1], techniques to prepare large seed crystals and to improve the quality still have some problems [2]. To understand the mechanism for improvement in the crystal quality during the growth, in this study, bulk single crystal diamond with millimetre thickness were grown by using plasma CVD and their cross sections were studied.

The right figure shows the structure of the prepared sample with 2.2mm thick in total, whose substrate at the bottom is 0.2mm, and the intensity distributions of the cathode-luminescence with 430 nm wavelength (band-A) [images (a-d)]. Horizontal dashed lines show the boundaries of the repetitive growth. The images (a) and (d) [(b) and (c)] were taken at the cross section without [with] the boundaries, whose surface layer with several micrometers thick was etched after polishing. Several line segments can be observed in all images. The line-segment density in the image (a) is higher than that in the image (d). If we assume that the distribution is isotropic on the plane perpendicular to the measured plane, the densities of the line-segments at (a) and (d) are roughly estimated to $6\times10^5$ and $3\times10^4/cm^2$, respectively. On the other hand, the image (c) seems more discontinuous structure than that of the image (b). This might be attributed to the differences in the growth conditions for the substrate [(d)] and the other overgrown layers. Above observations indicate that the importance to maintain the growth conditions between the substrate and the overgrown layers.

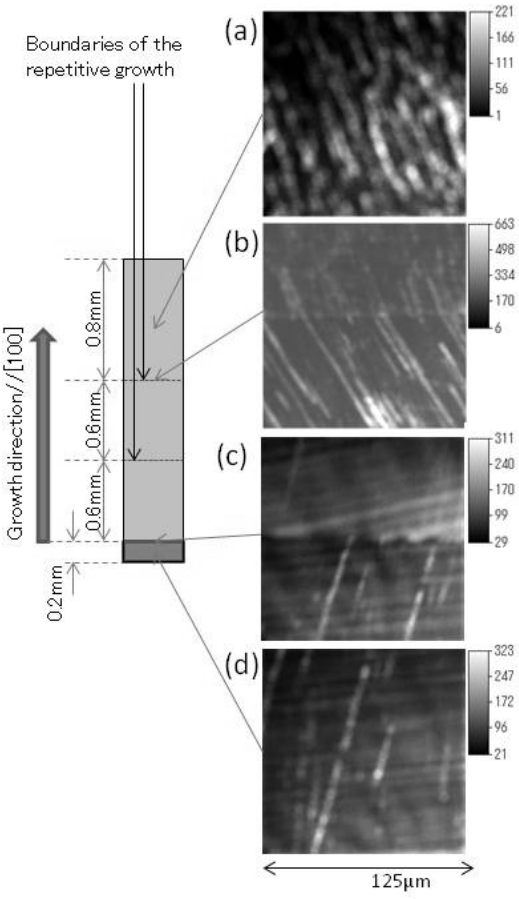


References

[1] Mokuno, et al., Appl. Phys. Lett. 104 (2014) 252109. [2] Feng, et al., Diamond Relat. Matter, 19 (2010) 1453.

Keywords: microwave plasma, cathode-luminescence, bulk crystal

**[P13.50]**

**Spectroscopic ellipsometry of nanocrystalline diamond film growth**

E. Thomas[1], S. Mandal*[1], A. Ahmed[2], E. Macdonald[1], T. Dane[3], J. Rawle[4], C. Cheng[2], O. Williams[1]

*[1]Cardiff University, UK, [2]National Dong Hwa University, Taiwan, [3]University of Bristol, UK, [4]Diamond Light Source, UK*

With the increased interest in the use of thin film diamond in a wide range of applications from micro-electro-mechanical systems to tribological coatings, compositional and structural analysis of the initial stages of diamond growth is required in order to optimise the growth conditions used. Unlike conventionally used characterisation techniques including Raman spectroscopy, X-ray photoelectron spectroscopy, scanning electron (SEM) and atomic force microscopy (AFM), spectroscopic ellipsometry (SE) has robustly demonstrated the quantitative estimation of the composition of diamond films with varying depth [1, 2]. The aim of this study is to therefore use SE to investigate the optical, compositional and structural properties of nanocrystalline diamond films during the early stages of growth.

To this end, a series of nanocrystalline samples of varying thickness (25-75 nm) were grown on nano-diamond seeded (100) silicon wafers. Characterisation with SE was performed within the spectral range 200-1000 nm using a simple 4-layer model to account for the surface roughness, grain boundary $sp^2$ and void fraction within the bulk, and SiC layer thickness at the interface with the Si substrate. With such a model the seeds and individual islands atop a 5-9 nm SiC layer are observed, before continued growth leads to coalescence at a thickness of ~30 nm as indicated by a reduction in the void content. The subsequent peak in non-diamond content from the addition of grain boundaries is then corroborated with Raman, while the increasing thickness of the surface roughness layer arising from columnar growth is validated with AFM, demonstrating the applicability of SE to the initial stages of diamond film growth. Lastly, the evolution from nano-diamond seeded Si to film was studied with SEM and x-ray diffraction.

1. J. Mistrik et al., Thin Solid Films 571, 230-237 (2014).

2. B. Hong et al, Diam Relat Mater 6 (1), 55-80 (1997).

Keywords: Ellipsometry, Nanocrystalline Diamond, NCD

**[P13.51]**

**Approach to the large-scale diamond synthesis using in-liquid microwave plasma CVD process**

Y. Sakurai*[1], Y. Harada[1,2], C. Terashima[1], H. Uetsuka[1,2], N. Suzuki[1], K. Nakata[1], K. Katsumata[1], T. Kondo[1], M. Yuasa[1], A. Fujishima[1] et al

*[1]Tokyo University of Science, Japan, [2]Asahi Diamond Industrial Co., Ltd., Japan*

Diamond (including boron-doped diamond) is a versatile material as cutting tools and electrodes. Thus, development of effective growth method is needed. In the last decade, a unique method of diamond growth from organic solvents called as “in-liquid microwave plasma CVD (IL-MPCVD)” has been studied [1]. The growth rate of diamond by IL-MPCVD exceeds 100 μm/h, however, growth area is limited by size of electrode (3-5 mm in diameter). To expand application field, it is essential to develop a method for uniform and large-scale diamond film.

Fig. 1 shows a schematic of IL-MPCVD system. Organic solvents are vaporized and decomposed at the apex of electrode by microwave plasma. Diamond films were deposited on substrate from mixture of MeOH and EtOH with or without tetra hydro furan (THF) at 60 kPa with microwave power of 440 W. In addition, the system has an XY substrate stage moving horizontally.

At first, effect of solvents was considered in order to achieve uniform diamond film. Fig. 2 represents summary of Raman measurements. Diamond film with THF tend to show higher crystallinity with a small disperse. On the other hand, quality of diamond film without THF is scattered and sometimes no diamond was grown.

Fig. 3 shows photographs of diamond film grown with or without the stage movement from MeOH and EtOH with THF. A large diamond growth area of 6 x 6 $mm^2$ was achieved along the stage moving. As shown in the SEM images taken at certain position on the large diamond film (Fig. 4), diamond grain size depends on its location. However, both (111)-oriented grains indicate growth condition was rather uniform.

In the current presentation, effect of solvents and uniformity of large-scale diamond film will be discussed in detail.

Reference

[1] Y. Harada *et al.*, *Diamond Relat. Mater.* **63** (2016) 12.

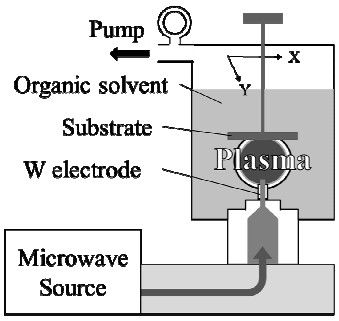


Fig. 1 A schematic of IL-MPCVD system.

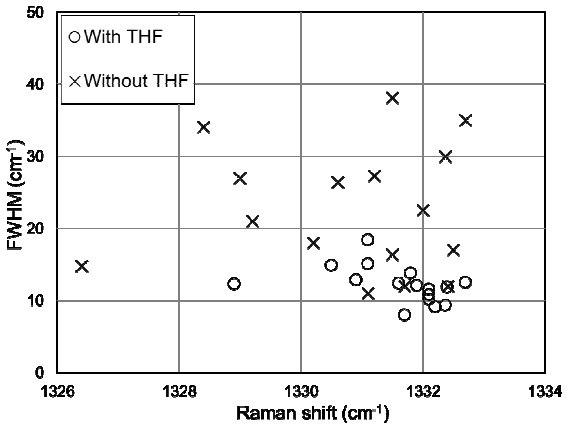


Fig. 2 Summary of Raman measurements.

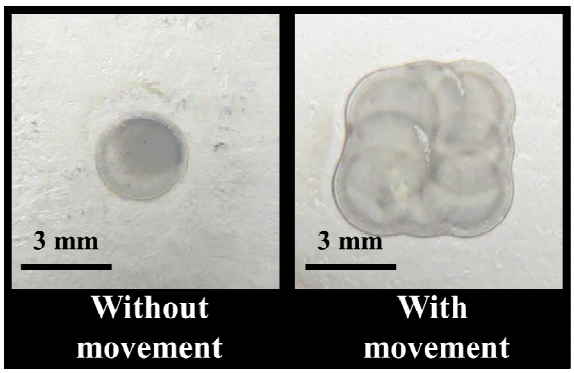


Fig. 3 Photographs of diamond film

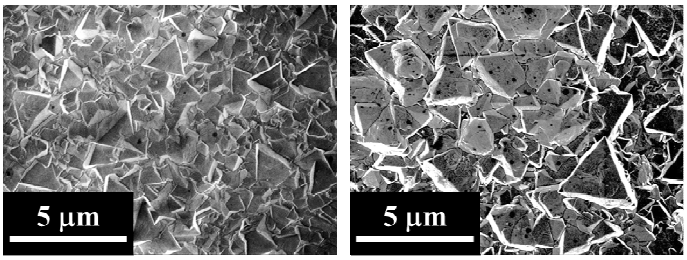


Fig. 4 SEM image of the large diamond film.

Keywords: In-liquid microwave plasma CVD process, Diamond synthesis, Effect of solvents, X-Y scnanning for large-scale diamond

**[P13.52]**

# Nano-polycrystalline diamond synthesized from neutron-irradiated highly oriented pyrolytic graphite

M. Terasawa[1], S. Honda[1], K. Niwase*[2] et al

*[1]University of Hyogo, Japan, [2]Hyogo University of Teacher Education, Japan, [3]Japan Atomic Energy Research Institute, Japan, [4]Japan Synchrotron Radiation Research Institute, Japan, [5]Ehime University, Japan*

The high-pressure synthesis of diamond from graphite and various other carbon sources has been extensively studied for several decades and widely applied for industrial and scientific purposes. Since a great breakthrough was made in the synthesis of pure binderless nano-polycrystalline diamond (NPD) from graphite, extensive studies have been conducted on conversion mechanisms and physical properties. Ultra-high hardness of NPD has drawn considerable attention for various industrial uses such as for cutting and wear-resistant tools and scientific applications such as for high pressure apparatuses.

In the present study, we have tried high-pressure synthesis of diamond from highly oriented pyrolytic graphite (HOPG), which was neutron-irradiated in nuclear reactor. Due to the neutron irradiation, the starting materials were heavily dislocated and many lattice defects were included. The purpose of this research is to elucidate the influence of the defects in the diamond synthesis process.

The starting material of the HOPG was neutron-irradiated at the irradiation fluence of 1.4 x $10^{24}$ n/m$^2$ (E > 1.0 MeV). The graphite materials were treated in high temperature and high pressure. At 15GPa and 1500□, the x-ray diffraction pattern indicated the formation of hexagonal and cubic diamond, although the graphite lattice was still remained. TEM observation showed the structure of sliding and/or buckling, together with the compressed lattice spacing. At 15GPa and 2300□, the x-ray diffraction pattern indicated the formation of pure cubic diamond crystals. In the TEM observation, polycrystalline diamond with the crystal size of 50 - 100 nm was also confirmed. The formation of nano-polycrystalline diamond would be promoted especially by enhanced diffusion of neutron-irradiation produced defects in high temperature at 2300 □. Thus, polycrystalline diamond was directly synthesized from neutron-irradiated HOPG in the high pressure and high temperature treatment.

Keywords: nano-polycrystalline diamond, graphite, high pressure, neutron-irradiation

**[P13.53]**

**Nanocarbon particles of colloid produced by electro-spark discharge (ESD) in ethanol as seeds for the CVD-synthesis of polycrystalline diamond**

M.A. Abakumov[4], A.M. Anpilov[1], N.R. Arutyunyan[1,2], E.M. Barkhudarov[1], I.V. Belashov[3], A.P. Bolshakov*[1], M.A. Borisenko[3], V.A. Ivanov[1,2], P.O. Kiryukhantsev-Korneev[5], I.A. Kossyi[1] et al

*[1]A.M. Prokhorov General Physics Institute RAS, Russia, [2]National Research Nuclear University MEPhI (Moscow Engineering Physics Institute), Russia, [3]CVD.SPARK, LTD, Russia, [4]Pirogov Russian National Research Medical University, Russia, [5]National University of Science and Technology MISIS, Russia*

The paper proposes a new method for obtaining a colloidal solution of finely dispersed carbon fractions produced in pulsed electric spark discharges in organic liquids (ethanol). Resulting stable nano-carbon colloid contains carbon-metal nano-particles, which after seeding on the substrate become sites of nano-diamond growth. Nano- and polycrystalline diamond films were synthesized in the microwave plasma by the MPACVD method, moreover the nucleation stage of nano-diamond film was similar to that as for the seeding with DND. The method of obtaining the colloid is described. The characterization of colloid particles by the method of light-dynamic scattering is performed to determine the colloid stability and sizes of particles. Samples of colloidal sedimentation on the substrate, obtained during the drying process, are studied by scanning and transmission electron spectroscopy to determine the element composition of particles. Various techniques for seeding nano-diamond sites are considered, in particular, both with the use of the colloid under the ultrasonic action and through sedimentation of the colloid to a substrate during natural evaporation.

The NCD film nucleation and growth on silicon substrates as the result of nano-carbon particles seeding, produced in the electro-spark suspension in ethanol are studied. The polycrystalline diamond plate have been grown at the electro-spark colloid seeding. The seeding nuclei particles pattern and grown films are investigated by Raman spectroscopy, scanning electron and optical microscopy. The structure and topology of nano-diamond layer formation at different seeding methods are studied. The growth of NCD films and the nature of the diamond nucleation at the carbon-metal nanoparticles are discussed.

Keywords: MPACVD diamond, carbon nanoparticles, colloidal solution seeding, nano and polycrystalline diamond films

**[P13.54]**

# Heteroepitaxial growth of iridium (001) on various substrates using a bias assisted RF-sputtering process

F. Meyer*[1], E. Reisacher[1], J. Preussner[1], A. Graff[2], A. Fromm[1], L. Groener[1], F. Burmeister[1]
*[1]Fraunhofer-Institut für Werkstoffmechanik IWM, Germany, [2]Fraunhofer-Institut für Mikrostruktur von Werkstoffen und Systemen IMWS, Germany*

Heteroepitaxially grown iridium (001) on sapphire (11-20) or YSZ (001) is one of the most promising substrates for large scale heteroepitaxial diamond growth [1, 2]. The best film qualities regarding crystallite size, orientational distributions and mosaicity were achieved with electron-beam evaporation; however, the very low evaporation rates (0.1-3 nm/min) [3] not suitable for cost-efficient large scale applications. Moreover, to the best of our knowledge, high quality epitaxial iridium films were only achieved at rather high substrate temperatures (> 600°C). RF-magnetron sputter deposition, on the other hand, is a widely used and industrially scalable process with a high potential for the fabrication of large scale [001]-oriented iridium film substrates.

Very recently, Tolstova et al. [4] were able to significantly reduce the temperature necessary for growing epitaxial platinum and gold films on MgO by using RF-sputtering with an additionally applied substrate bias. In this study we investigated the influence of the additional substrate bias, substrate temperature, target power and gas pressure on the growing Ir film on sapphire (11-20), YSZ (001), and $LaAlO_3$ (001). Crystallinity and morphology of the iridium films were characterized using X-ray diffraction, electron backscattering diffraction and scanning electron microscopy. We found that in the first seconds of the deposition process, an additional substrate bias creates a thin iridium seeding layer, which fosters epitaxial growth of iridium (001) on sapphire (11-20) and YSZ (001) already at temperatures slightly above 300°C.

[1] Z. Dai et al., Appl. Phys. Lett., 82, 3847 (2003)

[2] S. Gsell et al., Appl. Phys. Lett., 84, 4541 (2004)

[3] S. Gsell et al . Appl. Phys. Lett. 91, 61501 (2007)

[4] Y. Tolstova et al. Scientific Reports 6, 23232, (2016)

Keywords: Iridium, Heteroepitaxy, Sputtering, Substrate Bias

**[P13.55]**

# Ab initio studies of early stages of AlN growth process on oxygen-terminated diamond(111) surface

M. Sznajder*
*University of Rzeszow, Poland*

The AlN/diamond hybrid devices require an AlN layer with improved crystalline quality on the diamond surface. Recently, Imura et al. [1] demonstrated the single-crystal AlN/H-diamond(111) heterojunction with high-density interface hole channel, grown by MOVPE. However, the same method applied to O-diamond(111) substrate resulted in AlN layer of two-domain structure with poor crystalline quality [2].

Herein we study the early stages of wz-AlN growth process on diamond(111) surface within the DFT approach. First, we focus on the adsorption process of oxygen atoms on diamond(111) at various coverages, 0.25 ML, 0.5 ML, and 1 ML in the 2x2 lateral unit cell. For most coverages, independently from the starting position (H3, T4, bridge, ontop), the most stable adsorption sited is the ontop one. The corresponding $E_{ads}$ = -7.127989 eV/atom (1 ML), with the average C-O distance 1.3275 A. From the calculated atom-resolved DOS function follows that mainly oxygen p-states hybridize with p-, s-, and d-states of the four topmost C atoms, and these new states are created in the energy range of the forbidden gap of bulk diamond. Next, adsorption process of the subsequent four Al- and N-monolayers is studied on the preadsorbed O/diamond(111) surface. The corresponding energetically most stable adsorption sites are found. As a result, a wurtzite structure of AlN can be reproduced with slightly disturbed layer sequence. The corresponding p-DOS function confirms an interaction between oxygen and nitrogen p-states and d-states of aluminium. The computed laterally averaged profiles of the electron charge and total potential, as well as the spatial valence charge density distribution enable to trace the differences in charge transfer between the AlN layers and clean-, or O/diamond(111) surface. Finally, we discuss certain reconstruction patterns in analogy to those studied in [3], that lead to the enhanced adsorption energies of the Al-, N-monolayers of the diamond substrate.

1. M. Imura, R. G. Banal, M. Liao et al., J. Appl. Phys. **121** 025702 (2017).
2. M. Imura, K. Nakajima, M. Liao et al., J. Cryst. Growth **312**, 1325 (2010).
3. M. Sznajder, E. Wachowicz, and J.A. Majewski, J. Cryst. Growth **401**, 25 (2014).

Keywords: diamond, aluminium nitride

**[P13.56]**

# Simulation of the electromagnetic field and gas distribution in an improved microwave plasma reactor for diamond CVD

S. Fan*, R. Zhang, Z. Liu, H. Wang
*Xian Jiaotong University, China*

Single-crystal diamond has resent years been demonstrated as a promising candidate for semiconductor applications owing to the advantages of their electric and mechanical profiles such as large energy gap, large electron and hole mobility,high chemical stability, and large thermal conductivity. And some spin light sources in diamond, such as nitrogen-vacancy center, can be used in quantum information processes. As a result, developing high-quality and large area single-crystal diamond is a crucial subject and has been paid much attention. It is well know that nature diamond stored in earth is infinite, therefor man-made single-crystal diamond is an ideal alternative. Microwave plasma chemical vapor depositions (MPCVD) is wildly used to fabricate single-crystal diamond. However this system have the disadvantage of low crystal growth efficient and rate and, therefore, need to be taken more attention in the optimization for the system. The computer simulation is a commercial and convenient way to give theoretical predications for this optimization.

Here, we investigate the mechanism of electric and gas fields of MPCVD system, which are the key parameters that dominant crystal growth, by computer simulation. The system geometry has been optimized to give the most suitable parameters which make more electric power and reactive gases concentrated in the region above the substrate (Shown in Fig1). The experiment details and more results will be shown in the conference.

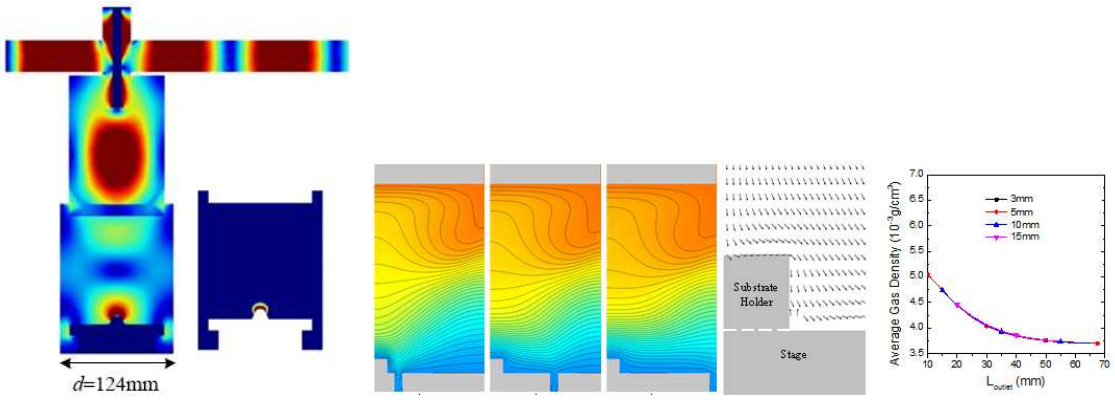


□a□ (b)

Figure 1. Electric field (a)and gas distributions(b) in the system.

Keywords: simulation, microwave cvd, diamond

**[P13.57]**

**Dependence of the density of diamond crystal dislocation from growth temperature**

V. Lysakovskyi*, O. Suprun, S. Ivakhnenko, Y. Milman

*[1]Institute for Superhard Materials NAS of Ukraine, Ukraine, [2]National Academy of Sciences of Ukraine, Ukraine*

Dislocations are defects that affect the properties of single crystals, so their study and the observation of their distribution makes it possible to obtain important information about the structure of grown samples and the conditions for their production. To observe dislocations, the selective etching method is used, and the advantages of this method are the relative simplicity of use.

For the selective etching method, the composition of the potassium hydrate mixture of oxide and potassium nitrate was used. The etching process of the crystals was carried out in a muffle furnace at a temperature of 550±10˚C÷660±10˚C and atmospheric pressure; the time ranged from 10 to 30 min.

The grown single crystals of diamonds of types Ib, IIa, IIb were obtained by the temperature gradient method with the help of the Fe-Ni, Fe-Al and Fe-Al-B alloys, respectively, to determine the dislocation density (ND). The study of etching patterns on various faces made it possible to establish that ND decreases with an increase in the growing temperature within the limits of:

- from 1,1÷2,1•103 cm-2 to 0,8÷1,8•102 cm-2 for type Ib, with the increase in temperature from 1280 to 1420 ºC
- from 1,3÷2,1•103 cm-2 to 1,5÷2,1•102 cm-2 for type IIa, with the temperature changing from 1450 to 1500 ºC;
- from 1,6÷2,2•103 cm-2 to 1,9÷3•102 cm-2 for type IIb, with an increase in temperature from 1450 to 1500 ºC.

It is also established that the dislocation density increases from 0,8÷3•102cm-2 to 1,1÷2,2•103cm-2 with an increase in the growth rate from 1-2 to 3,5-5 mg/h.

The results of the studies show that diamond single crystals obtained at temperatures of 1420-1500 °C have a high degree of perfection, the distribution of dislocations in crystals is uneven. The conclusion is made that the degree of crystal perfection increases with increasing growing temperature.

Keywords: Diamond, Dislocations, defects, alloys

**[P13.58]**

# Pyramid diamond synthesized with high pressure and high temperature technique

R. Fukuta*[1], N. Yamamoto[1], F. Ishikawa[1], M. Matsushita[1], H. Ohfuji[2], T. Shinmei[2], T. Irifune[2]
*[1]Graduate School of Science and Engineering, Ehime University, Japan, [2]Geodynamics Research Center, Ehime University, Japan*

Nanoscale structural design trying to obtain new functions of existing materials is a key issue for the realization of future devices and applications. Diamond is a material of interest for its application to next generation electronic devices due to is potential high carrier mobility, large breakdown voltage, hardness, and thermal properties. We then report our trial to make functional nano-structured material diamond.

We employed commercially available single crystalline diamond (001) substrate synthesized by chemical vapour deposition. We applied ion implantation on the substrate surface. By the damage induced from the ion implantation, the crystalline structure of the diamond surface was made to amorphous until the depth 100 nm from the surface. Subsequently, to re-crystallize and heal the damage of the diamond surface we applied high pressure and high temperature technique at 15 GPa and 2300ºC on the sample.

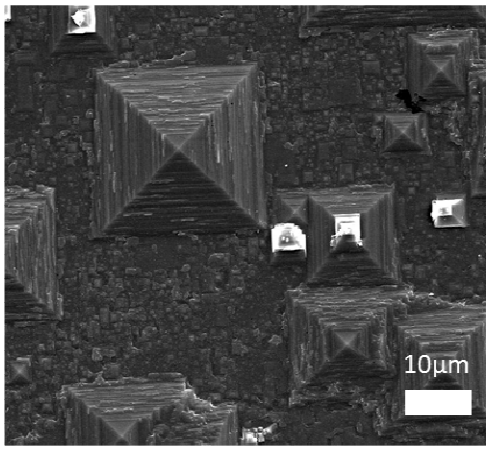


Fig. 1. Pyramid structures on diamond surface

The observation of the sample surface by scanning electron microscope is shown in Fug. 1 As clearly seen in the figure, we sample shows pyramid structures on the surface. The size of the pyramid largely varies between 1 and 30 μm on a side. Secondary ion mass spectrometry mapping shows reduced impurities density at the area existing the pyramid. That suggests there is a driving force synthesizing pure crystalline diamond at the pyramid structure. Transmission electron microscope revealed the generation of epitaxial growth at the substrate surface, which should induce the formation of pyramid structure. As a result, we have synthesized micro-nano scale pyramid diamond utilizing the combination of ion implantation and high pressure and high temperature technique.

**[P13.59]**

# Formation $Fe_3C$ in Fe implanted HOPG and CVD Diamond

K. Bharuth-Ram*[1], H. Masenda[2], H. Hofsäss[3], C. Ronning[4]

*[1]Durban University of Technology, South Africa, [2]University of the Witwatersrand, South Africa, [3]University of Göttingen, Germany, [4]Friedrich-Schiller-University, Germany*

The study of cementite phases is driven by several objectives ranging from their technological importance in influencing the mechanical properties of steel and iron alloys[1] to their role in the growth mechanism of carbon nanotubes [2]. Several methods, such as vapour deposition techniques, have been employed to produce cementite layers that would allow the study of their mechanical and thermal properties.

In this contribution, we report on $Fe_3C$ produced in highly oriented pyrolytic graphite (HOPG) and CVD diamond implanted with 40 keV $^{57}Fe$ ions to fluences of 1.0 x $10^{16}$/cm$^2$ and 5 x $10^{15}$/cm$^2$, respectively. The formation of the magnetic $Fe_3C$ phase was monitored with conversion electron Mössbauer spectroscopy (CEMS) measurement as a function of annealing up to 600 $^{o}$C.

Fig 1 (a) and (b) show the CEMS spectra for CVD diamond and HOPG, respectively. Fits to the spectra confirm the major contribution (>50%) to be from $Fe_3C$ hyperfine magnetic field of $B_{HF}$ ≈ 20 T (consistent with that of $Fe_3C$), with smaller contributions from $Fe_7C_3$ and other Fe-carbide phases[3].

The results will be discussed in comparison with other studies.

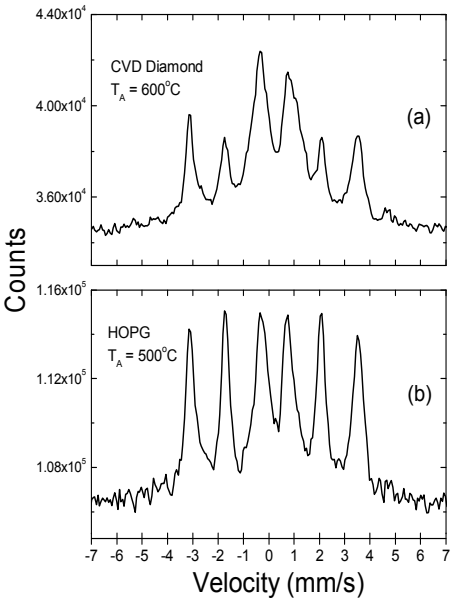


*Fig. 1. Room temperature Mössbauer spectra of CVD diamond and HOPG after annealing at temperatures indicated*.

## References

[1] E. Carpene and P Schaaf, Appl. Phys. Lett. (2002) 80:891- 893

[2] M. Perez-Cabero et al., Phys. Chem. Chem. Phys. 2006, 8, 1230-1235

[3] X–X. Bi et al., J. Mater. Research (1993) 8, 1666-1673

Keywords: Cementite, HOPG, Diamond, conversion electron Mössbauer spectroscopy

**[P13.60]**

**Adhesion of tungsten barrier layer and tungsten-copper multilayers on cemented carbide WC-Co, and growth mechanism of gradient nanocrystalline/microcrystalline diamond coatings in microwave plasma**

E.E. Ashkinazi*[1,2], P.A. Tsygankov[4,1], R.A. Khmelnitsky[1], V.S. Sedov[1,2], D.N. Sovyk[1,2], A.A. Khomich[1], A.V. Khomich[1], V.G. Ralchenko[5,1], R.I. Chelmodeev[4]

*[1]Russian Academy of Sciences, Russia, [2]National Research Nuclear University "MEPhI", Russia, [3]Troitsk Institute for Innovation and Fusion Research (GNTs RF TRINITI), Russia, [4]Bauman Moscow State Technical University "MSTU Bauman", Russia, [5]Harbin Institute of Technology, China*

Diamond-coated WC-Co tools are ideal candidates for machining Al-Si alloys and other hard composite materials due to their excellent wear resistance properties, chemical inertness and low friction coefficient. The gradient (with grain size variation within a single layer) micro/nanocrystalline multilayer diamond coatings with thickness of 3-13 microns with an upper nanocrystalline layer were produced using a microwave plasma-assisted CVD process on WC-6%Co substrates using an optimized pocket-type substrate holder.

We used the polycrystalline tungsten layers or multilayer W/Cu nanostructures as a diffusion barrier to prevent the Co diffusion, to hinder its catalytic activities and to relax the interfacial residual stress which enhances adhesion of diamond coatings (DC) on WC-Co substrates. Two methods of intermediate layer deposition on substrate at low temperature (75$^{o}$C) were investigated: magnetron sputtering and ion beam deposition. We determined the coatings adhesion immediately after deposition or after vacuum annealing under the diamond deposition temperature using scratch test method. The comparison results of these layer deposition methods are discussed. It is reported that adhesion strength of the intermediate layer reaches 80 N. It was shown that stub structure of WC-Co surface replicated by the intermediate layer supports the DC strength owing to formation of rigid elements in the coating.

The grain size of the diamond films was controlled by the adding of nitrogen to $CH_4/H_2$ mixture. Nitrogen induces secondary nucleation and therefore reduces the size of the diamond crystallites. It was found that adding of nitrogen to the gas mixture inside a microwave reactor in optimum concentration significantly improves the mechanical properties of the nanocrystalline DC. The Raman spectroscopy and SEM studies were used to examine the gradient structure profile of the DC. The cutting force and wear measurements of WC-Co substrates with a multilayer micro / nanocrystalline layers DC were performed for the turning of metal-matrix composites.

The results of experimental studies of the MW CVD nanocrystalline film growth on the diamond low-index {001}, {110}, {111}, {211} and {311} microcrystalline faces are discussed. It has been demonstrated that multiple twinning on {111} planes determines the morphology of nanocrystalline DC. According to scanning electron microscopy, Raman spectroscopy and photoluminescence studies the crystallites morphology evolution and the DC structure on the different diamond facets were examined vs. the nitrogen concentration in the gas mixture and vs. the deposition time.

This work was supported by Russian Science Foundation, grant No. 15-19-00279.

Keywords: diamond, chemical vapor deposition, nanocrystalline, intermediate layer

Keywords: diamond, chemical vapor deposition, tungsten carbide, intermediate layer

**[P13.61]**

# Effect of substrate particle size on the electrochemical properties of boron-doped diamond powder

T. Kondo*[1], K. Nakajima[1], T. Osasa[2], A. Kotsugai[2], T. Aikawa[1], M. Yuasa[1]
*[1]Tokyo University of Science, Japan, [2]Ricoh Co., Ltd, Japan*

Conductive boron-doped diamond powder (BDDP) is an attractive electrode material because it can enable fabrication of a new class of functional diamond electrodes, such as screen-printed electrode, fuel cell catalyst support and supercapacitor electrode. In order to widen the application field of BDDP, it should be important to reveal the relationship between the particle size and the electrochemical properties. In the present study, various size of BDDP was fabricated and electrochemical properties were investigated. In addition, BDDP-printed electrodes were prepared for detection of bovine serum albumin (BSA).

BDDPs were obtained by the deposition of a BDD layer on the surface of diamond powder substrate with a diameter of 300, 450, 1600 and 2600 nm by microwave plasma-assisted CVD for 8 h. BDDP-printed electrodes were prepared by screen-printing of an ink containing BDDP and polyester binder on a polyimide film substrate.

After the CVD process, the average diameter of the diamond particle was found by dynamic light scattering (DLS) to increase from 300, 450, 1600 and 2600 nm to 350, 650, 2000 and 3600 nm, respectively. This results indicates that growth rate of the BDD layer increased along with substrate particle diameter. In addition, Raman spectroscopy revealed that formation of $sp^2$ carbon impurities was suppressed for larger diamond particle substrates. From the results of cyclic voltammetry (CV) at BDDP-printed electrode, an obvious anodic peak for BSA was obtained at the electrode fabricated with 2000 and 3600 nm BDDP. Thus, BDDP in this size was found to be appropriate for the use in electroanalytical applications.

Keywords: Boron-doped diamond powder, Electrochemistry, Electroanalysis

**[P13.62]**

**Platinum on nanodiamond: A promising prodrug conjugated with stealth polyglycerol, targeting peptide and acid-responsive antitumor drug**

N. Komatsu*[1], L. Zhao[1], X. Chen[2]

*[1]Kyoto University, Japan, [2]Wuhan University, China*

In the field of nanomedicine, nanoparticles with various functions are required for in vivo applications such as biomedical imaging and drug delivery. Therefore, chemical functionalization of nanoparticles has been extensively investigated. Herein, nanodiamond (ND) coated with polyglycerol (PG) and its derivatives is reported to impart good solubility in a physiological environment, a stealth nature to avoid nonspecific uptake, a targeting property to be taken up by a specific cell, and an acid-responsive drug release property to kill cancer cells. ND is first grafted with PG and the resulting ND-PG has a high solubility in physiological media. Since a large number of hydroxyl groups in PG provide scaffolds for further surface functionalization, the targeting RGD peptide and Pt-based drug are immobilized to give ND-PG-RGD, ND-PG-Pt and ND-PG-RGD-Pt. The ND with intrinsic fluorescence is also functionalized by PG and RGD to confirm cellular uptake and intracellular localization fluorescently. The results of the cell experiments indicate that PG coating shielded fND from the uptake by HeLa and U87MG cells. In contrast, fND-PG-RGD is taken up by U87MG, not HeLa cells, exhibiting high targeting efficacy. When ND-PG-RGD-Pt is applied, U87MG is selectively killed against HeLa. The multi-functional ND is a promising prodrug in targeting chemotherapy.

References

1. X. Li, L. Zhao, J. Ye, Q. Liang, M. Xu, N. Komatsu,* G. Yuan, Q. Zhang, W. Gao, X. Chen,* "Cationic Polyarginine Conjugated Mesoporous Bioactive Glass Nanoparticles with Polyglycerol Coating for Efficient DNA Delivery" J. Biomed. Nanotechnol., 13 (3), 280-289 (2017).

2. L. Zhao, H. Yang, T. Amano, H. Qin, L. Zheng, A. Takahashi, S. Zhao, I. Tooyama, T. Murakami, N. Komatsu,* "Efficient Delivery of Chlorin e6 into Ovarian Cancer Cell with Octalysine Conjugated Superparamagnetic Iron Oxide Nanoparticle for Effective Photodynamic Therapy" J. Mater. Chem. B, 4(47), 7741-7748 (2016).

3. H. Qin, K. Maruyama, T. Amano, T. Murakami, N. Komatsu,* "Hyperbranched polyglycerol-grafted titanium oxide nanoparticles: Synthesis, derivatization, characterization, size separation, and toxicology" Mater. Res. Express, 3 (10), 105049 (2016).

4. L. Zhao, Y.-H. Xu, T. Akasaka, S. Abe, N. Komatsu, F. Watari, and X. Chen* "Polyglycerol-coated Nanodiamond as a macrophage-evading platform for selective drug delivery in cancer cells" Biomaterials, 35 (20), 5393-5406 (2014).

5. L. Zhao, Y. Nakae, H. Qin, T. Ito, T. Kimura, H. Kojima, L. Chan, and N. Komatsu,* "Polyglycerol-Functionalized Nanodiamond as a Platform for Gene Delivery: Derivatization, Characterization, and Hybridization with DNA", Beilstein J. Org. Chem., 10, 707-713 (2014).

Keywords: cancer, antitumor drug, carrier, platinum drug

**[P13.63]**

**Chemical purification for high purity and tunable grade of nanodiamond**

S.W. Lee*

*National Fusion Research Institute, Republic of Korea*

High purity and various grade of nanodiamond have attractive potential applications such as catalyst supporting materials, conducting nanodiamonds. Here, we demonstrate chemical purification process by using HClO4 to tune nanodiamond purity and get high purity compared to commercial one. Especially, chemical purification temperature, nanodiamond loading amount, and process time were studied to control nanodiamond purity. The purity was characterized with UV-Raman (325 nm) and evaluated by the intensity ratio ($I_{Dia}/I_G$) of diamond peak and G band peak which are assigned to 1324 $cm^{-1}$ and 1590 $cm^{-1}$, respectively. As the results, we can successfully fine control the nanodiamond purity and we demonstrate it is correlated to electrical conductivity of nanodimaonds.

Keywords: Nanodiamond, Chemical purification, High purity of nanodiamond, Purity control

**[P13.65]**

**Functionalization of nanodiamond's surface: A radiation chemistry approach**

J. Zhou*, C. Laube, W. Knolle

*Leibniz Institute of Surface Modification, Germany*

Thanks to their outstanding mechanical performance, unique photoluminescent and spin properties, superior biocompatibility and tunable surface, nanodiamonds find promising applications in fields of wear-resistance coating, sensing, biolabeling and drug delivery [1]. Modulation of surface functionality is of crucial importance for the desired properties. By using a radiation chemistry approach, we achieved surface chlorination of nanodiamonds (diameter approximetely 10-40 nm) with high efficiency [2]. The chlorination performance was tested with nanodiamonds carrying different surface functionalities in various media. The combination of XPS, ATR-FTIR and in-source thermal desorption mass spectrometry (IS-TD-MS) measurements confirmed a remarkable covalently chlorine-functionalized surface after irradiating hydrogenated nanodiamonds (HND) [3] in $CCl_4$ using an electron beam at doses ≥ 500 kGy. A chlorinated surface is expected to allow an easy further surface modification of nanodiamonds for novel applications.

[1] Krueger, A.; Lang, D., Functionality is Key: Recent Progress in the Surface Modification of Nanodiamond. *Advanced Functional Materials* **2012,** *22* (5), 890-906.

[2] Zhou, J. Functionalization of Nanodiamond's Surface: A Radiation Chemistry Approach. Master's thesis. Leibniz Institute of Surface Modification, Leipzig University, **2016**.

[3] Laube, C.; Riyad, Y. M.; Lohmann, F.; Kranert, C.; Hermann, R.; Knolle, W.; Oeckinghaus, T.; Reuter, R.; Denisenko, A.; Kahnt, A.; Abel, B., Optimized functionality and luminescence of nanodiamonds for sensoric and diagnostic applications by targeted high temperature gas-solid reactions and electron beam irradiation. Submitted for publication and under review.

Keywords: nanodiamond, chlorination, radiation chemistry

**[P13.66]**

# Plasma-assisted purification of nanodiamonds and their application for direct writing of a high purity nanodiamond pattern

S.P. Hong*[1], T.H. Kim[1,2], S.W. Lee[1]

*[1]National Fusion Research Institute, Republic of Korea, [2]Pusan National University, Republic of Korea*

In this paper, we demonstrate a new approach for purifying nanodiamonds using an atmospheric-pressure plasma jet. Oxygen gas is continuously dissociated in the plasma jet and generates reactive oxygen, which plays a key role in removing non-diamond carbon, including graphite and amorphous carbon. The purification process was evaluated by UV-Raman (325 nm) and X-ray photoelectron spectroscopy. This technique was applied to create a high purity nanodiamond pattern in the polymeric system of polyvinyl alcohol (PVA) and nanodiamonds using a localized plasma jet. Overall, the plasma-assisted purification of nanodiamonds enabled to the fabrication of patterns with low electrical conductivity and high thermal conductivity.

Keywords: Plasma, Reactive oxygen, Nanodiamond, Patterning

**[P13.67]**

# The novel method of functionalization on the surfaces of nanodiamonds for the preparation of polymer/nanofiller composite

D. Shiro*[1], K. Umemoto[1], H. Ito[1], T. Tasaki[2], Q. Meng[2], Y. Kasahara[2], A. Fujimori[2]
*[1]Daicel Corporation, Japan, [2]Saitama University, Japan*

Among various nano carbon materials, nanodiamonds (NDs) are expected to provide industrial advantages because of their unique properties. NDs are also easy to use as they can be dispersed in water or other polar solvents by adjusting their zeta potential and without any dispersants.

Meanwhile, combining NDs with polymers have been interesting to industries for long time as they also have noteworthy features, such as thermal stability or thermosetting property. However, choices of polymers for their purposes are limited, since neat NDs themselves show their affinity only to hydrophilic polymers, due to their hydrophilic surface compositions. Thus, efficient modification of the surfaces has been required to make them dispersible in wide variety of polymers.

In this study, we have investigated a new surface modification method to give NDs dispersibility in the wider range of solvents and polymers, and the unique behaviour of the polymer composites produced by using these newly modified NDs.

Phosphonic acid with long-chain alkyl groups was chosen as the modifying reagents. By using this surfactant, we found that both the modification and the nano-dispersion in less polar solvents can be effectively achieved simultaneously. FTIR and TG-DTA confirmed the successful modification. Modified NDs showed good dispersibility in less polar solvents such as toluene, and corresponding Langmuir-Blodgett films were prepared in order to estimate the particle size. We also found that the attached functional groups showed higher thermal stability when using this method, suggesting that polymers with higher processing temperature like engineering plastics can be combined.

Once obtaining the modified NDs, we prepared polymer composite including NDs as nanofiller in polymer matrix (Fig. 1). Only the small amounts of NDs improved Young's modulus of the composites while retaining their transparency. At the presentation, we will show other data to explain our speculation toward composite polymers with the modified NDs.

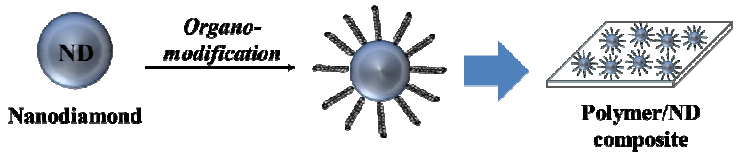


**Figure 1.** Schematic illustration of research strategy in this study.

Keywords: nanodiamond, functionalization, polymer, nanofiller

**[P13.68]**

# Novel fluorination of diamond materials using wet-chemical methods

B. Kiendl*[1], M. Drisch[1], F. Keppner[1], A-C. Pöppler[1], A. Venerosy[2], H. Girard[2], J-C. Arnault[2], M. Finze[1], A. Krueger[1]

*[1]University of Wuerzburg, Germany, [2]CEA-LIST, Diamond Sensors Laboratory, France*

The surface termination of diamond plays a key role in the actual material properties. Besides the usual hydrogenated and oxygenated diamond surface, the termination with halogens, particularly fluorine, is of special interest. Apart from the increasing hydrophobicity of fluorinated surfaces, the strong effects of fluorine on the electronic structure of diamond materials make it an attractive candidate for the preparation of functional diamond materials.

Fluorination of bulk diamond can be achieved either by using different plasma, electrochemical or thermal fluorination techniques.[1] However, for nanodiamond most of these methods are not easily accessible as either powders or dispersions need to be handled under the above mentioned conditions. In the case of powders, inhomogeneous surface modifications and irreversible agglomeration of the particle have to be considered. In the past, several methods including the thermal gas phase fluorination[2] and the fluorination using $XeF_2$[3] have been reported on submicron diamond.

Here, we report on a novel wet-chemical fluorination method using elemental fluorine in anhydrous HF under very mild conditions. The resulting diamond materials have been characterized using infrared, Raman, SS-NMR and XPS analysis. Thus, the efficient grafting of fluorine to the surface was proven and a quantification is possible. Further methods were applied to investigate the colloidal nature of the particles and the preservation of the diamond core. It was shown that the novel method achieves similar fluorination results in comparison to other methods, such as electrochemical fluorination.

After detailed investigations of the electronic and electrochemical properties of these particles, future work will focus on their use in catalysis and biomedical applications.

This work has received funding from the European Union´s Horizon 2020 Program under Grant Agreement n° 665085 (DIACAT).

[1] S. Cui, et al., *Appl. Phys. Lett*. **2013**, *103*, 051603; M. Kaviani, et al., *Nano Lett.*, **2014**, *14*, 4772.

[2] Y. Liu, et al., *Chem. Mater.* **2004**, *16*, 3924; E. M. Zagrebina, et al., *J. Phys. Chem. C* **2015**, *119*, 835.

[3] J. S. Foord et al., *Surf. Sci.* **2001**, *488*, 335.

Keywords: wet-chemical fluorination, surface termination, detonation nanodiamond, spectroscopic characterization

**[P13.69]**

**Surface and structural manipulation of diamond nanocrystals**

F. Picollo*[1,2], A. Barge[1], A. Battiato[2], K. Martina[1], L. Mino[1], M. Sacco[1], S. Tagliapietra[1], P. Olivero[1,2]

*[1]University of Torino, Italy, [2]National Institute of Nuclear Physics, Italy*

Innovative biological probes can be developed by engineering nano-scale materials to take advantage of their optical and chemical properties. In particular, the employment of nano-particles has been investigated in different environments, offering promising prospective in biomedical research, diagnostics and therapy. Diamond nano-crystals have received an increasing attention thanks to their non-toxicity, bio-compatibility and availability of a broad range of optically active centers.

A systematic study of surface chemistry of crystals with different dimensions (from 5 nm up to 1 μm), production synthesis (detonation and milling) and processing steps (thermal treatments and thermal oxidation) was performed with Raman spectroscopy, Diffuse Reflectance Infrared Fourier Transform spectroscopy (DRIFT) and X-Ray Photoelectron Spectroscopy (XPS).

The same characterization techniques were also employed to evaluate the quality of chemical functionalization after surface bonding of precursor for introduction of drugs (i.e. doxorubicin) or aliphatic chain to avoid aggregation.

Finally, the structural modification of 5 nm size nanodiamonds after proton irradiation processes was investigated by Raman spectroscopy, highlighting the formation of different types of H-terminated diamantoid structures.

Keywords: chemical functionalization, Diffuse Reflectance Infrared Fourier Transform, Raman spectroscopy, ion beam modification

**[P13.70]**

# Improvement of radiation-induced polymerization in presence of hydrogenated nanodiamonds

C. Coletta[1], H.A. Girard[1], D. Tromson[1], V. Simic[1], E. Nehlig[2], J.C. Arnault*[1], S. Saada[1]
*[1]CEA LIST, France, [2]CEA SCBM, France*

Since few years, hydrogenated diamond materials experience renewed interest with the work of Hammers' team revealing their use as a solid-state source of solvated electrons in water upon UV excitation [1]. Concerning nanodiamonds, if such electron emission in water has not been yet directly evidenced, several studies reported on the unusual behavior of the hydrogenated nanodiamonds (H-NDs) with water [2], especially under irradiation. For instance, we recently reported on the overproduction of hydroxyl radical induced by H-NDs under X-ray irradiation [3].

In this context of promising prospects around H-NDs as a source of reactive radical species during water radiolysis, we interested here to their combination with radiolytical chemistry. Indeed the overproduction of oxidant species in water radiolysis, particularly of hydroxyl radical, can be used to induce free radical polymerization. This radiolytical polymer synthesis is a new method largely investigated due to its advantages (synthesis in ambient temperature and pressure, no external oxidant, homogenous nucleation).

In our study, we investigated the polymerization behavior of monomers in presence of H-NDs in water under irradiation. Different kinds of hydrogenated nanodiamonds were studied, as well as different monomers (i.e. acrylamide). Oxidized nanodiamonds were used as negative control. The effect of the dose and energy of irradiation was also investigated. Several analysis techniques, such as NMR, FTIR, DLS, have been used to study the properties of the irradiated samples. From this study, we show an effect specific to H-NDs during the radiolytic polymerization, with the increase of the monomer conversion rate according to the concentration of H-NDs. This interesting result opens up the door for the synthesis of new nanocomposite materials as well as a new way of functionalization of NDs.

[1] Zhu et al., *Nature Materials*, 2013

[2] Petit et al., *J. Phys. Chem. C*, 2017

[3] Kurzyp et al., Chem. Comm., 2017

Keywords: hydrogenated nanodiamonds, radiolytic polymerisation, radical production, nanocomposite

**[P13.71]**

# Synthesis diamond powders using HPHT catalysts powder method containing boron and thermogravimetric characteristics

R. Oshima*, K. Iizuka
*Nippon Institute of Technology, Japan*

## Introduction

It has been proposed that boron doped diamond can growth by adding the boron when HPHT synthesizing with using graphite and metal catalyst alloy. However, the detailed crystallinity, quality and characterization are still unknown and it isn't produced in large quantities not yet been achieved. In this case, it was conducted using the catalyst method by adding boron to raw material powder to form diamond abrasive for the purpose of achieving large quantity production at a low cost, assuming that will be used as the industrial abrasives.

## Experiment

The diamond was synthesized using a large cubic-anvil HPHT apparatus same as muss production. The raw material powders were FeNi alloy, graphite powder, and boron powder. Boron powder were added at an amount equal to 5% of the graphite powder weight and mixed together completely. This starting material was then inserted into the 75mm cube high pressure cell made from pyrophyllite. The assembled this cell was compressed up to 5.5 GPa at 1450□ for a holding time of 15 min to synthesize the diamond. The diamond was refined from the high pressure cell, examined using some analyser.

## Result

The boron content in the produced diamond was approx. 1000 ppm, and the thermal characteristics in the atmosphere increased approx. 200ºC more than the normal diamond of same size. Furthermore, upon investigating this condition of the added boron within the diamond crystals, it was discovered that the boron incorporated into the diamond, which was grown by the synthesis conditions in this experiment, had “Puddle” as boron carbide and metal boride as a result of the metal catalyst when it converted into diamond from graphite.

## Discussion

We understood that the thermogravimetric characteristics improved as a result of the Percolation Theory due to the presence of this “Puddle” boride within the crystals.

Keywords: Synthesis diamond powders, HPHT, Boron dope, Thermogravimetric

**[P13.72]**

# Electrochemical deposition of metals with the explosive synthesis modified detonation nanodiamonds (MDND).

V.Y. Dolmatov*[1], G.K. Burkat[2], I.V. Safronova[1], G.S. Aleksandrova[2], A. Vehanen[3], V. Myllymaki[3]

*[1]FSUE "SCTB "Technolog", Russia, [2]St. Petersburg Institute of Technology, Russia, [3]"Carbodeon ltd. Oy", Finland*

Detonation synthesis MDND options were developed by including of modifying elements in free or bound state into the explosive charge or in the aqueous armor protection (sheath) of the charge.

The resulting purified MDND containing elements B, P, Si, Ge, S, Al, Sb, were dispersed in water and introduced into the chromium plating electrolytes, nickel plating electrolytes galvanizing, silver plating electrolytes, gold plating electrolytes and anodising aluminum electrolytes.

The following results were achieved after detailed working out of the deposition processes:

- An increase in microhardness: Cr hard - 1.6 times (up to 1427 kg / mm²); Cr wear-resistant - 1.5 times (up to 1280 kg / mm²); Al anodizing - 1.64 times (up to 1019 kg / mm²); Ni - 3.5 times (up to 800 kg / mm²); Ag - 1.3 times (up to 122 kg / mm²); Au - 1.2 times (up to 220 kg / mm²);

- An increase in wear resistance: Cr hard - 9.6 times; Cr wear resistant - wear is not detected (under conditions of detection); Al anodizing - wear is not detected; Ni - 28 times; Ag - 30 times; Au - wear is not detected (under conditions of detection);

- An increase in corrosion resistance: Cr hard - 1.25 times; anodizing Al - ≥ 2,4 times; Ni - 53 times; Zn - 2.6 times; Ag - the substrate is not corroded; Au - the substrate is not corroded;

- Reduction of porosity - Al anodizing - 2.3 times; Ni - 412 times; Ag -to 7.5 times.

Generally, the standard deposition conditions and electrolytes were used within normal limits.

It was increased electrical conductivity of electrolytes Cr, Ni, Ag. The scattering power of electrolytes (coating uniformity) was increased 1.5-2.0 times (Cr, Ni, Ag, Au), current efficiency of metal was increased.

Keywords: detonation nanodiamond, electrochemical deposition, modification, detonation synthesis

**[P13.73]**

# Influence of water armoring composition of the TNT-RDX charge on the yield and quality of detonation nanodiamonds.

V.Y. Dolmatov*[1], A. Vehanen[2], V. Myllymaki[2]
*[1]FSUE "SCTB "Technolog", Russia, [2]"Carbodeon ltd. Oy", Finland*

The easiest way to increase the diamond blend - DB, DND yield and reduce non-combustible impurities is a shift from aqueous armoring (shell) to aqueous solutions of organic and inorganic substances.

**Table:Armoring the explosive charge composition TNT+RDX 50/50, DND and DB yield.**

| № | Aqueous armoring composition, % wt. | DB Yield, wt.% | Incombustible impurities in DB, wt.% | DND content in DB, wt.% | DND Yield, wt.% | Incombustible impurities in DND, wt.% |
|---|---|---|---|---|---|---|
| 1 | $H_2O$ | 9,4 | 6,8 | 48,9 | 4,6 | 0,57 |
| 2 | $H_2O$+TrilonB,5% | 11,1 | 6,3 | 50,2 | 5,6 | 0,34 |
| 3 | $H_2O$+hydrazine hydrate,6% | 12,0 | 6,2 | 50,8 | 6,1 | 0,54 |
| 4 | Aqueous NH3,10% | 11,4 | 4,5 | 51,8 | 5,9 | 0,92 |
| 5 | $H_2O$+carbamide, 5% | 12,8 | 4,8 | 43,8 | 5,6 | 0,65 |
| 6 | $H_2O$+urotropin,5% | 12,7 | 2,52 | 52,0 | 6,6 | 0,18 |
| 7 | $H_2O$+urotropin,7% | 13,7 | 2,4 | 59,8 | 8,2 | 0,22 |
| 8 | $H_2O$+$H_3BO_3$,5% | 10,8 | 2,7 | 62,8 | 6,8 | 0,12 |
| 9 | $H_2O$+$NH_4H_2PO_4$,5% | 13,4 | 7,6 | 53,8 | 7,2 | 0,30 |

## Conclusions

1. In comparison with the explosive charge water armoring armoring, aqueous solutions of organic and inorganic compounds allows to: raise DND yield to 1.8 times; DB yield - to 1.5 times; reduce incombustible impurities in DND - 5 times, DB - to 3 times, increase DND content in DB to 14 wt.%.
2. Using urotropin or ammonium dihydrogen phosphate additive allows to obtain the maximum DB and DND yield.
3. The minimum amount of incombustible impurities in DB achieved by using boric acid and urotropin.
4. The maximum DND content in DB is achieved by using boric acid, ammonium dihydrogen phosphate and urotropin as the additives.
5. The minimum amount of incombustible impurities in DND is achieved by using boric acid, urotropin, ammonium dihydrogen phosphate and Trilon B.

Keywords: detonation nanodiamond, explosive charge composition, armoring, diamond blend

**[P13.74]**

**Comparative analysis of the electron paramagnetic resonance and X-ray diffraction of nanodiamonds doped with atoms of boron and phosphorus.**

V.Y. Dolmatov*[1], T.T.B. Nguyen[2], N.M. Lapchuk[2], V. Myllymaki[3]

*[1]FSUE "SKTB "Technolog", Russia, [2]Belarusian State University, Belarus, [3]"Carbodeon Ltd Oy", Finland*

The aim of the work was to establish the nature of the effect of the atoms of dopant impurities in detonation nanodiamond (DND) crystals and sintered tablets, on the spectra of electron paramagnetic resonance and X-ray diffraction.

The line width for the various samples of (a) original DND (DND20) and doped during detonation synthesis with the impurity atoms (b) of phosphorus (DND32) and (c) boron (DND36) varies: in the undoped sample: (8.8-8.9)±0.05Gs; in boron-doped samples (7.7±8.6)±0.05Gs; in phosphorus doped samples: (8.3-8.8)±0.05Gs. It was found that doping with impurities leads to a narrowing of nanodiamond powders EPR signal.

Based on the position and line width on the X-ray diffraction spectrum, the lattice parameter and the crystallite size were estimated (Table).

| Sample | The lattice parameter (Å) | The size of the crystallite (Å) |
|---|---|---|
| DND20 | 3,569±0,004 | 41÷50 |
| DND32 | 3,575±0,004 | 37÷44 |
| DND36 | 3,578±0,004 | 42÷47 |
| DND20-220<br><br>(Annealing at 220$^{o}$C) | 3,574±0,004 | 40÷50 |

The following results were obtained:

- the possibility of doping of diamond nanocrystallites with boron and phosphorus atoms during the detonation synthesis is demonstrated. EPR method can be used to diagnose the effectiveness of changes of uncompensated magnetic moments of electrons in DND with dopant and the establishment of optimal doping conditions;

- the results of X-ray diffraction studies of diamond nanocrystallites doped with boron and phosphorus showed the introduction of impurity atoms of boron and phosphorus into the lattice of nanodiamond, which correlates with the EPR spectroscopy data;

- it was found that by annealing the DND powders up to 600 ° C amorphous graphite phase is not formed in samples, EPR spectra parameters and X-ray diffraction are practically stable;

- EPR and X-ray diffraction methods show that, depending on the sintering conditions of the DND powders, it is possible to obtain sintered pellets samples, different in phase composition and paramagnetic properties.

Keywords: nanodiamond, electron paramagnetic resonance, X-ray diffraction, dopant impurity

**[P13.75]**

# Development of casting aluminium composites with TiC reinforcements synthesized from nanodiamonds

V.A. Popov*

*National University of Science and Technologu „MISIS", Russia*

Production of cast composites with TiC nano-size reinforcement particles by means of mixing nanoparticles into liquid alloy involves considerable difficulties, since, due to contamination on the particles surface, their wetting with liquid alloy is practically absent. To solve this problem, it was proposed to obtain, at first, composites with a higher concentration of reinforcing TiC nanoparticles by in situ synthesis from nanodiamonds directly within the metal matrix during mechanical alloying, and then to use it as a master alloy in casting technologies. In such a case, interface has no contaminations, wetting shall be high, and reinforcing particles shall be evenly distributed in liquid alloy during mixing.

The following materials were used as source materials for the research: aluminum (matrix material), nanodiamond powders (precursor for TiC synthesis), and titanium powder (precursor for TiC synthesis). Composite granules containing 40 %vol. of aluminum and 60 %vol. of TiC nanoparticles were obtained by 8 hours mechanical alloying in a planetary mill. Granules were mixed into aluminum liquid alloy at the temperature of 720°C and with volume proportion of liquid alloy to composite granules equal to 3:1. The liquid alloy was thoroughly mixed. After that, it was poured into molds for crystallization. Nanoparticles did not withdraw from the liquid alloy (depositing to the melting pot bottom did not take place). Study of samples cross-sections has shown uniform distribution of reinforcing nanoparticles within the matrix.

The study has shown an opportunity and efficiency of composite materials use with in situ synthesized TiC nanoreinforcements produced from nanodiamonds in capacity of master alloy within casting technologies.

The author is grateful to A.Prosviryakov, V.Cheverikin and E.Shelekhov for assistance in study. The research leading to these results has received funding from the Ministry of Education and Science of Russian Federation under the project with identifier RFMEFI58716X0030.

Keywords: nanodiamonds, titanium carbide nanoparticles, aluminium matrix nanocomposites, casting technology

**[P13.76]**

# Development of nickel matrix composites with reinforcing nanoparticles of titanium carbide obtained by in situ synthesis from nanodiamonds during mechanical alloying

V.A. Popov*

*National University of Science and Technology „MISIS", Russia*

Developing methods of in situ synthesis of nanoreinforcements inside metal matrix is actual task, because this technique allows obtaining absence of contamination at interface between reinforcing particles and metal. This paper is dedicated with elaboration of method of TiC nanoparticle formation inside nickel matrix from nanodiamonds and titanium powders as precursors during mechanical alloying. Primary nanodiamond particles sizes are 4-6 nm. It allows obtaining TiC nanoparticles practically with the same size level. Mechanical alloying was executed in planetary mill Retch-400 in sealed jars in argon atmosphere. The mechanically alloyed granules were investigated by X-ray diffraction, transmission electron microscopy and differential scanning calorimetry. For mechanical alloying, the following ratios of starting materials were employed: Ni – 8-25 g, Ti – 31.98 g, ND – 8.02 g.

The XRD investigation indicated that Ni content from 17%w up to 27%w allows obtaining complete in-situ synthesis of the TiC nanoparticles, but size of the TiC particles is depended from composition of initial components. The increased content of nickel interferes with TiC synthesis course.

The results of the mechanically alloyed granule structure investigation using TEM reveal that the titanium carbide particles have a regularly spaced distribution in the nickel matrix, and their sizes range from 10 to 40 nm. Thus, they can be classified as nanoscale particles.

DSC is considered a significant part of the study because it is used to obtain data on the functional capability of the composite under high temperature conditions. The DSC curve shows that no chemical reactions between the titanium carbide nanoparticles and the nickel matrix.

The author is grateful to A.Prosviryakov, B.Senatulin and E.Shelekhov for assistance in study. The research leading to these results has received funding from the Ministry of Education and Science of Russian Federation under the project with identifier RFMEFI58716X0030.

Keywords: nanodiamonds, titanium carbide nanoparticles, mechanical alloying, in situ synthesis

**[P13.77]**

# The application of DSC, XRD at high temperatures, and synchrotron radiation for the investigation of metal matrix composites with non-agglomerated nanodiamond reinforcing particles

V.A. Popov*

*NUST „MISIS", Moscow, Russia*

The size of primary nanodiamond particles is 4-6 nm. However, they are combined in agglomerates. It is the major peculiarity of nanodiamonds as well as most nanopowders. The size of these agglomerates can be hundreds micrometers. This study is dedicated to the development of metal matrix composites (MMC) with non-agglomerated nanodiamond reinforcements based on mechanical alloying as production method. This technique allows achieving the deagglomeration of nanodiamonds inside the metal matrix (resulting in separate nanodiamond particles that are uniformly distributed in the matrix). Such processing can be extended to the point where there is no connection, even between 2 to 3 nanoparticles, and each separate nanodiamond particle is completely surrounded by the metal matrix. Such a distribution of nanoscale-reinforcements leads to an enhancement of the performance properties of the composites. This paper is about application of DSC, XRD at high temperatures and synchrotron radiation to study developing composites. MMCs with copper, aluminium and nickel matrixes were investigated. The results show that the production process did not lead to a transformation of nanodiamonds into any graphite-like nanoparticles: reinforcing particles after treatment still have diamond structure. In aluminium matrix composites, the formation of aluminium carbide starts at 450°C. Reactions between copper and nickel matrixes and nanodiamonds are absent, but oxides of matrix materials starts to react with nanodiamonds at 500-550 °C. Non-agglomerated nanodiamonds as reinforcing particles lead to the stabilization of matrix structure: changes of crystallite size of matrix materials are absent after 4 hour annealing at 400 °C. Study of the developed composites demonstrates the possibility of their application up to 400 °C.

The authors are grateful to A.Prosviryakov, B.Senatulin, S.Kannykin and E.Shelekhov for assistance in study. The research has received funding from the Ministry of Education and Science of Russian Federation under the project with identifier RFMEFI58716X0030.

Keywords: non-agglomerated nanodiamonds, mechanical alloying, metal matrix composites, structure stabilization

**[P13.78]**

# Development of metal matrix composites with non-agglomerated nanodiamond reinforcing particles

V.A. Popov*, V.V. Cheverikin

*National University of Science and Technology „MISIS", Russia*

Size of primary nanodiamond particle is mainly 4-6 nm but a minor part of particles can be smaller up to 2 nm, and the size of approximately 5-10% of particles can exceed the medium size and reach even 30 nm. It should be noted that particles with correct single-crystal structure predominate in initial detonation-synthesized particles, however, a considerable part of the particles have various crystal structural defects, most often crystal twins. The major peculiarity of nanodiamonds as well as all nanopowders is agglomeration. If primary particle size is 4-6 nm, then their agglomerates can be hundreds micrometers and even millimeters in size. Agglomeration is the primary barrier to the wide commercialization of nanodiamonds. There are various methods to obtain metal matrix composites with nanoscale reinforcing particles. Several of these methods are not able to achieve the deagglomeration of nanodiamonds, while others (e.g., mechanical alloying) effectively deagglomerate, resulting in separate nanodiamond particles that are uniformly distributed in the metal matrix. The disintegration of agglomerates of nanodiamond reinforcing particles in a metal matrix upon mechanical alloying is studied in this paper. The developed technological scheme includes use of phase transformation in matrix during mechanical alloying. Phase transformation leads to additional microstresses and microstrains arising in local zones due to variations in the density and molar (gram-atom) volumes of phases and parameters of the metal lattice. Such processing can be extended to the point where there is no connection, even between 2 to 3 nanoparticles, and each separate nanodiamond particle is completely surrounded by the metal matrix. Such a distribution of nanoscale-reinforcing particles leads to an enhancement of the performance properties of the composites.

Keywords: nanodiamonds, mechanical alloying, metal matrix composites, phase transformation

**[P13.79]**

**On thermodynamics of diamond nanocrystal**

B.V. Spitsyn*[1], S.N. Zhevnenko[2]

*[1]Institute of Physical Chemistry and Electrochemistry of RAS, Russia, [2]National University of Science and Technology „MISIS", Russia*

The thermodynamic stability of diamond nanocrystals considered in a number of papers, largely theoretically. Because in nanodiamond (ND) crystal of 4-5 nm size, the fraction of the surface atoms is ~15 %, the main influence to the enthalpy provide the chemical state of the surface atoms . Experimental data show enhanced ND enthalpy to 30.72 kJ / mol measured through combustion, far exceeding the difference for bulk diamond and graphite ( 1.8 kJ / mol) [1]. In this paper, we attempt to estimate the diamond nanooctahedra standard enthalpy in the approximation to the C - C, and C -H bond energies. Obviously, the highest value of the enthalpy should have a diamond nanocrystals with unreconstructed (111 ) faces covered with broken ( 'dangling' ) bonds, it consider unreconstructed monohydride (111 ) faces with a monolayer of C-H bonds formation with dramatic enthalpy decreasing. Undoubtedly deviation of the considered nanocrystals from bulk diamond energy will increase with a decrease in the size **a** - the length of the edge of the octahedron. Assuming that the excess energy of the surface atoms on the unreconstructed (111 ) is 177.82 kJ/ mol, we can show that for an octahedron with **a** = 5 nm have excess relative the bulk diamond crystal enthalpy amounted 28.1 kJ/mol. Chemisorption of hydrogen provides significant reduction in surface energy and further reduction of the diamond nanocrystals enthalpy. Abovementioned looks as helpful approach to the size ranges consideration between higher diamantoids and diamond nanoparticles.

Moreever, according to many CVD diamond studies the hydrogen plays an important role in the diamond nucleation, because a significant decrease in the sub-nm crystals enthalpy and their surface energy takes place.

Keywords: Nanodiamond,, Surface energy

**[P5.01]**

# Effects of an ethanol addition on the growth of carbon nanotube during combustion in a diesel engine

S. Suzuki*, S. Mori
*Tokyo Institute of Technology, Japan*

A variety of applications using carbon nanotube (CNT) have been expected. However, applications are quite limited because production costs of CNT are still high although CNT mass production is achieved by some processes. Recently, flame process has been focused on due to its advantages such as low investigation cost and easy scale-up. Among flame processes, we utilized a diesel engine for the synthesis of CNT. The reduction of CNT production cost using a diesel system can be expected since power generation in addition to CNT production is achieved.

In our diesel system, normal dodecane, methyl laurate and 1-decanol were used as main fuel and ethanol was blended with them. Ferrocene whose amount was 5,000 ppm by weight was used as a floating catalyst and sulphur and molybdenum acetate dimer were added as promoters so that atomic ratio S/Fe and Mo/Fe to be 2.2 and 0.01, respectively. An ethanol fraction in fuel and an engine load were varied as experimental parameters. Influences caused by an ethanol addition on CNT synthesis were explored by an experimental approach and a theoretical approach.

Growth of CNTs tended to occur at a high ethanol fraction in fuel and a large engine load. Under these conditions, an exhaust gas possessed larger CO and low molecular hydrocarbons like ethylene and acetylene which might behave as a CNT precursor. Our investigations through intensive analysis revealed that CO amount most strongly affected CNT formation than other factors. Calculations by simulation software and a modelling work for CNT growth rates using CO disproportionation reaction supported experimental results. Therefore, it can be concluded that major effects of an ethanol addition were to produce CO which acted as a CNT precursor, and we believe that this finding will provide useful information for CNT synthesis in a flame process.

Keywords: carbon nanotube, flame synthesis, diesel engine, combustion reactor

**[P5.02]**

# Spontaneous diameter control synthesis of single-walled and a few layers carbon nanotubes

S. Inoue*[1], S. Lojindarat[2], T. Kawamoto[1], Y. Matsumura[1], T. Charinpanitkul[1]
*[1]Hiroshima University, Japan, [2]Chulalongkorn University, Thailand*

In order to separate carbon nanotubes we must conduct complicated procedures, such as purification, dispersion, and centrifuge; however, these procedures often invite damages in carbon nanotubes. Diameter control synthesis is useful technique due to omit these negative procedures. So far authors succeeded in selective synthesis of single-walled carbon nanotube by controlling catalyst species and diameter in chemical vapor deposition method. In this study, we expand this technique to control even a number of layers of carbon nanotubes, such as double-walled and triple-walled carbon nanotube; especially, we focused on seeking conditions for synthesizing double-walled carbon nanotube.

Cobalt and molybdenum were used as catalysts and supported on a quartz glass by dip coat method. A quartz glass was sunk into the solution and gradually pulled up at the constant rate. Then, the substrate was calcined at 500 °C for 5 minutes. First, molybdenum was dipped and then cobalt was dipped. This procedure was for 1 layer of catalyst. In order to achieve spontaneous control synthesis of carbon nanotube, we examined multi-layered catalyst. Carbon nanotube was synthesized by chemical vapor deposition in a vacuum oven employing ethanol as a source gas. Before CVD, we reduced catalysts by using $Ar/H_2$ gas, and hold the substrate in the oven for 0–180 min in order to induce sintering of catalysts.

In order to grasp the diameter distribution, we referred to Raman spectroscopy with its exciting wavelength were 488, 515, and632 nm. Though the radial breathing mode of CNT is resonance mode, we used Raman for the simplicity but referred three kinds of wavelength. Then, we observed TEM for measuring actual diameter. Consequently, adjusting the number of dip coat, the density of catalyst solution, sintering time, we succeeded in controlling the number of layers as shown in the figure.

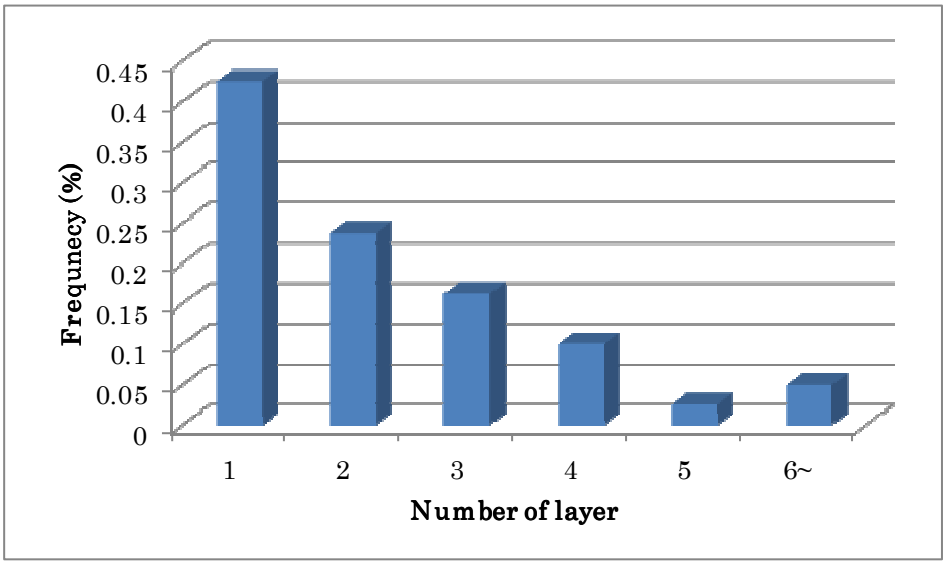


Keywords: double-walled, diameter, selective synthesis

**[P5.03]**

**Carbon nanofibers on si substrate by simple process of microwave-assisted physical vapor deposition**

J. Onsopa*[1], M. Thepnurat[2], D. Wongratanaphisan[1], A. Gardchareon[1], S. Phadungdhitidhada[1], P. Ruankham[1], S. Choopun[1]

*[1]Chiang Mai University, Thailand, [2]Chiang Rai Rajabhat University, Thailand*

In this work, carbon nanofibers (CNFs) was synthesized on silicon substrate by using a simple process of Microwave-assisted Physical Vapor Deposition technique (M-PVD) under normal atmospheric condition. Precursor of activated carbon (8 ,12 and 16 grams by the weight) was heated in a household microwave oven for only one cycle of 2-5 mins at the power of 700 and 800 watts. The silicon substrate was placed into the microwave and surrounded by the activated carbon. The as-synthesized products were characterized by Field Emission Scanning Electron Microscopy (FE-SEM), High Resolution Transmission Electron Microscopy (HRTEM) and Raman spectroscopy. The results showed that the as-synthesized products exhibited fiber-like structure of carbon. The diameters of CNFs were in a range of 30-50 nm with the length was up to several micrometers. The TEM and SAED analysis indicated that the CNFs exhibited platelet structure of CNFs with the growth direction of [111] and similar to the other reports [3]. Raman spectra of CNFs showed the two typical peaks of carbon nanostructure form, D-band (1360 $cm^{-1}$) and G-band (1582 $cm^{-1}$) with no radial breathing mode peak. The relative intensity ratio ($I_D/I_G$; R-value) was 1.1 which indicated the good crystallinity of CNFs. These results suggest that the CNFs can be successfully synthesized with simple and fast process by using a household microwave oven.

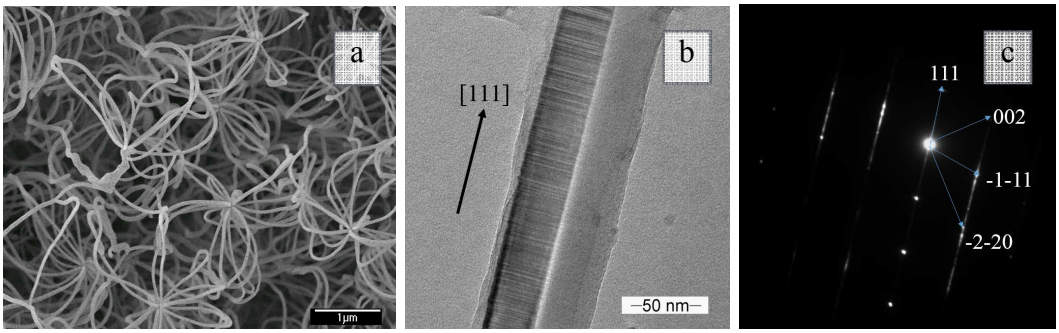


Fig. 1 a) FE-SEM image at heating time of 3 mins , b) HR-TEM image

and c) SEAD pattern of platelet CNFs.

References

[1] S. Bigdeli ,S. Fatemi, Journal of Chemical Engineering 2015, 269, 306-315.

[2] A. Undri, B. Sacchi, E. Cantisani, N. Toccafondi, L. Rosi, M. Frediani, P. Frediani, Journal of Analytical and Applied Pyrolysis 2013, 104, 396-404.

[3] R. Zheng, Y. Zhao, H. Liu, C. Liang, G. Cheng, Journal of Carbon 2006, 44, 742-746.

Keywords: CNFs, Physical Vapor Deposition, platelet Carbon Nanofibers, Nanofibers

**[P5.04]**

**Longitudinal splitting of multi-walled carbon nanotubes via acid vapor toward controllable synthesis of high-quality graphitic nanoribbons**

M. Yang*, T.X. Fan, D. Zhang

*Shanghai Jiao Tong University, China*

Graphene/graphitic nanoribbons (GNRs) are promising qusai-1D carbon nanomaterials for use in a variety of applied fields such as optoelectronics and electronics, electrochemical devices, assembling into macroscopic structures, composite nanofillers and so forth. Despite significant efforts to develop ways to produce customized carbon-based nanostructures, facile synthesis of mass GNRs without losing the intrinsic sp2-structure and properties remains challenging. Here we report that bulk of multi-layered graphitic nanoribbons can be prepared by gas-phase oxidative splitting of multi-walled carbon nanotubes (MWCNTs) using $HNO_3$ vapor. Three key factors substantially determining the tube-to-ribbon transforming behavior of MWCNTs were identified: i) the selecting of highly-crystallined CNTs with larger diameter may avoid cutting off the tubes transversely; ii) the utilization of gaseous oxidant contributes to the unidirectional splitting of CNTs; iii) the high-pressure autoclaving condition facilitates the penetration and selective oxidation of HNO3 vapor. Moreover, this splitting process was evidenced to be edge-selective and nonaggressive as opposed to traditional wet chemical oxidation, for which the obtained GNRs show minimized oxidation level, highly intact crystalline and robust electrical conductance ($2.2\times10^4$ S $m^{-1}$). This study suggests a simple yet effective strategy for producing mass high-quality GNRs.

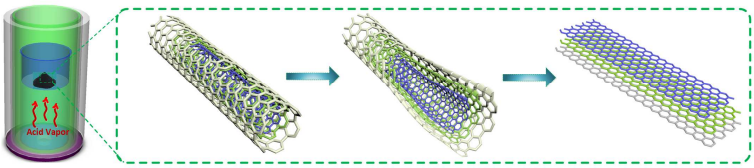


Keywords: graphene nanoribbon, multi-walled CNTs, gas phase oxidation, longitudinal splitting

**[P5.05]**

**Transient behaviour of as-grown carbon nanotube thin film on the occasion of molecular adsorption**

Y. Tomita*, S. Inoue, Y. Matsumura

*Hiroshima University, Japan*

Unlike conventional semiconductor gas sensor, carbon nanotube can detect even at the room temperature, so that it can be a particular candidate for sensing. So far, considerable number of studies was focused on the response to gas molecules using an isolated carbon nanotube. We demonstrated sensing using as-grown carbon nanotube and detecting mechanism. However, almost all of studies observed only steady states and have not treated transient states. When we use this as a gas sensor, it is important to specify gas species. Embedding modifiers into carbon nanotube is definitely a good method but it requires a sophisticated technique. Observing a transient state during molecular adsorptions possibly useful for specifying gas molecules. In this study, we observed the transient behaviour on the occasion of molecular adsorptions on the carbon nanotube thin film.

An as grown carbon nanotube this film was fabricated on the quartz glass by spin coating method using CNT dispersion solutions. This substrate was placed in the sample holder made of alumina with heater and some electrodes in order to measure the electric resistance. This sample was set in the small vacuum chamber connected to the larger vacuum chamber, which was used for buffer chamber. After the pressure of both chambers reached below 2 Pa, the gate valve between chambers was closed. Then, the buffer chamber was filled with a certain gas at the target pressure and opened the valve. The change of the electric resistance was recorded.

As shown in the figure, non-polar gas exhibited overshooting behaviour unlike the polar molecule such as water. It is considered that polar molecules tend to stick on as their electrostatic potential becomes minimum; on the other hand, as for non-polar molecules stick by physisorption, so that it may be overshooting.

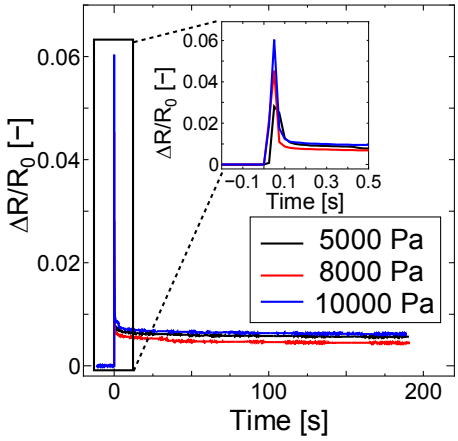


(a) $CO_2$

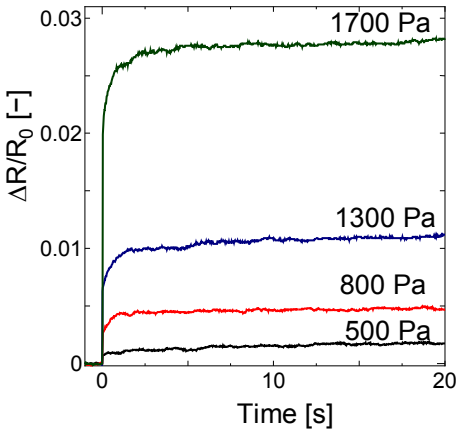


(b) $H_2O$

Keywords: gas sensor, electric conductance

**[P5.06]**

**Little by little addition of CNTs to Al/Ti powder composite to achieve uniform distribution of nanotubes**

M. Haddad-Sabzevar*, F. Saba, S.A. Sajjadi
*Ferdowsi University of Mashhad, Iran*

A novel strategy called little by little (LbL) CNT adding was used to achieve a uniform distribution of carbon nanotubes (CNTs) in Al/Ti powders and thus synthesis a composite sample. This method consists of solving some problems such as incompatibilities between Al/Ti powders with CNTs, uniform adsorption of CNTs onto the Al/Ti flakes and consolidation of as-prepared CNT/Al composite powders by spark plasma sintering (SPS). At first, Al and Ti powders were mixed together for 2 hours by mechanical milling. After mixing them, two routes were used for producing composite powders: (I) a common mechanical milling of Al/Ti and CNT powders for 6 hours and (II) a novel LbL method for 6 hours (use 6 one hour stages instead of continuously 6 h). Scanning electron microscope (SEM) equipped with energy-dispersive X-ray spectroscopy (EDS) was used to microstructural evaluation of the samples. It was shown that the present novel method can produce uniform and individual distribution of CNTs in Al/Ti powders as a comparison with typical mechanical milling.

Keywords: CNT, TiC, microstructure, spark plasma sintering

**[P5.07]**

**Multi-wavelength Raman investigation of carbon fibers produced from conventional and sustainable precursors towards online monitoring feasibility**

P. Jagdale*[1], M. Rovero[1], D. Dragatogiannis[2], E. Koumoulos[2], A. Khan[2], P. Mandrachi[1], C. Charitidis[2], A. Tagliaferro[1]

*[1]politecnico di torino, Italy, [2]National Technical University of Athens, Greece*

There are few non-destructive evaluation techniques available to evaluate the carbon fibre quality in online process. The goal of this research is to evaluate the potential of non-destructive Raman spectroscopy assessment for carbon fibre. Raman spectroscopy investigates vibrational, rotational, and other low-frequency modes of interaction between molecules. Early studies on graphitic materials revealed that two regions are of particular interest, namely 1100-1800 $cm^{-1}$ and 2500-3100 $cm^{-1}$. In the first region two main contributions are found, one near 1550 $cm^{-1}$ related to C=C vibrations (usually labelled 'G' peak) and the other around 1350 $cm^{-1}$ related to the finite size of graphitic regions (usually labelled as peak 'D'). These two peaks are also evidenced in carbon fibers Raman spectra and exhibit different relative intensities in different fibers.

In this work, we will discuss the relative variation of the 'D' and 'G' contributions for a number of different carbon fibers. Further information on the structure of the fibers will be gained from the other wavenumber region were the overtones of the 'D' and 'G' peaks are observed. To gain further insight, Raman spectra were recorded for three different laser wavelengths (457.9 nm, 514.5 nm, 785 nm). Commercial PAN based carbon fibers and in-house generated cotton based carbon fibres were investigated and their Raman spectra compared. The Raman spectral features are correlated with other properties of interest of the fibers, with the purpose of exploring possible correlations between Raman spectral features and physical properties.

This work has received funding from the EU FP7 Project (FIBRALSPEC) under Grant Agreement No. 604248.

References

1. F. Tuinstra, J. L. Koenig, *The Journal of Chemical Physics*, 53, 3, 1126 (1970).
2. N. Melanitis, P. Tetlow, C. Galiotis, *Journal of Materials Science*, 31, 4, 851,( 1996).
3. G. Washer, F.Blum Jr., *Research Letters in Materials Science,*2008,1(2008)
4. P. Jagdale, E. P. Koumoulos, I. Cannavaro, A. Khan, M.Castellino, D. A. Dragatogiannis, A. Tagliaferro, C. A. Charitidis, submitted, *Manufacturing Review* (2017)

Keywords: Multi-wavelength Raman, carbon fibre, PAN

**[P5.08]**

**The carbon nanotubes (CNTs) filled poly(2,6-dimethyl-1,4-phenylene oxide) hybrid membranes for the air separation**

A. Rybak*[1], A. Rybak[1], W. Kaszuwara[2], S. Awietjan[2], R. Molak[2], S. Boncel[1]

*[1]Silesian University of Technology, Poland, [2]Warsaw University of Technology, Poland*

Carbon nanotubes (CNTs) are currently the most intensively studied allotropic form of carbon. These nanostructures are characterized by an unusual combination of the physicochemical and biological properties. Therefore, they are widely used in many fields, such as the electronics, energy, industrial catalysis, material's engineering, medicine, etc. Due to the many advantages of the CNTs, they may also find the application as fillers of the inorganic-organic hybrid membranes with potential medical and industrial usage (air separation, hydrogen recovery). Such inorganic-organic hybrid composites are materials of great interest because of their adjusted properties obtained by control of the composition, content and morphology of the particle addition and by modification of the polymer matrix.

This work concerns the study of the inorganic-organic hybrid membranes based on a poly(2,6-dimethyl-1,4-phenylene oxide) matrix and various additions of FeMWCNT's as a filler. We have examined the gas transport ($N_2$, $O_2$, synthetic air), magnetic, mechanical and rheological parameters of the homogeneous PPO and SPPO membranes and the hybrid membranes (CNTs:0.5-5.0 wt%) based on these polymer matrices. The membranes were prepared from the CNTs dispersion in the polymer solution, using the casting method. It was introduced the magnetic field during the casting process for the filler arrangement in the polymer matrix. To improve the interaction between the CNTs and the polymer matrix, the PPO was sulfonated and the CNTs were chemically functionalized. The results showed that the introduced magnetic field and chemical modifications caused the increase in CNT's dispersibility, in membrane's gas permeability, diffusivity and permselectivity. It was found that the mechanical and rheological parameters and gas transport properties of hybrid membranes were improved with the increase of CNT's addition and selection of appropriate type of polymer matrix.

***Acknowledgments***

This publication was supported under the Rector's grant in research and development. The Silesian University of Technology, Grant no.***04/040/RGJ17/0058***.

Keywords: CNT's, hybrid organic-inorganic membranes, synthetic air separation

**[P5.09]**

**TiC/CNT dual-nanoreinforced aluminum-matrix composite fabricated by a pressureless spark plasma sintering (SPS) method**

S.A. Sajjadi*, F. Saba, M. Haddad Sabzevar
*Ferdowsi University of Mashhad, Iran*

Carbon nanotubes (CNT) and nano-titanium carbide (nTiC)-reinforced aluminum-matrix composite powders were fabricated using wet ball milling and a novel pressureless-spark plasma sintering (SPS) method. After preparing the powders, consolidation process was performed through a common spark plasma sintering (SPS). Nano TiC, in addition to CNT, was used as a tool of inducing fine particle strengthening. Scanning electron microscopy (SEM), Transmission electron microscopy (TEM) and X-ray diffraction (XRD) were used to study the microstructure and composition of the samples. In addition, Improvements of Young's modulus and nanohardness were achieved by doping of 1.0 wt.% TiC/CNTs into the aluminum matrix. It was found that the proposed dual-reinforcing strategy can be a versatile route for fabricating other nano-hybrid composite materials.

Keywords: Carbon nanotubes, nano-titanium carbide, aluminum-matrix composite, spark plasma sintering

**[P5.10]**

**Unzipped carbon nanotube films converted from spun multi walled carbon nanotubes for growth and phase transition characteristics of nanostructured $VO_2$**

H-S. Jang*[1], K-C. Kim[2]

*[1]World Tech. Co. Ltd., Republic of Korea, [2]Mokwon University, Republic of Korea*

Unzipping process of the spun multi-walled carbon nanotubes (MWCNTs) was performed to produce networked graphene nanoribbon (GNR) sheet films using an $O_2$ plasma etching method, after which we produced the spun MWCNT film by continually pulling MWCNTs down from the vertical well aligned MWCNTs on the substrate. The electrical resistance was slightly decreased and the optical transmittance was significantly increased. Plasma etching for the optimized time, which does not change the thickness of the spun MWCNT films, improved the electrical resistance and the optical transmittance. GNR sheet films were heated by applying a direct current, and showed rapid thermal responses and uniform temperature distribution. The rate of temperature change was found to depend on the power applied. GNR sheet films reached temperature of ~ 70 °C at 12 V. Vanadium dioxide ($VO_2$) is a thermochromic material that exhibits a reversible metal-insulator phase transition at 68 °C, which accompanies rapid changes in the optical and electrical properties. Nanostructured vanadium dioxide was grown on catalytic layer of GNR sheet films by thermal CVD using vapour transport process. The phase transition characteristic of nanostructured $VO_2$ on the GNR sheet films was investigated by *in-situ* measurement using GNR sheet film heater.

Keywords: Carbon nanotubes, Unzipping, Film heater, Graphen nanoribbon

**[P5.11]**

**Synergistic Reinforcement of Tungsten Carbide and Carbon Nanotubes for Improving the Fracture Toughness of Titanium Carbide based Ultra High Temperature Ceramic**

M. Sribalaji*[1], B. Mukherjee[1], A. Islam[1], T. Laha[2], A.K. Keshri[1]

*[1]Indian Institute of Technology Patna, India, [2]Indian Institute of Technology Kharagpur, India*

TiC (TiC-SD), TiC-3.5 wt.% WC (TW-SD) and TiC-3.5 wt.% WC-2 wt.% CNT (TWC-SD) pellets were consolidated using spark plasma sintering technique at 1600°C 1600°C and 50 MPa pressure. Spray drying technique was used for achieving uniform distribution of CNTs in TiC-WC matrix. The HR-TEM and Raman analysis has confirmed the survival of CNTs in TWC-SD with increased defect concentration. Incorporation of WC increased the density of TiC from 89% to 94%, while the addition of CNTs to TiC-WC matrix has further increased the density value to 99%. The average grain size of TW-SD and TWC-SD pellets were reduced by ~17% and ~31% respectively compared to TiC-SD pellet. In addition to that, the interfacial analysis performed at the TiC-CNT interface shows that a shear stress greater than 0.28-0.33 GPa is required for removal of CNT from TiC interface. Both hardness and elastic modulus of TWC-SD pellet were found increased by ~20% compared to TW-SD pellet. The CNTs are more effective in enhancing the fracture toughness of TW-SD pellet, which was ~76% compared to TW-SD pellet. In addition to conventional toughening mechanism like, CNT pull out, CNT stitching and CNT grain gluing, the increase load transfer behaviour of TWC-SD pellet was found responsible for the significant improvement in toughness value.

Keywords: Titanium Carbide, Spray Drying, Spark Plasma Sintering, CNT Toughening

**[P5.12]**

**Nickel doped diamond-like carbon thin film electrodes: Effect of annealing and implications for physical and electrochemical properties**

N. Wester*, E. Leppänen, J. Etula, T. Laurila, J. Koskinen
*Aalto University, Finland*

Tetrahedral amorphous carbon (ta-C) thin films show promise as electrode materials for detection of neurotransmitters and drugs. We have shown recently that reversible electron transfer can be achieved with ta-C thin film electrodes [1,2]. Moreover, ta-C has several other attractive properties, including large water window, good biocompatibility and resistance to bacterial adhesion. The sensitivity and selectivity of ta-C is however insufficient for detection of neurotransmitters and painkillers in biological samples, due to interference with ascorbic acid (AA) [1,3].

Nickel and its oxides are known to have electrocatalytic properties [4,5]. Thus, by alloying carbon thin films with Ni we expect that electrochemical properties of the resulting carbon based electrodes will be significantly improved.

The carbon based Ni alloyed films were deposited with cathodic arc. The Raman spectra in Fig. 1 a) shows a clear increase in ID/IG ratio after annealing (650 °C, 20 min). The appearance of a 2D peak further confirms the graphitization of the amorphous carbon. Initial experiments show that Ni doping only slightly reduces the water widow to 3.2V from 3.5V for ta C [1]. More reversible electron transfer of dopamine (DA) was also observed at the nickel doped electrode as shown in Fig. 1 b). The Ni doping and annealing also effected the measurement of AA and paracetamol (PA) with cyclic voltammetry (CV) and differential pulse voltammetry (DPV) as shown in Fig. 1 c) and d), respectively. The electrochemical properties of these materials will be evaluated with CV, DPV and electrochemical impedance spectroscopy (EIS). Combined with characterization, including Raman spectroscopy, SEM, XPS and TEM, the results can be correlated to changes in both chemical and physical properties. Hence, this new thin film electrode material provides a very promising CMOS compatible platform for biomolecule detection that can enable the realization of the next generation diagnostic and therapeutic devices.

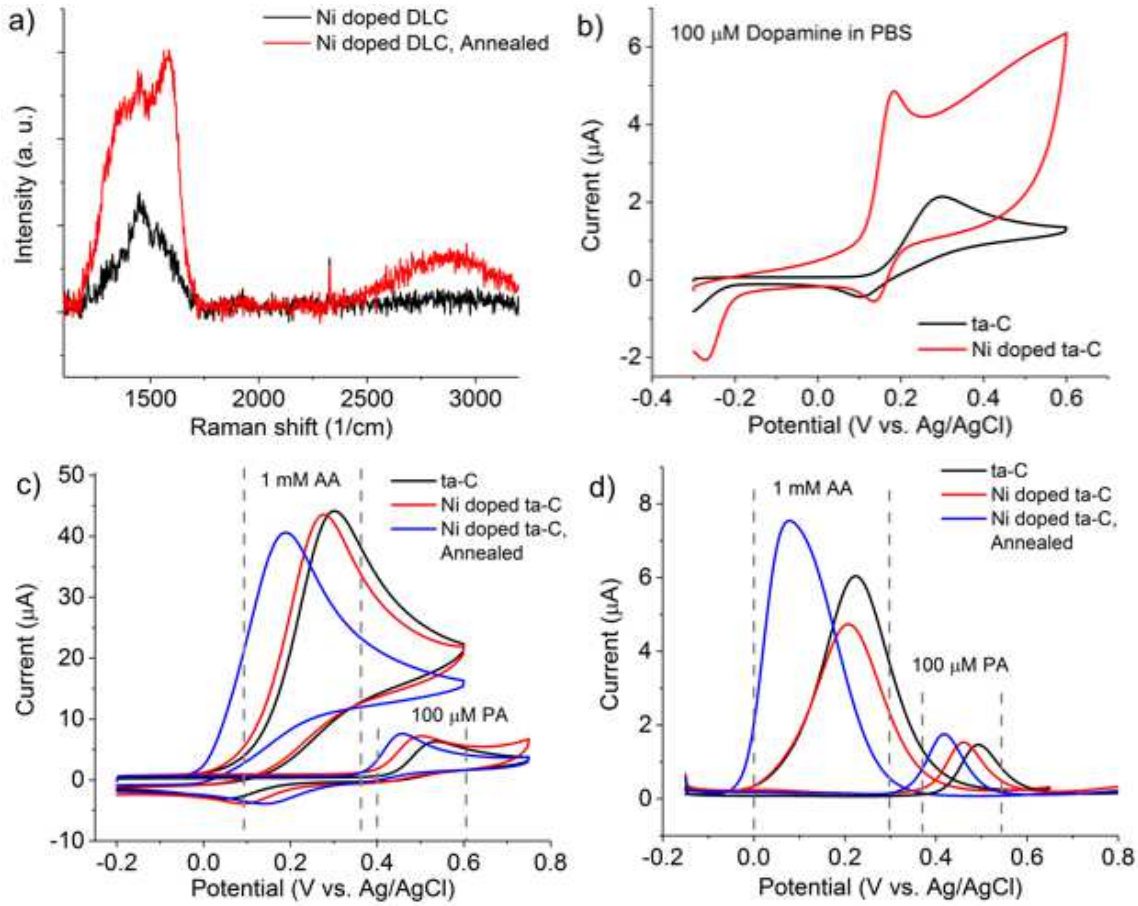


Fig. 1 a) Raman spectra for the as deposited and annealed Ni doped ta-C electrodes b) cyclic voltammogramms of 100 μM DA in PBS for ta-C and as deposited Ni doped ta-C electrodes as well as c) cyclic voltammogramms and d) differential pulse voltammograms of 1 mM ascorbic acid (AA) and 100 μM paracetamol (PA) in PBS.

References:

[1] T. Laurila, V. Protopopova, S. Rhode, S. Sainio, T. Palomäki, M. Moram, J.M. Feliu, J. Koskinen, New electrochemically improved tetrahedral amorphous carbon films for biological applications, Diam. Relat. Mater. 49 (2014) 62–71. doi:10.1016/j.diamond.2014.08.007.

[2] T. Palomäki, N. Wester, M.A. Caro, S. Sainio, V. Protopopova, J. Koskinen, T. Laurila, Electron transport determines the electrochemical properties of tetrahedral amorphous carbon (ta-C) thin films, Electrochim. Acta. 225 (2017) 1–10. doi:10.1016/j.electacta.2016.12.099.

[3] N. Wester, S. Sainio, T. Palomäki, D. Nordlund, V.K. Singh, L.-S. Johansson, J. Koskinen, T. Laurila, Partially Reduced Graphene Oxide (PRGO) Modified Tetrahedral Amorphous Carbon (ta-C) Thin Film Electrodes as a Platform for Nanomolar Detection of Dopamine, J. Phys. Chem. C. (2017) acs.jpcc.6b13019. doi:10.1021/acs.jpcc.6b13019.

[4] L.M. Lu, L. Zhang, F.L. Qu, H.X. Lu, X.B. Zhang, Z.S. Wu, S.Y. Huan, Q.A. Wang, G.L. Shen, R.Q. Yu, A nano-Ni based ultrasensitive nonenzymatic electrochemical sensor for glucose: Enhancing sensitivity through a nanowire array strategy, Biosens. Bioelectron. 25 (2009) 218–223. doi:10.1016/j.bios.2009.06.041.

[5] T.E.M. Nancy, V.A. Kumary, Synergistic electrocatalytic effect of graphene/nickel hydroxide composite for the simultaneous electrochemical determination of ascorbic acid, dopamine and uric acid, Electrochim. Acta. 133 (2014) 233–240. doi:10.1016/j.electacta.2014.04.027.

Keywords: Tetrahedral amorphous carbon, Thin films, Electrochemistry, Biomaterials

**[P5.13]**

**Electronic Properties, Bonding Structure and Mechanical Behaviours of a-CNx:Si(:B) thin films**

S.C. Ray*[1], W.F. Pong[2]

[1]*University of South Africa, South Africa,* [2]*Tamkang University, Taiwan*

Amorphous carbon nitride (a-CNx), silicon doped a-CNx (*a-CNx:Si*) and boron doped a-CNx (*a-CNx:B*) thin films alloys were prepared on silicon substrate using plasma enhance chemical vapour deposition process keeping (C/N) ratio constant in all films. The electronic properties, bonding structure and mechanical behaviours of a-CNx, *a-CNx:Si* and *a-CNx:B* thin films alloys were studied by the C *K*-edge, N *K*-edge x-ray absorption near edge structure (XANES) and valence band photoelectron spectroscopy (VB-PES). The *a-CNx:Si* and *a-CNx:B* shows higher Young's modulus compare to a-CNx thin film that are due to increase of carbon $sp^3$-hybridized cluster in *C* and *N K*-edge XANES spectra. From *C* and *N K*-edge XANES spectra formation of different carbon, nitrogen, silicon and boron bonding structure are observed. A valence band PES spectrum showed that the *p*-□ band became more intense than the *p*-□band upon silicon and boron addition, which confirmed the role played by the □bonds in controlling the electronic structure of *a-CN$_x$* films and hence their mechanical behaviour. All these films could be used in surface coating technology.

Keywords: Amortphous nitrogenated carbon, Silicon doped amorphous nitrogenated carbon, Boron doped amorphous nitrogenated carbon, Electronic structure

**[P5.14]**

**Laser irradiation to self-supporting ta-C film prepared using T-shape filtered arc deposition**

T. Harigai*[1], M. Yamano[1], T. Kawano[1], Y. Suda[1], H. Takikawa[1], M. Nishiuchi[2], H. Sakaki[2], K. Kondo[2], S. Kaneko[3], S. Kunitsugu[4] et al

*[1]Toyohashi University of Technology, Japan, [2]Kansai Photon Science Institute, Japan, [3]Kanagawa Industrial Technology Center, Japan, [4]Industrial Technology Center of Okayama Prefecture, Japan, [5]University of Hyogo, Japan*

Self-supporting tetrahedral amorphous carbon (ta-C) films have been expected a film target material for the laser-driven carbon ion acceleration method. The self-support of a ta-C film with several 10 nm in film thickness is difficult due to the high internal stress of the film. In this study, 110-nm-thick self-supporting ta-C film is prepared, and its laser irradiation damage is evaluated. The assumed high-intensity laser for the ta-C film target is the J-KAREN laser (the wavelength: 800 nm, the power density: $10^{12}$ W/cm$^2$, the pulse width: 40 fs) in Japan.

Self-supporting ta-C film was obtained by a sacrificial layer dissolving method. In the sacrificial layer dissolving method, a sacrificial layer formed between an objective film and a base substrate is dissolved, and then the film released from the substrate is dried on a perforated substrate. A ta-C film was deposited using the T-shape filtered arc deposition (T-FAD) on a dextran sacrificial layer. In the T-FAD, droplet-free ta-C films with high film density are obtained. The deposited ta-C film had laminated structure (the film thickness 35 nm, the film density 3.0 g/cm$^3$ / 40 nm, 2.7 g/cm$^3$ / 35 nm, 3.0 g/cm$^3$ / sacrificial layer) to suppress the film delamination on the sacrificial layer. In the laser irradiation experiment to the self-supporting films, CW laser for Raman spectroscopy (the wavelength 785 nm) was used.

The 110-nm-thick laminated ta-C film exhibited enough resistance to laser irradiation as shown in Fig. 1 because the prepulse energy intensity of the J-KAREN laser is approximately 35 J/cm$^2$. In addition, the ta-C film had flat surface. It was suggested that the laminated structure relaxed the internal stress of the film. For the laser-driven carbon ion acceleration method, 110-nm-thick ta-C film with high film density and flat film surface was obtained by film structure design using T-FAD.

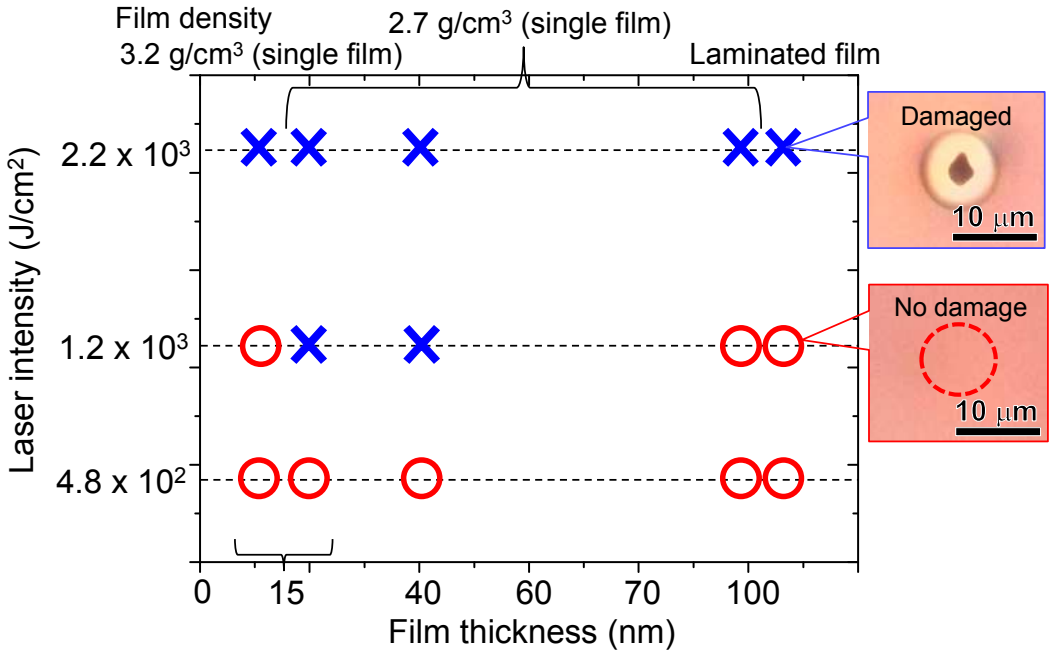


Fig. 1. Results of the laser irradiation experiment to the self-supporting ta-C films.

Keywords: ta-C, film target, laser-driven ion acceleration, self-supporting film

**[P5.15]**

**Influence of microstructure and chemical composition of different steels on DLC films adhesion**

P.C.S. Silva*[1,2], D.C. Lugo[1], M.A. Ramirez[1], E.J. Corat[1], V.J. Trava-Airoldi[1]

*[1]National Institute for Space Research - INPE, Brazil, [2]Science and Technology of Sao Paulo - IFSP Pirituba, Brazil*

DLC films have attracted attention due to their unique properties, such as high hardness, excellent wear and corrosion resistance, low friction coefficient and chemical inertness. DLC tridimensional deposition by PECVD technique allows its applications on steel pieces and surfaces. Nevertheless, this coating adhesion on steel substrate is hindered mainly due to high residual compressive stress that occurs in film formation and thermal expansion coefficient mismatch between steel and DLC film, which generates delamination effects. In this work, DLC films were grown on different types of steel, in order to evaluate how microstructure and composition influences the films adhesion. A silicon interlayer was deposited prior to the film growth, by using different bias voltages. Both silicon and DLC films were grown by using a pulsed DC-PECVD system, with an additional cathode. This technique enhancement allows depositing films with very low pressure, due to the increase on mean free path, and ion energy distribution narrowing, which makes the subimplantation process more efficient. DLC films structure was analyzed by Raman spectroscopy. Scracth tests were performed in order to evaluate DLC films adhesion. Rockwell C impressions was also analyzed with the same purpose. SEM images showed the microstructure differences while EDX analysis showed the chemical composition variation. According to results, bias voltage variation have different influence for each type of steel, resulting in different levels of adhesion.

Keywords: DLC, Adhesion, Steel, PECVD

**[P5.16]**

# Nanotexturing amorphous carbon films by reactive ion etching

A. Godoy Junior*[1], F.G. Carlucci[1], W. Miyakawa[1], D.M.G. Leite[1], M. Massi[2], A.S.S. Sobrinho[1]
[1]*Technological Institute of Aeronautics, Brazil,* [2]*Mackenzie Presbyterian University, Brazil*

## Introduction

In the last decades, the research and development of carbon-based nanostructured materials has become increasingly critical to the advancement of the aerospace, electronics, biomedical and other industries branches. The proposal was the deposition of thin films of amorphous carbon by magnetron sputtering (MS) on glass and silicon (Si) substrates, followed by a thermal treatment (TT) to increase the film roughness and decrease its electrical resistance. Using the reactive ions etching process, the surface roughness was enhanced aiming to applications in electrodes of batteries and dye-sensitized solar cells DSSCs. This procedure of texture/roughness modification using plasma is known as plasma texture (PT).

## Methods

Carbon thin films were deposited by MS onto crystalline Si and FTO substrates, and then annealed at 600°C to improve the films conductivity. In order to enhance the surface roughness the films were finally etched in $SF_6$ plasma combined with $H_2$ (during 30 and 45 seconds), $O_2$ (during 6 and 12 seconds), and Ar (during 14 and 28 seconds) in different experiments. The films produced were characterized by profilometry, MEV, AFM, RAMAN, FT-IR and goniometry.

## Results and Discussion

The analyses showed that the films submitted to the TT and to the PT processes presented nanostructural surface (see Fig. 1) patterns strongly depend upon the secondary plasma etching gas ($H_2$, $O_2$, or Ar).

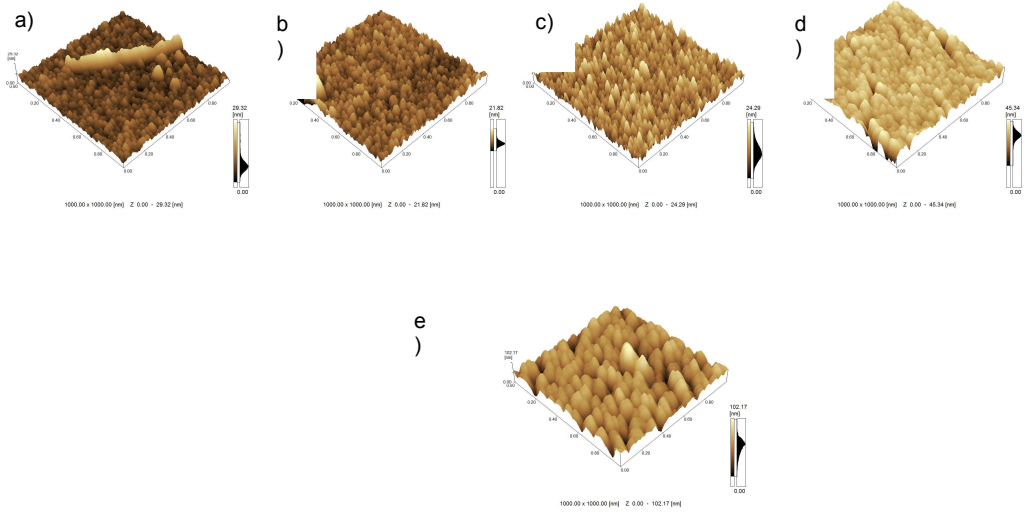

Fig. 1: Representative AFM images with 1 μm x 1 μm scanning area, in 3D visualization of some carbon films a) C, b) CT c) H30 d) O6 and e) Ar28 sample.

Regarding to microstructure, the TT allowed the increase of $sp^2$ hybridization and nanoclusters formation leading to a nanocrystalline structure. The films submitted to the $SF_6$+Ar plasma exhibited the highest surface roughness. The goniometry analyses revealed that the TT was responsible for a clear hydrophilic to hydrophobic surface transition. However, super hydrophilic behavior was observed after the PT processes (see Table 1).

Table 1: Water-surface contact angle for each sample

| **Samples** | C | CT | H30 | H45 | O6 | O12 | Ar14 | Ar28 |
|---|---|---|---|---|---|---|---|---|
| **Contact angle (degrees)** | 40±1 | 89±1 | 25±2 | 20±1 | < 20 | < 20 | 34±5 | 31±4 |

The increases on the surface roughness and hydrophilicity of these textured carbon thin films are extremely important characteristics for its applications as DSSCs electrodes and batteries.

Keywords: Plasma texture, Nanostructured amorphous carbon, Carbon thin films, Surface roughness

**[P5.17]**

## Wear property of DLC coating for medical devices

K. Sakurai*[1], K. Terai[1], H. Nakamori[2], M. Hiratsuka[2], K. Namiki[3], K. Hirakuri[1], K. Sato[1]
*[1]Tokyo Denki University, Japan, [2]Nanotec Co. Ltd, Japan, [3]Namiki-Mi Co. Ltd, Japan*

Metal materials such as stainless-steel (SUS) and titanium are used for the current therapeutic devices and medical devices. It may cause aching pain, discomfort, and laceration due to high friction when metal made medical devices are inserted into the body. It is not enough to use the metal made medical devices in case of any friction. Diamond-like carbon (DLC) has been applied as a coating technique on rubbing surface because its friction coefficient is extremely low. Furthermore, DLC coating has excellent properties such as biocompatibility and chemical stability. It is expected as a surface modification of a medical device. In this study, we have investigated the reduction effect of friction coefficient of SUS substrate by DLC.

In this experiment, DLC films were deposited on SUS substrate (DLC/SUS) by using an ionized vapor deposition method. The structure of SUS and DLC/SUS were evaluated by X-ray photoelectron spectroscopy and Raman spectroscopy. The friction coefficient was measured under the dry condition (Dry) and the moist atmosphere of physiological saline (Wet), due to simulation environment for a living organ.

According to the result of the friction measurement, the friction value was dramatically decreased by DLC coating in case of Dry condition, that is, the friction coefficient was reduced from 0.529 to 0.176 by DLC coating. Furthermore, in Wet condition, the friction coefficient was 0.556 at SUS substrate and 0.117 at DLC coating substrate, respectively. It was confirmed that the friction coefficient of DLC/SUS is lower than that of SUS in both Dry and Wet condition. DLC films is a key technology for improvement of sliding properties of medical devices.

Keywords: DLC, Wear property

**[P5.18]**

**Surface coating of aluminium alloys sintered products for automotive applications using DC and RF sputtering**

I. Solomon, C. Deb, N. Chhatral, B. Sarma, V. Umasankar, A. Sarma*
*VIT University Chennai, India*

DLC formation on Al alloys and its purity were obtained by characterizing the samples with Raman spectroscopy, X-ray diffraction and scanning electron microscopy/energy dispersive spectroscopy. Initial evaluation of DLC coatings was performed using scratch, micro-hardness, fracture toughness and surface roughness tests. Raman measurements showed the presence of a broader peak in the region of 1000 to 1600 $cm^{-1}$ after coating which shows clear indication of DLC. X-ray diffraction and energy dispersive spectroscopy confirmed the presence of carbon phases in the coatings. Scanning electron microscopy examination showed a fairly uniform and dense coating with a nominal thickness of 5-10 μm and a heat affected zone of 60–80 μm. These coatings exhibited micro-hardness in the range of 2000 to 2300 $kg/mm^2$ when measured using a Vickers diamond pyramid indenter at a load of 0.5 N. In some localized regions, even more hardness (> 5000 $kg/mm^2$) was obtained. Scratch tests revealed a fairly homogenous coating with strong adhesive nature having almost four times the average critical force when compared against the electro-statically deposited sample. Fracture toughness and surface roughness are well within the acceptable ranges of DLC coatings. The capability of laser sintering to produce thick DLC coatings with outstanding mechanical and tribological properties and excellent bonding with aluminium offers the possibility to tailor an extreme lightweight, strong and wear-resistant material.

Keywords: Diamond, Hardness, Adhesive, Tribological properties

**[P5.19]**

**Improving the mechanical properties of amorphous carbon films by silicon doping**

A.S. Chaus*[2], D.G. Piliptsou[1], P. Pokorný[2], X.H. Jiang[1], A.V. Rogachev[1]

*[1]Nanjing University of Science and Technology and Francisk Skorina Gomel State University, China, [2]Slovak University of Technology in Bratislava, Slovakia*

In this study the microstructure and mechanical properties of a-C:Si films, in relation to C/Si concentration ratios, were studied. The films were formed via sputtering a composite silicon-graphite target by pulse arc discharge. The C/Si atomic concentration ratio was changed varying the C/Si mass concentration ratio of the cathode.

The atomic element concentration in the films was determined using SEM equipped with EDS. AFM was used to evaluate the surface morphology, in particular, its roughness and the grain distribution vs. average size. Micro-hardness measurements (Knoop method) and the tribological tests (sphere-plane method, speed 10 mm/s, Hertz pressure 478 MPa) of the films were also carried out.

Raman spectrometry showed that Si doping leads to a reduction in size of $Csp^2$ clusters and to an increase of degree of disorder in the film microstructure with increasing the Si concentration. XPS analysis revealed the presence of the C-Si bonds in the films, which are typical for silicone carbide, with $Csp^2/Csp^3$ reducing at the increase of Si concentration in the film.

It has been shown that the growth of C/Si leads to a decrease in both the residual stresses and the surface energy, and influences the films friction kinetics, primarily friction coefficient. In general, the a-C:Si films properties depend on the silicone concentration and the certain Si concentration threshold value can provide the surface microstructure stabilisation, which is dealt with the graphitisation temperature increase due to $Si_xO_y$ formation on the film surface that leads to the improved tribological properties of the a-C:Si films.

The financial support of the grants VEGA 1/0520/15 and VEGA 1/0477/14, and the project Centre of Excellence of Five Axis Machining Experimental Base for High Tech Research ITMS 26220120045 (Co-financed by European Funds for Regional Development) is gratefully acknowledged.

Keywords: Diamond-like carbon, Si doping, Structure, Mechanical properties

**[P5.21]**

**The impact of diamond-like-carbon coating on the function abilities of port fuel injectors**

J.Y. Lambongang*, P. Suwanpinij

*The Sirindhorn International Thai-German Graduate School of Engineering, Thailand*

Port fuel injectors are the components that injects fuel into the intake manifold of the engines of automobiles. The harsh environments that port fuel injectors are subjected to make their material selection and coating selection a very important area that is worth investigating. Nowadays, certain Port fuel injectors are of similar designs and have virtually similar coating materials. However, these similar injectors are sometimes different in certain areas of their function abilities. Some can run on both gasoline and ethanol while others can only run on gasoline even though they are of similar designs and virtually of similar coating materials. To understand the reason behind their difference in certain areas of their function abilities it was imperative to have an inverse engineering on the similar injectors with diverse function abilities and then investigate both coatings in detail. The coating was the target point because it comes into direct contact with which ever fuel that the injector runs on. In this study, both coatings were examined with X-Ray Photoelectron Spectroscopy (XPS). The various experiments with XPS revealed that both injectors were of diamond-like-carbon coating. However, the diamond-like-carbon coating of both injectors were analyzed further and it was discovered that the types of diamond-like-carbon coating varied in each injector. Further studies were done and it was realized that the several types of diamond-like-carbon coating possess their distinct features. Hence, having a significant impact on the function abilities of the injectors on which they were applied.

Keywords: Impact, Diamond-like-carbon, coating, functionabilities

**[P5.22]**

**Effect of kink structure and chlorine on the magnetism of carbon nanowires array**

C.H. Wong*, E.A. Buntov, A.F. Zatsepin

*Ural Federal University, Russia*

The ab-initio calculation predicts the existence of magnetism in the chlorine doped linear carbon nanowires array. The theoretical analysis is based on the calculation of the differential DOS of spin up and spin down electrons. Through monitoring the bond distance between the chlorine and carbon atoms, the magnetic signal is stronger upon decreasing the bond distance. Despite no magnetism is detected in the un-doped linear carbon nanowires, the differential DOS is non-zero in the presence of kink structure surprisingly. The key of generating unbalanced DOS in the pure carbon nanowires is to twist the kink angle at least 50 degree periodically. The direction of the easy axis shows kink-dependence interestingly. The easy axis switched to opposite direction when the kink is above 57 degree and the optimal magnetic signal of takes place at 60 degree. Apart from this, the lower differential DOS is occurred if the branch length is extremely long under the same kink angle. We also observe that doping chlorine opens an opportunity to intensify magnetism at any kink angle. The largest differential DOS per atom in the chlorine doped carbon nanowire is 0.345 electron/eV which is comparable to the pure iron of 0.355 electron/eV.

Keywords: magnetism, carbon nanowire

**[P5.24]**

**Surfen-assembled graphene oxide for fluorescence turn-on detection of sulfated glycosaminoglycans in a biological matrix**

Y-T. Wang, W-L. Tseng*
*National Sun Yat-sen University, Taiwan*

**Introduction:** Sulfated glycosaminoglycans (GAGs) have been reported as biomarker for mucopolysaccharidoses disease and as an important role in various biological processes, such as blood clot medication (heparin) and signal transduction (heparan sulfate). However, few fluorescent sensors have been developed for the detection of sulfated GAGs in the real world. A cationic dye, 1,9-dimethylmethylene blue (DMMB), is commonly used to detect sulfated GAGs based on electrostatic attraction. However, this probe suffers from poor selectivity and sensitivity toward sulfated GAGs.

**Methods:** We propose that a surfen/few-layer graphene oxide (FLGO) nanocomplex could be utilized for sensitive detection of sulfated GAGs. At the beginning, surfen molecules are self-assembled onto the surface of FLGO through electrostatic attraction. Subsequently, FLGO quenches the fluorescence of surfen through a static and dynamic quenching process. Since the complexes of surfen and sulfated GAGs have strong electrostatic repulsion for FLGO, the presence of sulfated GAGs can allow the removal of surfen from the surface of FLGO. As a result, GAGs not only restore the fluorescence of surfen, but also enhance their fluorescence through the formation of the complex.

**Results and Discussion**. To overcome this challenge, we fabricated a surfen/FLGO nanocomplex for sensing sulfated GAGs in biological fluids. Surfen molecules were self-assembled onto the surface of FLGO through electrostatic attraction and their fluorescence was then quenched by the creation of the FLGO-surfen complex (static quenching), and partially combined with the energy transfer from surfen to FLGO (dynamic quenching). The strong electrostatic attraction forced surfen molecules to self-assemble on the FLGO surface, which was supported by deep chemical and morphological characterization. The presence of sulfated GAGs resulted in fluorescence recovery through the formation of the surfen-GAGs complex, which exhibits weak binding to FLGO and keeps surfen molecules away from the FLGO surface. Because FLGO efficiently reduced the fluorescence background from surfen and competed with sulfated GAGs for binding to surfen, surfen-assembled FLGO exhibited higher sensitivity and better selectivity for sulfated GAGs than surfen did. The aforementioned strategy was exemplified by the analysis of heparin in human plasma and sulfated GAGs in artificial cerebrospinal fluid; the limits of detection (LOD) at a signal-to-noise ratio of 3 for heparin, dermatan sulfate, and heparin sulfate were determined to be 30, 30 and 60 ng/mL, respectively. The LOD of heparin detected by surfen-assembled FLGO is the lowest among all organic dye-based sensors reported so far. Moreover, this sensor was capable of sensing heparin in human plasma without the need for the standard addition method and sulfated GAGs (a mixture of chondroitin sulfate A, dermatan sulfate, and heparan sulfate) in artificial CSF. Undoubtedly, surfen-assembled FLGO coupled with a high-throughput screening plate reader holds remarkable potential for use in routine assays of sulfated GAGs in clinical samples.

Keywords: Graphene oxide, Sulfated Glycosaminoglycans, Fluorescence, Biosensor

**[P5.25]**

# Graphene oxide and MWCNTs as promising additives for stand-alone reverse osmosis membranes for water desalination

W. Falath*
*King Fahd University of Petroleum and Minerals, Saudi Arabia*

Introduction:

Graphene Oxide (GO) and MWCNTs attracted research interest in fabrication of water treatment membranes, due to their special inherent properties, such as great surface area, large amount of hydrophilic functional groups, good mechanical strength, and ability to mitigate bacterial growth upon direct contact with cells. Incorporating GO and MWCNTs within membrane surfaces improved Chlorine resistance and fouling resistance of the surfaces. In this study, novel crosslinked Poly (vinyl alcohol) reverse osmosis (RO) membranes infused with GO and MWCNTs were synthesized.

Methods:

Membranes were synthesized using dissolution casting methodology. GO and MWCNTs were infused into the polymer solution after sonication. The overall RO performance of the membranes including hydrophilicity, surface roughness, water permeability, salt rejection, Chlorine resistance and biofouling resistance was evaluated using a dead end RO filtration unit. Membranes were characterized using ATR-FTIR, SEM, AFM, contact angle measurements and mechanical strength analysis.

Results and Discussion:

The synthesized membranes showed improved overall RO performance. It was found that the modified membranes surfaces became highly hydrophilic compared to the pristine PVA membranes surfaces. Surface roughness decreased as well and that could be explained by the fact that MWCNTs loading leads to an increase in viscosity of the casting solution which obstructs the exchange rate of solvent and non-solvent diffusion during the dissolution casting process, and hence, smoother membrane surfaces are formed. This study indicated that the membranes provided excellent permeability, salt rejection, Chlorine and biofouling resistance and mechanical strength. The antibacterial property of the membrane has improved by more than 80 % after the inclusion of MWCNTs and GO. In this research, the synthesized modified PVA membranes had a much better Chlorine resistance compared to commercial RO membranes. Chlorine resistance is a very important membrane property since it diminishes the need for the de-chlorination process.

Keywords: Graphene Oxide, MWCNTs, Membranes, Water Desalination